

UNIVERSITÀ DEGLI STUDI DI PADOVA
DIPARTIMENTO DI INGEGNERIA INDUSTRIALE
CORSO DI LAUREA MAGISTRALE IN INGEGNERIA CHIMICA E
DEI PROCESSI INDUSTRIALI

**Tesi di Laurea Magistrale in Ingegneria
Chimica e dei Processi Industriali**

**Modeling the bicarbonate uptake in
Arthrospira maxima as a function of pH:
batch and continuous experiments**

Relatore: Prof.ssa Eleonora Sforza

Laureanda: Anna Tagliaferro

ANNO ACCADEMICO 2022 – 2023

Riassunto

Gli ultimi decenni sono stati caratterizzati da un'attenzione crescente rivolta alla possibilità di produrre industrialmente elevate quantità di microalghe e cianobatteri, sia in termini di biomassa che di prodotti da questi estratti. L'interesse rivolto a questi microorganismi è principalmente dovuto al loro notevole e differenziato campo di applicazioni cui possono essere destinati. Infatti, a seconda della specie considerata, è possibile sfruttarne i differenti componenti bioattivi utili non solo nel settore alimentare, nutraceutico e cosmetico, ma anche in quello energetico e dei materiali.

Tuttavia, oggi, l'effettiva applicazione su scala industriale di tali sistemi produttivi rimane ancora notevolmente limitata, sia per le scarse produttività ottenibili sia per gli elevati costi operativi. Uno tra i principali fattori che maggiormente incidono sui costi operativi è dato dall'utilizzo di stream gassosi d'aria arricchita con percentuali variabili di CO₂. L'utilizzo dell'anidride carbonica è essenzialmente legato a due aspetti: primariamente, come per tutti gli organismi fotoautotrofi come le microalghe, essa rappresenta la principale fonte di carbonio inorganico da cui origina l'intero macchinario metabolico atto a sostenere le normali attività cellulari; in più, nelle colture in grande scala, vi è la necessità di tamponare il pH del mezzo di coltura, il cui aumento incontrollato dovuto alla crescita cellulare può impattare negativamente la produttività finale del processo. Tuttavia, per poterne usufruire, la CO₂ deve essere previamente purificata e trasportata al sito di produzione, facendo aumentare i costi di produzione per le aziende. In più, le microalghe stesse utilizzano una esigua parte della CO₂ insufflata (1-5%), per cui una buona parte di gas utilizzato viene perso in atmosfera. Tutti questi aspetti incidono negativamente sulla fattibilità del processo, soprattutto quando sono richiesti grandi volumi di produzione. Una soluzione alternativa emergente è rappresentata dall'approccio BICCAPS (*Bicarbonate Integrated Carbon Capture and Algae Production system*), che prevede di minimizzare il più possibile o eliminare l'utilizzo della CO₂, fornendo alle microalghe fonti di carbonio inorganico alternative, come il bicarbonato di sodio (NaHCO₃). In particolare, questi sistemi di coltivazione sono applicabili per specie alcalofile (cioè in grado di sopravvivere a pH piuttosto basici), dotati di un metabolismo in grado di sfruttare lo ione bicarbonato (HCO₃⁻), in accordo con le reazioni di equilibrio chimico nelle quali l'NaHCO₃ viene coinvolto e che sono strettamente dipendenti dal pH della coltura stessa.

Tra i diversi organismi sfruttabili in BICCAPS, i rappresentati del genere *Arthrospira*, risultano estremamente interessanti non solo per la loro spiccata capacità di sfruttare il bicarbonato per la fissazione del carbonio, ma anche per il notevole interesse commerciale acquisito. A scala industriale, il bicarbonato per spirulina è già ampiamente utilizzato, ma spesso con un approccio combinato al supply di CO₂, con conseguente grande spreco di carbonio, dal momento che le informazioni relative agli aspetti cinetici e regolatori non sono completamente chiari. Pertanto, in questo progetto di tesi, sono stati svolti degli esperimenti finalizzati a descrivere con approccio quantitativo la coltivazione del cianobatterio alcalifilico *Arthrospira maxima* simulando il funzionamento di un fotobioreattore operante in continuo (approssimato da un CSTR – *Continuous Stirred Tank Reactor*) dove sono state mantenute costanti l'intensità luminosa, la composizione dell'aria e il tempo di residenza, variando la concentrazione di bicarbonato di sodio in ingresso. L'obiettivo è quello di verificare quale sia la concentrazione di NaHCO₃ in grado di garantire la massima concentrazione di biomassa. Dopo aver individuato la condizione ottimale a 30 g L⁻¹ di NaHCO₃, è stato possibile verificare l'effetto di diverse composizioni di aria insufflata (aria arricchita con CO₂, aria atmosferica e senza nessun bubbling) sulla produzione di biomassa. Anche in questo caso, si sono mantenute costanti le altre variabili di processo. In particolare, non è stata individuata una differenza significativa tra l'uso di aria arricchita con CO₂ o aria atmosferica quando il sistema tampone viene ottimizzato, e mantenendo la coltura in continuo alla fase esponenziale, a supporto della possibilità di poter evitare l'uso del diossido di carbonio per la coltivazione. Tale considerazione è ulteriormente supportata dal fatto che operando in continuo, ad elevate concentrazioni di bicarbonato, il pH tende a stabilizzarsi naturalmente a valori accettabili per la crescita.

Sulla base dei dati sperimentali, è stato proposto un modello matematico capace di descrivere l'andamento della concentrazione di biomassa, ione bicarbonato e pH nel mezzo di cultura. Nello specifico la velocità di crescita della biomassa contiene al suo interno un termine cinetico che segue il modello di Monod. Tuttavia, a differenza di altri modelli presenti in letteratura, soltanto la concentrazione di bicarbonato è stata considerata come substrato limitante. I parametri sono stati determinati attraverso una procedura di fitting realizzata grazie all'uso del software MATLAB®. In generale, il modello riesce a predire correttamente l'andamento del pH, dello ione bicarbonato e della biomassa. Tuttavia, non contiene specifici termini derivanti da possibili fenomeni di inibizione da salinità che non potranno pertanto essere adeguatamente descritti, pur verificatisi a livello sperimentale.

Abstract

Microalgae industrial cultivation is still currently limited by high costs related to biomass production and harvesting. Among the others, the supply of CO₂ by bubbling is one of the major costs related to CO₂ insufflation in photobioreactors, due to the low solubility of CO₂ and the slow uptake by microalgae, causing a consistent loss of the gas in the atmosphere. Hence, research efforts have been focused on the investigation of suitable alternative inorganic carbon sources. Some microalgae and cyanobacteria, called alkali halophilic species, are able to exploit bicarbonate ions for carbon fixation with efficiency comparable to that of CO₂. *Spirulina*, one of the most cultivated microalgal species for industrial purposes, is able to use bicarbonate, and it was chosen as a model organism to describe the effect of bicarbonate on growth, accounting for the effect of pH on carbonate speciation.

In this master thesis, *Arthrospira maxima* has been cultivated in continuous photobioreactors under different bicarbonate concentration, pH and under enriched CO₂ bubbling. Experimental data were subsequently applied to implement a kinetic model for a numerical description of such a phenomenon.

Index

Introduction.....	11
Chapter 1: Microalgae and Cyanobacteria.....	13
1.1 Industrial relevance of microalgae and cyanobacteria.....	13
1.2 Photosynthesis and carbon fixation.....	15
1.2.1 Photosynthetic pigments.....	15
1.2.2 Photosynthesis: light phase and dark phase.....	17
1.2.3 Carbon fixation and the Calvin-Benson cycle.....	17
1.3 Microalgae growth parameters.....	18
1.4 Microalgae industrial production systems.....	20
1.4.1 Open systems.....	21
1.4.2 Photobioreactors.....	21
1.4.2.1 Photobioreactors illumination technologies.....	22
1.4.2.2 Photobioreactors design.....	23
1.4.3 Hybrid systems.....	26
1.5 Cultivation modes.....	27
1.6 Alkalophilic cyanobacteria and BICCAPS.....	29
1.6.1 CO ₂ supplying issues.....	30
1.6.2 BICCAPS and alternative inorganic carbon source.....	30
1.6.2.1 Sodium bicarbonate as carbon source.....	31
1.6.2.2 The pH drives the chemical equilibrium reactions.....	32
1.6.3 Alkaliphilic cyanobacteria and <i>Arthrospira</i> spp.	34
1.6.3.1 <i>Arthrospira</i> spp. relevance in microalgae market.....	36

1.7 Purpose of the thesis.....	38
Chapter 2: Materials and methods.....	41
2.1 Arthrospira maxima cultivation conditions.....	41
2.1.1 Laboratory-scale photobioreactors.....	43
2.1.2 Experimental conditions.....	44
2.2 Analytic measurements.....	45
2.2.1 Optical density.....	45
2.2.2 Dry cell weight.....	45
2.2.3 Analytical measurements.....	47
2.2.3.1 Titration.....	47
2.2.3.2 Chlorophyll a and carotenoids extraction and quantification.....	49
2.2.3.3 Phycobiliproteins extraction and quantification.....	49
2.2.3.4 Exopolysaccharides quantification.....	50
2.3 Statistical analysis.....	52
Chapter 3: Kinetic model description.....	53
3.1 The importance of a mathematical model.....	53
3.2 Material balances.....	55
3.2.1 Biomass material balance.....	56
3.2.2 Carbonaceous species material balance.....	59
3.2.2.1 Additional terms.....	60
3.2.3 Hydrogen species material balance.....	60
3.3 Kinetic parameters determination.....	64
Chapter 4 – Results and discussion.....	65
4.1 Experimental results.....	65
4.1.1. Effect of different sodium bicarbonate concentrations.....	67

4.1.1.1 Effect of NaHCO ₃ on biomass concentration and on carbonaceous species concentration.....	69
4.1.1.2 Effect of NaHCO ₃ on pigments production.....	70
4.1.2 Effect of different air composition.....	72
4.1.2.1 Effect of different air composition on biomass growth.....	73
4.1.2.2 Carbonaceous species distribution.....	74
4.1.2.3 Pigments and PBPs production.....	75
4.1.3 The effect of pH.....	77
4.2 Kinetic parameters.....	79
4.5.1 Input data.....	79
4.5.2 Fitting results.....	81
Conclusions.....	85
References.....	87

Introduction

In the last decade, the society has been characterised by a relevant growth of the population and consequently also the demand of different everyday life products (such as food, energy, chemicals etc.) raised. According to this aspect, combined with the necessity to develop more sustainable industrial processes, the attention has been focused on alternative technologies and production systems: microalgae represent one of the most suitable solutions. Nowadays, many examples of microalgae industrial applications could be reported since they can promote different advantages, such as the high photosynthetic efficiency, if compared with terrestrial plants, the possibility to use non arable lands for their cultivation and their high content of valuable bioactive components, just to cite some examples. However, there are still important drawbacks that limit their production at large scale. Among the others, LEDs important to consider the high biomass production costs mainly linked to the supply of CO₂ as carbon source: sodium bicarbonate seems to be an interesting alternative for alkaliphilic microalgae or cyanobacteria able to exploit bicarbonate ion. In fact, this is the basic idea of BICCAPS (*Bicarbonate Integrated Carbon Capture and Algae Production System*) approach, which is an alternative microalgae production system recently proposed.

This thesis project is divided in two main parts: an experimental assessment and a mathematical model presentation. In the first case, the aim is to verify the real possibility to cultivate the alkaliphilic commercially-relevant cyanobacterium *Arthrospira maxima* in continuous mode (through a laboratory-scale photobioreactor simulated with a *Continuous Stirred Tank Reactor-CSTR*) and with different concentrations of sodium bicarbonate fed. Additionally, once the optimal concentration has been found, also the effect of different air stream supplied has been considered, in order to check if the only atmospheric air is sufficient to guarantee acceptable results in terms of biomass concentration. At the end, some experiments will be performed controlling the pH of the culture to different set-point, and according to the most suitable conditions found from the two previous experimental campaigns. This might be important, since the pH is one of the most important process variables which could affect the microalgae cultivation and it could impact on the biomass composition.

In the second part of the work, a mathematical model to describe the bicarbonate uptake from *Arthrospira maxima* is presented. In particular, a suitable kinetic model able to describe the biomass growth and to determine the speciation of carbonate species was needed. For this purpose, the software MATLAB® will be used to perform a fitting

procedure between the material balances equations (namely, the model) and the experimental data collected. The work of this thesis project is presented in four main chapters.

Chapter 1 contains a general overview concerning microalgae importance at industrial level, besides the key information regarding their metabolism briefly describing the photosynthesis and carbon fixation activities. Then, the most important process variables which affect the microalgae cultivation, the different cultivation mode and devices are described. At the end, it is presented one of the most important issues concerning the industrial production. It is mostly related to the carbon dioxide supply, presenting the use of BICCAPS as a suitable alternative.

In Chapter 2, the experimental conditions and the main features of the experimental set-up are described. Additionally, particular references to the method to perform the analytical measurements are reported.

Chapter 3 contains the details of the mathematical model considered and, at the end, in Chapter 4, the results are presented and discussed. Specifically, concerning the experimental assessment, they are divided according to the different experimental campaigns and focusing on the most significative data collected. Concerning the model, the fitting results (and the parameters values obtained) are reported.

Chapter 1

Microalgae and Cyanobacteria

In this chapter, a briefly overview regarding the economic importance of microalgae and cyanobacteria is presented, describing the most common modes and technologies developed for their cultivation. Particular references to *Arthrospira* spp. are reported since it is the cyanobacteria species investigated through this thesis work.

1.1 Industrial relevance of microalgae and cyanobacteria

Cultivation of microalgae and their industrial exploitation have been trending topics in the last decade, both among researchers and companies. This is due to their promising applications in a wide variety of industrial sectors, ranging from everyday products to high-value compounds, since they accumulate a quite high varieties of valuable chemicals (Barbera et al., 2020; Pastore et al., 2022). This is a consequence of their versatile and heterogeneous metabolism, through which microalgae are able to synthesize and accumulate a huge variety of specific molecules (Abreu et al., 2022; Vale et al., 2020). These microorganisms also show high growth and photosynthetic rates, with the capability to capture inorganic carbon faster than terrestrial crops and without herbicides and pesticides requirement (Hernández et al., 2014). In addition, for their cultivation non-arable lands, saline water and agro-industrial wastewaters could be used (Hernández et al., 2014; Trentin et al., 2021). Moreover, they can grow exploiting sun light and exhibit a photosynthetic efficiency 10-50 times higher than terrestrial plants (Zhou et al., 2017). Microalgae assume a key role also in the perspective of a future sustainable and bio-based industry (Barbera et al., 2020). For example, the European Green Deal and other related EU policy initiatives (such as the *Farm to Fork* or the *Sustainable Blue Economy Communication*) recognised their potential importance to promote the transition to a green-circular and carbon-neutral economy (Vazquez & Sanchez, 2022).

In fact, by exploiting their nutritional requirement, they can be applied to capture CO₂, both from the atmosphere and flue gasses emission, but also to remove nutrients (e.g., nitrate, ammonium and phosphate) from industrial or urban wastewaters (Vale et al., 2020). Also, microalgae become suitable in the case of a biorefinery approach (Shankar et al., 2022). In fact, the valorisation of the residual biomass after the extraction of valuable biomolecules, such as pigments or fatty acids, could help make microalgae

cultivation more remunerative for companies (Thevarajah et al., 2022; Vale et al., 2020). Nevertheless, some potential uses could be also the biodiesel synthesis, with an oil yield about 16-70 times higher than the one obtained from coconut, sunflower and palm, or the synthesis of bioplastic, derived from the extraction of a wide range of intermediate ingredients, ensuring more environmentally friendly and biodegradable properties than ordinary fossil-based plastics (Hernández et al., 2014; Fernández et al., 2021), even though the production of biodiesel from microalgae was demonstrated to be not compatible from an economic point of view.

A summary of potential microalgae application is reported in *Figure 1.1*.

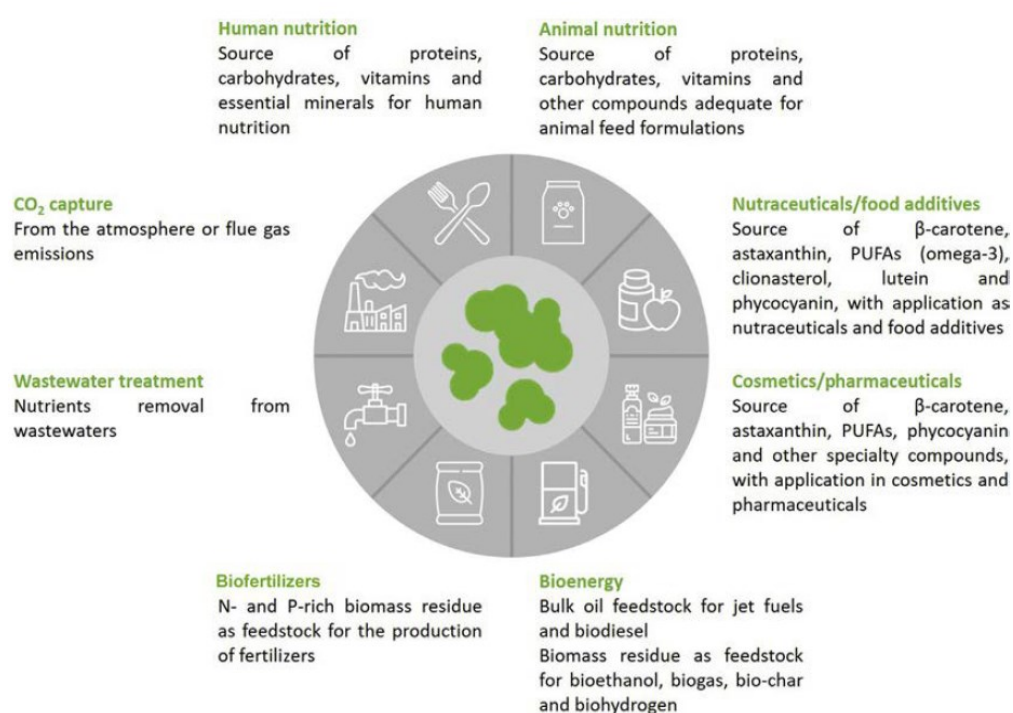


Figure 1.1: Summary of the most common possible microalgae applications (Vale et al., 2020).

The microalgae global production is estimated to be 25,000 t year⁻¹, with a total market volume of 50 M€ and this is set to grow to 70 M€ by 2025 (Fernández et al., 2021).

Thus, the microalgae market is continuously growing and it is expected that the *Compound Annual Growth Rate (CAGR)* could rise up to 5.6% (~ half billion dollars/year) by 2030 (Abreu et al., 2022).

However, massive microalgae cultivation and commercialization is still far from reality. The main bottleneck that microalgae producers, as well as researchers, are facing concerns the high production costs (Zhu et al., 2022) and the small-scale of current production systems (Garrido-Cardenas et al., 2018). In particular, according to the cultivation technology design, the capital costs vary between 33,042 \$/acre for an open

pond to 510,617 \$/acre for a flat panel photobioreactor (Clippinger & Davis, 2019). A precise estimation of the productivity of different systems is quite difficult to obtain, since it could be affected by many aspects, especially among the different photobioreactors designs and also for the same one, when different operative conditions are set (Clippinger & Davis, 2019). Anyway, in general, the biomass target areal productivity could achieve $25 \text{ g m}^{-2} \text{ day}^{-1}$ for an open system and around $50 \text{ g m}^{-2} \text{ day}^{-1}$ for closed photobioreactors. However, nowadays is very difficult to reach such theoretical values in large and full-scale plants (Clippinger & Davis, 2019; Devadas et al., 2021). This, apart from the metabolic limitations of microalgae, is typically caused by operation costs, namely the exploitation of artificial light in PBR, the supply of nutrients and of CO_2 (Abreu et al., 2022; Chen et al., 2011). For this reason, research efforts are to date focused on the development of more robust and efficient production systems (Garrido-Cardenas et al., 2018).

1.2 Photosynthesis and carbon fixation

Even though they are capable to grow heterotrophically (that is, by mean of organic carbon uptake), generally microalgae better exploit photosynthesis for their growth both in nature and industrial cultivation (photo-autotrophy). Thanks to a complex cellular and metabolic machinery (i.e., pigments and associated proteins), microalgae can use light as the solely energy source, through which inorganic components (mainly CO_2) are transformed into macromolecules (carbohydrates, proteins, lipids etc.) that are essential in sustaining cellular growth and maintenance. For the purpose of this thesis, the main metabolic reactions that constitute photosynthesis and carbon fixation as well as pigments and enzymes that mediate such processes are briefly described (Vale et al., 2020).

1.2.1 Photosynthetic pigments

When considering photo-autotrophic growth, light represents an important variable to consider, since it is the only energy source to sustain the whole metabolic machinery. In general, the portion of light exploited to perform photosynthesis corresponds to the visible light wavelength ($\sim 400\text{-}700 \text{ nm}$) and it is usually defined as photosynthetically active radiation (PAR) spectrum. Light harvesting and energy transfer to the reaction centres in photosystems (PSI and PSII) is due to particular molecules able to absorb and emit light, called pigments. They are structured in the form of antennae located in thylakoid membranes, placed inside the chloroplast or close to the cellular membranes for eukaryotic and prokaryotic microalgae respectively. The main pigments classes are: chlorophylls, carotenoids and phycobiliproteins. Each group is able to absorb in a specific

range of wavelengths as represented in *Figure 1.2*. Most represented pigments in microalgae are chlorophyll *a* and beta-carotene, even though a plethora of diverse accessory pigments can be found among different species (Pagels et al., 2020; Yarish & Kim, 2012).

Chlorophyll, a green coloured pigment, is the leading molecule in light harvesting. Six different types exist, according to the different molecular structure, and the main absorption range is between 430-465 nm and 630-675 nm (Pagels et al., 2020).

Phycobiliproteins (PBPs) are characteristic blue-red pigments typically found in cyanobacteria and red-algae. They can be divided into three main proteins: phycocyanin (PC, $\lambda_{MAX} = 650$ nm), phycoerythrin (PE, peculiar of red algae, $\lambda_{MAX} = 565$ nm) and allophycocyanin (APC, $\lambda_{MAX} = 620$ nm) (Pagels et al., 2020). They are in turn organised into a macromolecular multi-protein complex, called phycobilisome (PBS) that is attached through linker proteins to the photosystems I and II. They are hydrophilic and, together with carotenoids, their main role is to widen the absorption spectrum of photosynthetic machinery, by funnelling more photons (i.e., more energy) towards reaction centres.

Carotenoids (which absorb light between 400-550 nm) are crucial for the cell survival capability and many types exist, also according to their biochemical composition. They can assume two main roles in the cells: they can work as accessory light-harvesting pigments, as explained above, or can serve as important anti-oxidant molecules, so protecting photosynthetic machinery from oxidation stress and damage (Pagels et al., 2020).

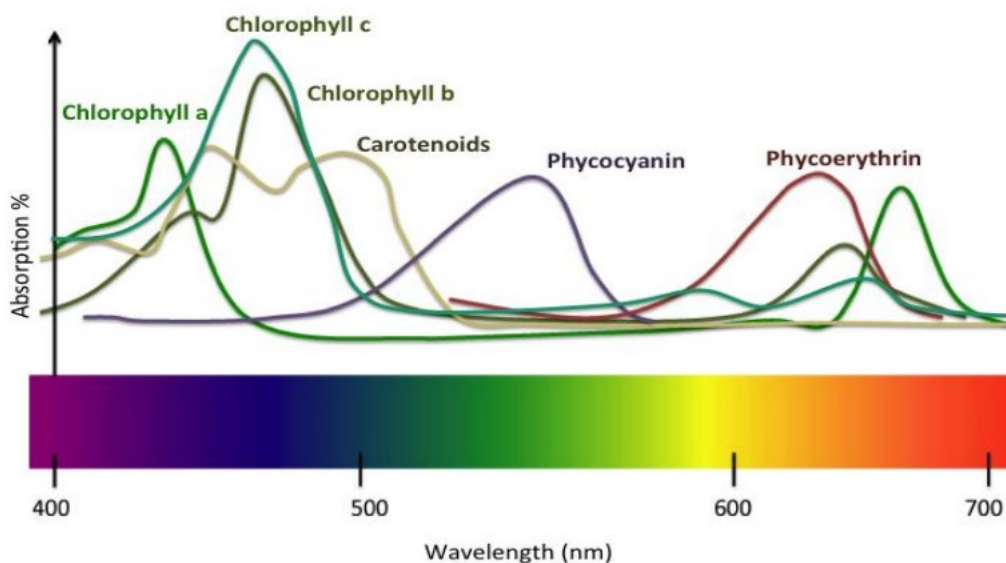
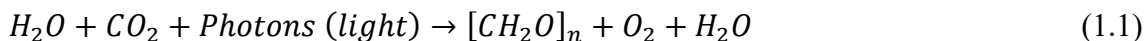


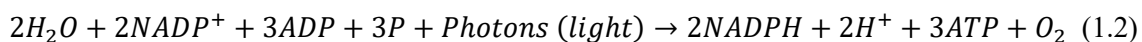
Figure 1.2: Light absorption spectra for different photosynthetic pigments (Yarish & Kim, 2012).

1.2.2 Photosynthesis: light phase and dark phase

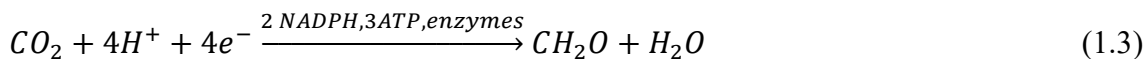
According to photoautotrophic cultivation, the main aspect to consider concerns the role of carbon and light because they are crucial to undergo photosynthesis, as described by the following equation (Chai et al., 2021):



Photosynthetic metabolism can be divided in two main phases, i.e., light-dependent and light-independent phase, respectively. During the light dependent reactions, water serves as an electron donor and oxygen is released after hydrolysis: both photochemical and redox reactions are involved (Chai et al., 2021). The main purpose of this process is to generate the biochemical reductant (NADPH) and the chemical energy (ATP) necessary to further assimilate the inorganic carbon (Vale et al., 2020). It can be briefly synthesized in the following equation, even though there are several biochemical steps involved as well as proteins and enzymes: equation (Chai et al., 2021; Vale et al., 2020):



During the light-independent reactions carbon assimilation and photorespiration occur (Vale et al., 2020). Also, in this case the main reaction is reported:



Inorganic carbon, such as atmospheric CO₂, undergoes through a series of reactions that together constitute the Calvin-Benson cycle.

1.2.3 Carbon fixation and the Calvin-Benson cycle

The Calvin-Benson cycle (CBC) refers to a series of metabolic activities which are performed to assimilate the inorganic carbon and, in turn, convert it into organic compounds, mainly glucose. CBC consists of three main phases: (1) carboxylation, (2) reduction and (3) regeneration. During the carboxylation phase, carbon dioxide is added to ribulose 1,5-bisphosphate (RuBP), by RuBisCO enzyme to synthesize a six-carbon atoms compound which is further transformed in two molecules of 3-phosphoglyceric acid (3-PGA). During the reduction phase, ATP and NADPH₂ (previously produced during the photosynthetic light phase) are consumed in a series of enzymatic reactions that end in a three-carbon sugar molecule (glyceraldehyde 3-phosphate, G3P). Finally, in the regeneration phase, a series of enzymatic activities take place to regenerate RuBP

from one remaining G3P molecule, while the other one enters the anabolic metabolism of sugars (Ighalo et al., 2022; Zhou et al., 2017).

1.3 Microalgae growth parameters

In photoautotrophic cultivation of microalgae, not only light must be addressed to boost growth performance. Other culture parameters, described below, can strongly affect the cultivation process, making important to find the optimal value to enhance biomass productivity. The cultivation system configuration is important as well and should be considered for an efficient scale-up of the process.

Growth temperature of most microalgae ranges between 15°C and 30°C (Daneshvar et al., 2022; Zhou et al., 2017) and strongly depends on the cultivated species (Ighalo et al., 2022). Even if a broad range of temperatures can be tolerated by various strains, an optimal value must be chosen to boost enzymatic activity, which reaction's rate agree with the Arrhenius Law, and to reach the highest productivity possible (Vale et al., 2020). To be more precise, temperature is linked with photosynthesis: it affects the carbon fixation activity through its influence on the affinity of ribulose for CO₂ (Khan et al., 2018). The activity of the RuBisCO (which could act as oxygenase or carboxylase according to the CO₂ and O₂ concentrations in the chloroplast) increases with rising temperature until up to a certain level and then declines (Khan et al., 2018). At the same time, temperature doesn't have to exceed a threshold for which a heat stress causes inactivation and/or denaturation of enzymes or proteins involved in photosynthesis as well as other metabolic pathways (Barbera et al., 2019; Vale et al., 2020). However, in some cases, stressful temperatures can be exploited to induce the production of valuable metabolites (Khan et al., 2018). In addition, temperature affects the chemical equilibrium among chemical species in the medium, the gas solubility and the pH (Huang et al., 2017). Thus, a cost-effective and a reliable temperature-control device is essential for the microalgae cultivation systems (Huang et al., 2017).

Another important aspect is the nutrient requirement: microalgae necessitate of macronutrients, such as nitrogen (N), phosphorus (P) and Carbon (C), as well as micronutrients such as magnesium (Mg), potassium (K), iron (Fe), cobalt (Co) and vitamins, essential for enzymatic activity and microalgae growth (Zhou et al., 2017).

Regarding the most abundant components, carbon is usually supplied in inorganic form (such as CO₂ or flue gas) when photoautotrophic cultivations are considered and it represents more or less the half of biomass composition. However, some microalgae species are able to grow in heterotrophic and mixotrophic mode: they can exploit organic carbon which usually comes from monosaccharides (such as glucose, fructose) volatile

fatty acids, glycerol and urea. This particular ability makes microalgae interesting for cultivation in which wastewaters are implied.

Instead, nitrogen ranges between the 5-10% of dry weight and represents the main component of essential biochemical compounds such as nucleic acids, proteins and pigments (both chlorophylls and phycobiliproteins). Usually, it is supplied in the form of NaNO_3 , even if some reasonable alternative could be considered with their advantages and disadvantages (some examples might be ammonia, urea or eventually N_2 for those species capable of fixing it from the atmosphere).

Moreover, phosphorous is important because it contributes to synthesize nucleic acids, membrane phospholipids and ATP. The most common form in which is supplied is orthophosphate (Markou et al., 2014).

Also in this case, the amount of nutrient required varies among the different microalgae species and strictly affects the accumulation of carbohydrates, lipids, and proteins as well (Khan et al., 2018). Specifically, microalgae and cyanobacteria can adjust their nutrient uptake and requirements according to the nutrient availability. What is interesting, is their capability to grow also when nutrients are available in limiting concentrations, regulating their biomass composition either triggering the accumulation of carbohydrates or lipids or by altering the content of other components (usually proteins and pigments). Thus, a cultivation in such conditions is still an important research field both to stimulate microalgae to produce specific compounds and to minimize as much as possible the nutrient demand (Markou et al., 2014).

Light intensity and photoperiod are crucial for photoautotrophic microorganisms, since they influence photosynthesis, cell composition and metabolic pathways (Vale et al., 2020). Light sources can be sunlight, artificial light or a combination of the two (Zhou et al., 2017). Optimal values for these parameters vary according to the culture characteristics such as microalgae species, cell density and depth of the culture (Soni et al., 2017; Vale et al., 2020; Carvalho et al., 2011). Suitable light intensity is important to allow photosynthetic machinery to process the maximum number of photons (photo-saturation) and so maximize photosynthetic efficiency (the ratio between energy supplied to microalgae by light illumination and the energy content of the microalgae biomass produced by photosynthesis), avoiding either light-limited conditions (photo-limitation) either the photo-inhibition effect where an excess of photons lead to reactive oxygen species (ROS) accumulation, photosystems damages and, finally, cell death (Ahmad et al., 2021; Carvalho et al., 2011; Di Caprio et al., 2019). Moreover, the light intensity distribution is usually non uniform and the attenuation of the radiation is dependent on the light wavelength, cell concentration, geometry of the PBR and penetration distance of light (Huang et al., 2017).

Many research activities have been performed on light quality effect since it might impact on both microalgae growth and physiology (Schulze et al., 2014). In particular, as a result of microorganisms' evolution in environmental niches, different microalgae species preferentially absorbs specific wavelengths, even if the most common are the ones associated with red and blue light (Schulze et al., 2014). Specifically, the main absorption peak of these microorganisms depends on the pigment composition, for example, red light is necessary to supply enough energy for chlorophyll a or b, instead the blue one, plays a crucial role for cell metabolism and growth (Borella, Ortolan, et al., 2021). To guarantee an adequate amount of light, both in quantity and quality, is one of the major bottlenecks when PBRs design and the light source is considered. In particular, the self-shading phenomenon, the exponential decrease of light intensity as it penetrates in the culture medium and the strictly correlation between temperature and light intensity, makes the control of this process variables quite complex (Carvalho et al., 2011).

pH is another important variable to consider; the optimal values change according to the microalgae species but most of them can survive at pH in the range between 7-9 (Wang et al., 2012). The role of pH is crucial because it affects the CO₂ concentration, and so its solubility, and the concentration of carbonaceous species in the culture medium as well (Lafarga et al., 2021).

Even if not to be intended as a nutritional requirement, it is important to improve the efficiency of gas-liquid mass transfer of gaseous components (CO₂ in particular, but also O₂ whose accumulation is toxic for microalgae) as well as guarantee the homogeneous distribution of nutrients, through the use of *mixing devices* (i.e., impeller, paddlewheels, air sparging etc.). They also reduce the self-shading and guarantees that all the cells are equally exposed to the incident light, increasing photosynthetic and carbon fixation efficiency (Huang et al., 2017; Zhou et al., 2017). Additionally, mixing prevents from cell sedimentation, cell clumping and biomass adhesion to the walls of the cultivation system (Huang et al., 2017)

1.4 Microalgae industrial production systems

In general, microalgae can be cultivated with two different technologies: open systems and closed systems, namely photobioreactors (Wang et al., 2012). Both present specific features, advantages and drawbacks, but also subsets.

1.4.1 Open systems

Open systems mainly differ each other for the shape of the pond: they could be shallow big ponds, tanks or raceway ponds/circular ponds, but also for the water source (for example lagoons or lakes water) (Soni et al., 2017). Apart from more rudimental open systems (such as lagoon), generally ponds distinguish into *raceway* and *circular* (Figure 1.3). They are both equipped with a mixing system (such as paddlewheels or pivoted agitator) to ensure an adequate turbulence (Thevarajah et al., 2022). Circular open ponds have a 40-50 cm diameter and a depth of 20-30 cm (Ahmad et al., 2021).

Raceway-type ponds, instead, consist of two or four parallel channels with the same dimensions and connected by 180° curves; rotating blades are used to create fluid flow. A length/width ratio between 10-20 is useful to reduce heat losses (Thevarajah et al., 2022). The recirculation of microalgae culture along the racetrack loop is the main feature (Ahmad et al., 2021).

In general, these systems are characterized by low investment and maintenance costs, the simple construction and the ease of cleaning operations, making them to date the most used cultivation system at industrial scale (Soni et al., 2017; Wang et al., 2012). However, productivity of open ponds is lower than that of closed systems, mainly due to the high risk of contamination, the lack of process variables control, the gas escape as well as the poor light penetration (Mitra et al., 2023; Soni et al., 2017).

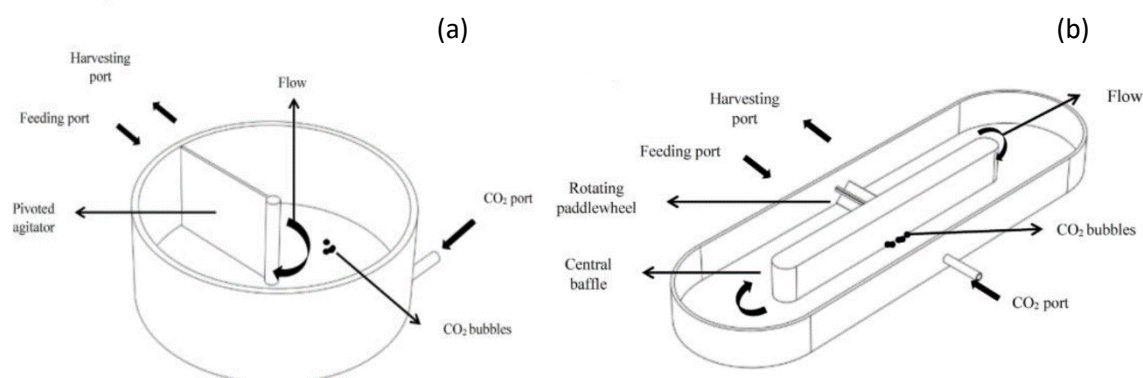


Figure 1.3: Schematic representation of (a) a circular pond and (b) a raceway pond (Ahmad et al., 2021).

1.4.2 Photobioreactors

Photobioreactors (PBRs) in general consist of a transparent vessel illuminated by natural or artificial light. Even though a plethora of designs exists, photobioreactors, unlike open ponds, guarantee a closed and controlled environment for microalgae growth: light can be supplied continuously, the risk of contamination is low and crucial growth parameters

(such as pH, temperature and gas exchange) can be carefully modulated. As a result, PBRs allow to reach a higher biomass productivity and quality as well as to establish a robust and reproducible cultivation process.

1.4.2.1 Photobioreactors illumination technologies

Photoautotrophic cultivation of microalgae is nowadays the most employed strategy of cultivation both at laboratory and at industrial scale. Anyway, the exploitation of light as the main energy source comes at a cost. Even if sunlight is the cheapest illumination source, it is very difficult to control because of seasonal and diurnal light cycle. Moreover, only wavelengths between 400-700 nm are used for photosynthesis while the others are dissipated as heat (Huang et al., 2017). Using natural illumination leads, hence, to a poor energy conversion efficiency by microalgae and this reflects on final productivity of the system. The use of artificial lighting can solve these bottlenecks. It ensures a controlled and continuously illuminated environment, avoiding photo-limiting or photo-inhibiting effects on microalgae cells (Blanken et al., 2013). Additionally, the use of artificial light sources allows to finely modulate not only the photosynthetic photon flux density (defined as the amount of photosynthetic active photons in μmol striking a surface of 1m^2 in 1s) but also the photoperiod and the light spectra, improving biomass productivity and quality (Schulze et al., 2014).

Among the different possibilities, two examples can be considered: the fluorescent lamps and LEDs. Fluorescent lamps consist of long glass tubes, containing mercury vapor at low pressure. They emit light in the visible region and have been mostly used for laboratory scale cultivation (Carvalho et al., 2011). Between the innovative possibilities, in the last years, particular attention has been reserved to light-emitting diodes (LEDs) (Chen et al., 2011; Schulze et al., 2014). They allow a Photosynthetically Active Radiation (PAR) which is greater than that of high intensity discharge and of fluorescent lamps (for LEDs it is $2\text{-}2.55 \mu\text{mol photons s}^{-1} \text{W}^{-1}$, for fluorescent tubes it is $1.25 \mu\text{mol photons s}^{-1} \text{W}^{-1}$) (Blanken et al., 2013; Borella, Ortolan, et al., 2021). Moreover, they are mercury-free, with a longer life-expectancy (up to 50,000 h against, for example, 10,000 h for fluorescent lamps). LEDs are also more suitable in an economic perspective due to light intensity supplied ($14.7\text{--}55.5 \text{ W m}^{-2}$ for LEDs and 5.9 W m^{-2} for fluorescent lamps), lower heat generation and an overall higher conversion efficiency, (Carvalho et al., 2011; Chen et al., 2011; Schulze et al., 2014). Nowadays, LEDs can be also manufactured to emit the desired monochromatic wavelengths as well as to combine different ones in order to boost cellular metabolism towards a desired compound (Borella, Ortolan, et al., 2021; Schulze et al., 2014). In general, the selection criteria of artificial light sources for cultivation of photosynthetic microorganisms include low heat dissipation and, so, high

energy conversion efficiency, good reliability, long lifetime and reasonable compactness (Carvalho et al., 2011; Ragaza et al., 2020). The use of Light Emitting Diodes (LEDs) could possibly accomplish all above mentioned features in microalgae cultivation with respect to other artificial lamps available. LEDs, in fact, allows to reduce the energy consumption of about 50% if compared with fluorescent lamps (20.16 kW-h against 40.32 kW-h respectively) (Zhu et al., 2022). Moreover, to overcome the poor light conversion efficiency which could affect photobioreactors, besides the necessity to guarantee a short light path and a high incident light intensity, not only illumination technologies have been addressed but also alternative design solutions (Blanken et al., 2013; Chen et al., 2011).

1.4.2.2 Photobioreactors design

PBRs presents in a variety of forms and design, each one with a specific feature engineered: the most common are tubular, vertical, horizontal and flat-panel type PBRs (Shankar et al., 2022; Soni et al., 2017). With respect to open ponds systems, generally photobioreactors are more compact and so the land use is more efficient (Shankar et al., 2022). Anyway, PBRs allow a better control of process variables with respect to open ponds, increasing biomass productivity. Also, the risk of contamination is drastically reduced as well as water and CO₂ losses due to evaporation and degassing phenomena. On the other hand, the costs for the initial investment and for the biomass production are significative (Soni et al., 2017). Photobioreactors could be classified according to their design:

Vertical-column PBR is the most suitable design for large scale production and the main advantages are the low cost, the facility of operation and the compact design (Soni et al., 2017). The main feature is a gas sparger system linked at the bottom of the tube which allows to convert the gaseous inlet stream into tiny bubbles that represent the driving force for the mixing, mass transfer of CO₂ and O₂ removal (Ahmad et al., 2021). In particular, these reactors can be classified as bubble columns or airlift photobioreactors (Ahmad et al., 2021); a schematic representation is reported in *Figure 1.4*.

In general, Vertical-column PBR can reach a final biomass concentration and a specific growth rate comparable with tubular photobioreactors (Soni et al., 2017).

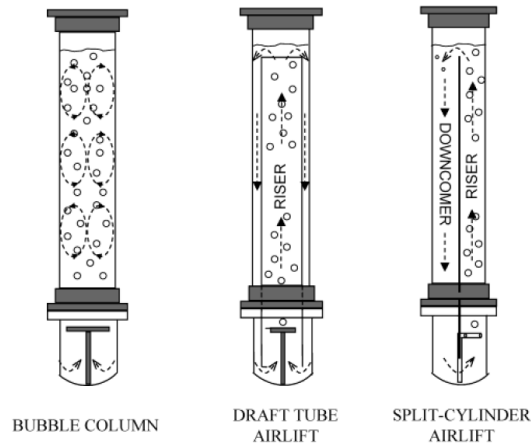


Figure 1.4: Schematic representation of bubble column and airlift PBR (Ahmad et al., 2021).

Flat plate PBRs, are reactors with a cuboidal shape where panels are made of a transparent material, usually plexiglass or polycarbonate (Figure 1.5). They are characterised by a high surface to volume ratio allowing to reach higher cell density than other PBRs. Mixing is ensured by air bubbling or by the mechanical rotation of a motor through the perforated tube (Sirohi et al., 2022). High photosynthetic efficiency is achieved, and it is possible to overcome self-shading issues by using LED as light source (Ahmad et al., 2021; Soni et al., 2017). Self-shading limitation can also be overcome by using *Internally Illuminated PBRs*. They have the same structure of conventional PBRs but with the specific feature that illumination comes from inside the reactor itself. It is resalable applying optics fiber, increasing the average irradiance and the depth to which light reaches (Wang et al., 2012). An important advantage is the vast illumination area, determined by the optical fibers rather than the PBR surface and it is possible to minimize contamination with heat sterilization under pressure (Soni et al., 2017; Wang et al., 2012). Nevertheless, the capital costs, the cleanability, and the loss of light energy in transmission in optical fibers strongly limit their effective construction (Wang et al., 2012).

Tubular PBR is one of the most appropriate and feasible configurations for outdoor mass cultivation because it has a relatively large available surface area for illumination (Huang et al., 2017). It consists of transparent tubes of high-grade plastic or glass, the orientation is different, such as vertical, conical, inclined or horizontal/serpentine to capture the maximum sunlight (*Figure 1.6*) (Shankar et al., 2022; Sirohi et al., 2022). The aeration

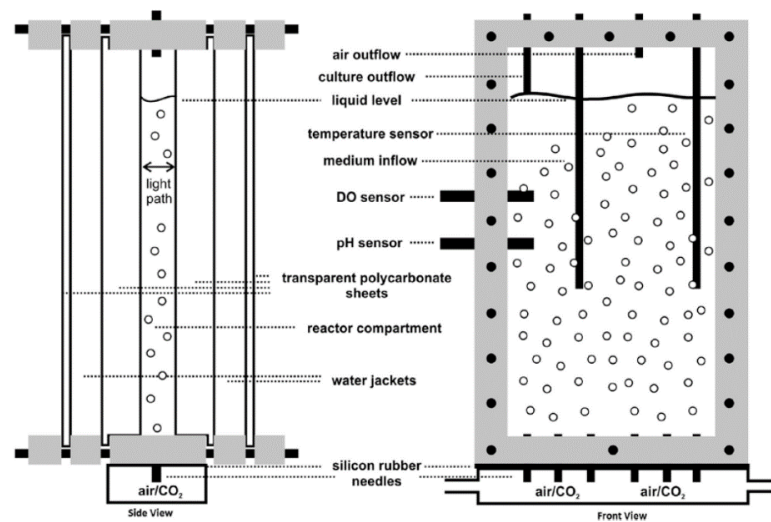


Figure 1.5: Schematic representation of a flat plate PBR (Ahmad et al., 2021).

and the mixing of the culture are provided by airlift systems or by air pump (Soni et al., 2017). In addition to the tube where biomass grows, there is a degasser unit which is used to remove the gas and the pump system which provides circulation and mixing of the microalgae culture (Ahmad et al., 2021). Light is captured more efficiently so photosynthesis rate is high as the CO₂ dissolution if compared with conventional open ponds. However, they are expensive because of the construction and operation costs (Thevarajah et al., 2022). Additional drawbacks are the difficulty on control the temperature during the operation and the mass transfer during the scale-up. These PBRs are strongly affected by fouling also, due to microalgae adhesion to transparent surfaces (Soni et al., 2017).

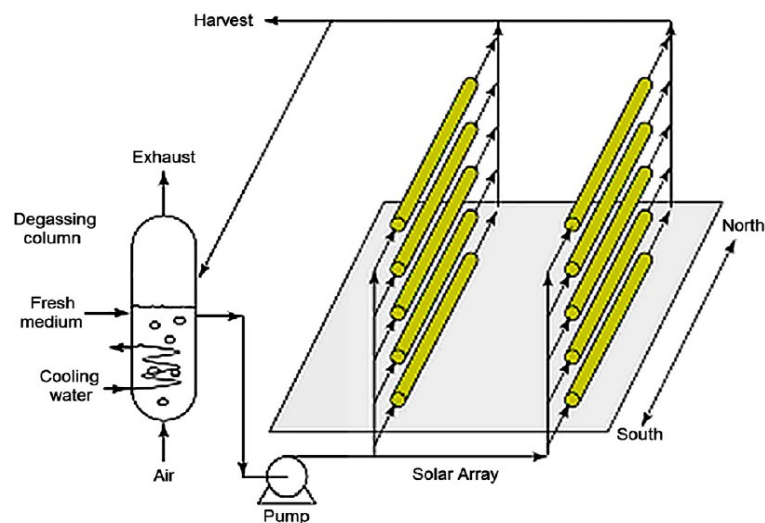


Figure 1.6: Schematic diagram of a tubular PBR (Wang et al., 2012).

1.4.3 Hybrid systems

It can be possible to conjugate advantages of both open and closed system into an innovative hybrid system for microalgae cultivation.

For instance, open ponds can be equipped with artificial lamps or covered to reduce contamination risks and evaporative losses. Similarly, PBRs can be designed to reduce overall cultivation costs by simplifying the geometry and the operation, as it is with floating PBRs (Soni et al., 2017).

Floating PBRs usually consist of plastic bags floating on marine or freshwater. They are interesting because of both the use of low-cost materials and the zero-energy consumption for mixing (wave driven) and bubbling, making this technology interesting for future high-scale and low cost microalgae cultivation (Soni et al., 2017). Anyway, this system is characterized by an inadequate mixing as well as frequent “culture crashing” (Wang et al., 2012). Photolimitation occurs due to the distortion of the bags by gravity and the lifespan of the bags is short because of frequent cleaning procedures required and leakage issues (Huang et al., 2017).

Despite this wide range of possibilities, majority of the system recently optimized and engineered are still limited to laboratory scale exploitation, since many challenges have to be faced. Among the others, it is important to consider the optimization and the strictly control of process variables to guarantee an increase of process profitability (Barbera et al., 2019; Lafarga et al., 2021). Open systems and raceway ponds are, to date, the most widespread configuration in industrial microalgae cultivation due to techno-economic advantages explained (Fernandes et al., 2015).

1.5 Cultivation modes

Microalgae cultivation can be performed in different modes. Most common are batch, semi-continuous and continuous mode. In this paragraph the main features of each one is briefly described.

In a *batch* cultivation all the requirements for microalgae growth are provided at the beginning of the run, without any feed or culture withdrawn streams present (Vale et al., 2020). During the growth, microorganisms go through different growth stages, drawing a specific growth curve characterised by four main phases: lag, exponential, stationary and death phase (Figure 1.7) (Lee et al., 2013). During the lag phase, generally, there is no biomass growth mainly due to cells acclimation to light and nutrient conditions imposed. When cells start to actively duplicate with a constant rate, they enter the exponential growth phase following an exponential trend. The following equation can be used to describe cells growth as long as they are dividing exponentially:

$$\frac{dC_x}{dt} = \mu C_x \quad (1.4)$$

where t is the time [h], C_x is the biomass concentration [g L^{-1}] and μ is the specific growth rate [h^{-1}], that represents the average growth rate of all cells present in the culture (but not necessarily the maximum specific growth rate of the individual cells).

After all nutrients have been consumed and/or toxic by-products have been released, the curve comes at a plateau (stationary phase) representing an equilibrium between microalgae division and death. If culture is prolonged over the stationary phase, cells death becomes prevalent and a decrease in culture density is observed (Lee et al., 2013; Stanbury et al., 2017).

So, batch culture works discontinuously since the medium and the microorganism's inoculum are injected in a single dose and the harvesting takes place when cell density achieves its maximum value. Despite being the most common method used in microalgae and cyanobacteria cultivation, due to ease of operation and maintenance as well as economic feasibility, the productivity can be low and final biomass specifics can vary from a batch run to another as well as within the same run (Fernandes et al., 2015; Pastore et al., 2022). Moreover, cells require a longer lead time to be matured after the harvesting is done and the operational costs are high when the process starts up (Peter et al., 2022). Among the others, another important drawback is that substrates are depleted and product accumulates, causing a growth cease due to a lack of limiting substrate or growth-inhibiting products accumulation (Fernandes et al., 2015).

Such disadvantages can be overcome in a continuous system, since fresh culture medium and the culture broth (including cells and metabolites) are continuously added and removed respectively (Fernandes et al., 2015). An example of the biomass trend is reported in *Figure 1.7*. The material balance of a bioreactor working at steady state can be considered:

$$V \cdot \frac{dC_X}{dt} = \mu C_X \cdot V - F_{out} \cdot C_{X,out} \quad (1.5)$$

where V is the working volume [L], C_X is the biomass concentration [g L^{-1}], μ is the specific growth rate [h^{-1}] and F is the volumetric flowrate [L h^{-1}] (in all cases subscript “out” refers to the outlet condition). Assuming a constant volume Equation 1.5 becomes:

$$\frac{dC_X}{dt} = \left(\mu - \frac{F_{out}}{V} \right) \cdot C_{X,out} \quad (1.6)$$

Moreover, regulating the dilution rate (defined as the reciprocal of residence time, $D = F_{out}/V$) it is possible to control the biomass growth rate (Borella, Sforza, et al., 2021; B. D. Fernandes et al., 2015). It is important that the dilution rate is lower than the maximum specific growth rate in order to avoid the washout condition, for which cells are withdrawn by the reactor before to have time to duplicate (Stanbury et al., 2017). Additionally, the culture’s volume is kept constant and a steady-state condition is attained (Fernandes et al., 2015). Steady state is a particular state of the system, it is self-regulatory and it is achieved when biomass concentration does not change during the time (Lee et al., 2013). To be set, steady state requires that about four total volume changes of the system take place (“transient state”) (Lee et al., 2013). The possibility to keep the process variables constant, including biomass and substrate concentration, is important to optimize the operating conditions (Borella et al., 2021). The productivity is 2.3-5 times higher than that achieved in batch mode (Borella et al., 2021) and it is possible to achieve higher cell densities allowing to reduce harvesting costs. Moreover, smaller equipment requires a lower space utilization, the process is almost automatic, there is a significant reduction of time necessary for cleaning and sterilization operations and of investment and operational costs (Fernandes et al., 2015). Steady-state operations allow to achieve a robust control of major parameters (such as CO_2 supply, light intensity, fresh medium flowrate) and the downtime for the harvesting process is not so long (Peter et al., 2022). Additionally, residence time manipulation allows accumulation of a specific compound of interest (Trentin et al., 2021). Thus, this cultivation mode seems to be the most suitable for large-scale applications where it is crucial to guarantee reliability, efficiency and

constant product quality, as in the case of photosynthetic microorganisms' cultivation (Fernandes et al., 2015, Pastore et al., 2022).

Semi-continuous mode represents a compromise between the modes described above: fresh medium is replaced only once the desired growth phase is reached and the harvesting operation is completely done (Pastore et al., 2022; Peter et al., 2022). Since the dilution has the same duration of the cell cycle, the inoculum and the specific growth rate are kept constant (Reichert et al., n.d.). So, it is possible to minimize the time for cleaning and filling, other to ensure a more stable productivity once the culture is adapted to external conditions (Pastore et al., 2022). The productivity depends on the frequency of harvesting, which, on a mean value, can be approximated to the residence time (Pastore et al., 2022).

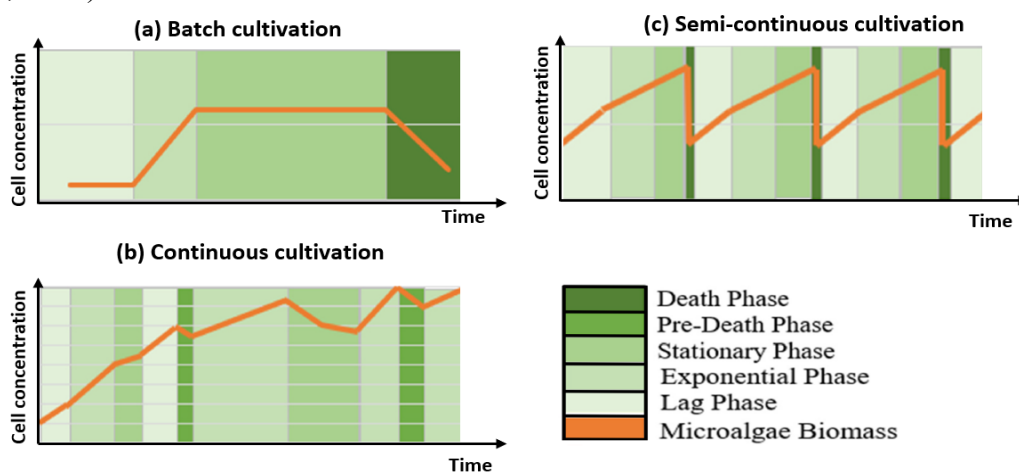


Figure 1.7: Comparison of microalgae growth pattern with biomass trend in the case of a batch cultivation (a), continuous cultivation (b) and semi-continuous cultivation (c). Image adapted from (Peter et al., 2022).

1.6 Alkalophilic cyanobacteria and BICCAPS

In the following paragraphs, the main features regarding cyanobacteria cultivation are described, focusing on one of the most relevant bottlenecks: improving cultivation economics by reducing as much as possible the carbon dioxide supply for carbon fixation. Thanks to the metabolic activity of certain microalgae and cyanobacteria species to uptake alternative inorganic carbon forms, research efforts have been focused to integrate such abilities into the cultivation process, in order to reduce CO₂ dependence. Bicarbonate-based Integrated Carbon Capture and Algae Production System (BICCAPS) is then presented as suitable alternative for all of those species that are able to exploit alternative carbonaceous forms.

1.6.1 CO₂ supplying issues

Inorganic carbon supply assumes a crucial role in microalgae photoautotrophic cultivation which accounts for 20,000-ton year⁻¹ of biomass produced at global scale (Abreu et al., 2022). In particular, CO₂ is the main carbon source for substantially all photosynthetic and carbon fixing microorganisms around the world, due to its abundance and ability to solubilize into water. Although the pivotal role of CO₂ supply, its exploitation and management better represent an issue which microalgae producers have to cope with. The first aspect to consider is the necessity to ensure the correct amount of carbon dioxide to avoid inhibition of photosynthesis or microalgae growth, but at the same time it has to be enough to sustain the metabolic reactions (Zhou et al., 2017). The maximum photosynthetic efficiency is usually obtained when carbon dioxide concentration is in the range of 1-5% by volume (Di Caprio et al., 2019; Huang et al., 2017). CO₂ must be supplied into the culture by direct injection for both open and closed systems. This is because CO₂ diffusion from the atmosphere to the culture suspension is limited by its low partial pressure in pure air (≈ 0.04 kPa) (Huang et al., 2017), low solubility in water (1.5 g/L at 25°C and 1atm) (Markou et al., 2014) and low mass transfer rate, which result in a faster CO₂ escape than its utilization by microalgae (Kim et al., 2019). The optimal CO₂ level for growth and its tolerance level vary among different microalgal strains (Ighalo et al., 2022). In fact, in some applications, CO₂ is also exploited to buffer fluctuations of pH towards alkaline values due to microalgae growth (Lafarga et al., 2021). However, an excessive CO₂ sparging and consequent medium acidification can lead to culture crash or lower accumulation of interesting products (Mehar et al., 2019). Moreover, a series of preliminary expensive operations, such as purification, transportation and storage of CO₂ are required to allow its utilization, heavily impacting on the overall operating expenses (Kim et al., 2019; Zhu et al., 2021). The cost of carbon dioxide for microalgae production ranges from 1.47-7.33 \$ kg⁻¹. However, by estimating a carbon utilization efficiency (CUE, expressed as the ratio between the mass of carbon fixed in microalgae and the carbon fed) of 1.0-5.0 % and by considering ash free dried biomass composed for 50% of carbon, the cost can raise up to 40 \$ Kg⁻¹ (Zhu et al., 2022). These costs further increase if it is considered that energy-requiring devices for its utilization are needed (Kim et al., 2017; Zhu et al., 2022). It results that, for example, the microalgae biomass production in an open raceway pond could account until 50% of overall costs derived from the use of CO₂ (Kim et al., 2019; Magwell et al., 2023b).

1.6.2 BICCAPS and alternative inorganic carbon source

A suitable alternative to CO₂ exploitation is represented by an emerging approach: BICCAPS (Bicarbonate-based Integrated Carbon Capture and Algae Production System).

According to BICCAPS, the common CO₂ supply for carbon fixation is replaced by sodium bicarbonate contained in the medium fed (Zhu et al., 2022). It is possible to underline the main advantages and drawbacks concerning BICCAPS technology. Of course, the use of bicarbonate as sole carbon source represents a relevant economic advantage when compared with CO₂ insufflation (see par. §1.6.1): managing with solid substrates allows to reduce transportation costs among the others (purchase, supply, storage etc.). Moreover, the unnecessary for bubbling systems allows to simplify the PBRs geometry and easily scale-up the production. However, there are also important drawbacks to take into account. For example, a precise and intelligent technology to provide an on-time control is needed. Moreover, without an adequate buffer system, culture pH tends to increase towards alkaline values. This represents a relevant issue when considering that only few species are able to survive in such conditions. Moreover, high pH values induce the precipitation of salt nutrients such as Ca⁺ and Mg²⁺ and enhance the carbonaceous species equilibrium to be shifted in the CO₃²⁻ (as explained in paragraph §1.6.3.2) that cannot be up-taken by microalgae for carbon fixation. According to all these aspects, alkaliphilic cyanobacteria and microalgae, such as *Arthrospira* spp., *Dunaliella* spp. or *Eubalotheca* spp., seem to be good candidates for BICCAPS feasibility. All these microorganisms share the ability to grow in a broad range of alkaline pH (8-12) due to the efficient bicarbonate ion uptake for carbon fixation. Being *Arthrospira* spp. one of the main cultivated cyanobacteria species around the world, BICCAPS can be implemented and optimized to further reduce cultivation costs (Zhu et al., 2022).

1.6.2.1 Sodium bicarbonate as carbon source

To overcome the high costs due to CO₂ sparging, some other suitable alternative can be considered. For instance, flue gases could be used, even if some issues have to be considered: the utilization efficiency is quite low, usually the gases have to be transported to algae ponds at high pressure (requiring additional energy and costs) and some components, such as SO_x and NO_x, can exhibit an inhibiting effect on microalgae growth (Kim et al., 2019). Another possibility might be the exploitation of wastewaters containing large amount of P and N, but also in this case, the presence of toxic compounds (such as heavy metals, drugs and disinfectant by-products) could definitely compromise the biological activity of cultivated microorganisms (Zhou et al., 2017).

In the last years, researchers have proposed the use of bicarbonate (NaHCO₃) as alternative carbon source in microalgae cultivation.

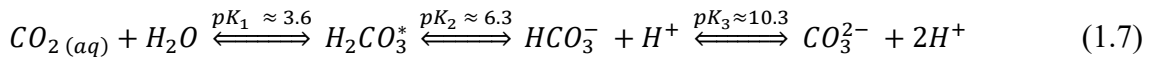
Bicarbonate shows a high-water solubility (9.21% w/w at 25 °C) leading to a higher CUE with respect to CO₂. Moreover, being a solid component, bicarbonate feeding does not require additional costs for its transportation in a compressed form (Kim et al., 2019). In

BICCAPS, bicarbonate allows to absorb (by generating an alkaline medium) and to store CO₂, playing the role of a carrier (Zhu et al., 2022). This allows to increase the CUE and so to reduce the production costs in microalgae cultivation systems. By assuming a CUE between 50-90% and a price of NaHCO₃ equal to 200 \$t⁻¹, the cost to produce algal biomass is around 0.778-1.40 \$ kg⁻¹, significantly lower than the one previously reported for CO₂ (Zhu et al., 2022).

CUE could be further improved increasing the carbon dioxide mass transfer coefficient or increasing the pH of the culture, but this point will be better explained in the next paragraph. Additionally, the use of sodium bicarbonate can lead to an increase of the culture alkalinity: it can be useful to enhance the production of specific products from the microalgae but also to prevent contaminations by predator or other photosynthetic microorganisms which are inhibited by pH >8 (Zhu et al., 2022).

1.6.2.2 The pH drives the chemical equilibrium reactions

Among all the process variables, pH plays a crucial role in microalgae growth performances (Fernández et al., 2021). Simultaneously, pH must be carefully considered when choosing bicarbonate as major carbon source. In fact, when either CO₂ or bicarbonate are supplied in the liquid microalgae suspension, they dissolve forming a weak acid-base buffer system (Markou et al., 2014). The equilibrium established is described by the following equations:



The relative amount of the dissolved inorganic species is driven by the pH of the solution as represented in *Figure 1.8* (Markou et al., 2014). Decreasing the pH value (pH < 6.5) the CO₂ is the predominant species, in fact, more H₂CO₃* is gradually formed: when pH is equal to pK₂ the concentration of H₂CO₃* is equal to HCO₃⁻ and at lower values H₂CO₃* becomes predominant (Markou et al., 2014). On the contrary, at higher pH values, (pH > 10) CO₃²⁻ concentration increases: its amount is the same of HCO₃⁻ when pH is equal to pK₃ and it starts to be predominant at pH higher than pK₃ (Markou et al., 2014).

So, in microalgae cultivation it is fundamental to set the correct pH value to guarantee a sufficient concentration of the carbon species that can be up-taken by the specific species considered (Mehar et al., 2019).

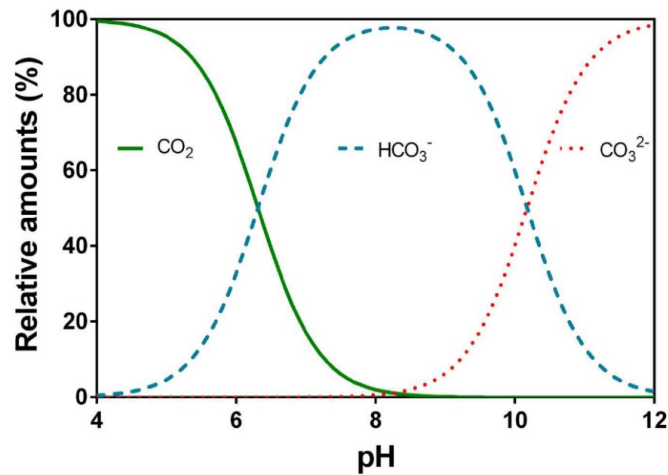


Figure 1.8: Relative speciation (%) of carbon dioxide (CO_2), bicarbonate (HCO_3^-) and carbonate (CO_3^{2-}) in water as a function of pH. The example given is at $20^\circ C$ and electrical conductivity of $250 \mu S cm^{-1}$ (Pedersen et al., 2013).

Additionally, pH affects the CO_2 mass transfer rate that is described by the following equation (Markou et al., 2014):

$$M_{CO_2} = k_L \alpha (CO_2^* - CO_2) \quad (1.8)$$

where M_{CO_2} is the mass transfer rate [$mol m^{-3}$], k_L [$m s^{-1}$] is the mass transfer coefficient between gas-liquid phase, α is the specific area available for the transfer, CO_2^* [$mol m^{-3}$] and CO_2 [$mol m^{-3}$] are the carbon dioxide concentration at equilibrium (in water) and dissolved in the liquid, respectively (Markou et al., 2014).

To improve the mass transfer rate between the gas-liquid phase, it is required to increase the pH of the culture (Zhu et al., 2022) or to increase k_L (or α) (Van Den Hende et al., 2012). According to Equation 1.8 with a fixed mass transfer coefficient, CO_2 can be either outgassed or absorbed according to the difference between dissolved concentration and the equilibrium one (Kim et al., 2019). At higher pH values ($pH \approx 10$) the reaction between carbon dioxide and hydroxide ion is faster than the hydration of CO_2 to H_2CO_3 (Markou et al., 2014; Van Den Hende et al., 2012); instead, when pH is lower than 8, hydration becomes the preferential pathway (Van Den Hende et al., 2012). Specifically, when there is a high alkalinity condition carbon dioxide can be efficiently captured and

stored as a high concentration of bicarbonate-carbonate pool, so enough carbon quantity is ensured for microalgae carbon fixation (Zhu et al., 2022).

All these considerations are important also when sodium bicarbonate is involved as inorganic carbon source since it enters the circuit of the chemical equilibrium reactions described by *Equation 1.2* and because, as anticipated in the previous paragraph, it is a carrier for the carbon dioxide.

Moreover, a deeper correlation between bicarbonate and pH of the culture exists. The pH^* (pH value at which dissolved CO_2 is in equilibrium with the one that is in the air) impacts on the effect that bicarbonate has on the CUE (Zhu et al., 2022).

When the bicarbonate concentration is low, its buffering ability decreases causing an increase of pH; when the pH becomes higher than the pH^* the concentration of dissolved CO_2 is less than the one at equilibrium condition, so it is easily absorbed from the air and it replenishes the consumed carbon (Zhu et al., 2022). Instead, when pH is lower than pH^* , CO_2 outgassing occurs (Zhu et al., 2022). For this reason, it seems to be preferential to work at lower bicarbonate concentration to enhance CUE, that can be improved also with high pH or $K_{L\alpha}$ (Zhu et al., 2022).

The previous discussion highlights the difficulties on choosing the correct pH range and carbon source for the microalgae cultivation, since many aspects are interconnected and they influence each-other.

1.6.3 Alkaliphilic cyanobacteria and Arthrospira spp.

Cyanobacteria (Cyanophyta), also known as blue-green microalgae, are photosynthetic prokaryotic microorganisms (Lafarga et al., 2020). They show a heterogeneous morphology spanning from unicellular to filamentous and colonial (Lau et al., 2015). Cyanobacteria are diverse in physiology: in fact, they can easily colonize different aquatic and terrestrial habitats, ranging from marine and freshwater to brackish and alkaline environments, as well as terrestrial and desertic substrates (Lau et al., 2015). Moreover, only light (usually sunlight), carbon dioxide, water and minimal amounts of nutrients are required for growth, besides a metabolic activity that can rapidly switch from one mode to another (Lau et al., 2015). Cyanobacteria are interesting for a series of advantages and suitable possible applications, which are also common to microalgae as previously described in paragraph 1.1 (Lau et al., 2015).

They are mainly cultivated autotrophically, so, carbon is one of the most important nutrients (Zhu et al., 2021). Even though the majority of cyanobacteria exploit mainly CO_2 for carbon fixation, there are few species that adapted to survive in alkaline environments (such as soda lakes), where the concentration of carbon salts is extremely high. Alkaliphilic microorganisms evolved not only the ability to grow at pH greater than

8-9 but also to exploit both carbon salts (such as bicarbonate) and CO_2 when possible. In the first case, in fact, carbon salts could derive from the reaction of CO_2 with water forming a weak acid-base buffer system (Markou et al., 2014) but also from specific salts such as sodium bicarbonate. Between the two forms, CO_2 is usually preferred because it can be up taken inside the cytosol through membrane diffusion (passive mechanism) and through membrane transport mechanism (active mechanism). When pH is higher, HCO_3^- becomes prevalent and is up taken through active membrane transportation (Markou et al., 2014).

HCO_3^- is then converted into CO_2 through the Carbon Concentrating Mechanism (CCM). The main actor in CCM is represented by a specific class of enzymes, called carbonic anhydrases (CAHs): thanks to their catalytic activity HCO_3^- ions are converted into CO_2 . In this way, carbon dioxide concentration around RuBisCO (Ribulose-1,5-Bisphosphate Carboxylase Oxygenase) is elevated if compared to its concentration in the extracellular surrounding environment (Wang et al., 2012). So, RuBisCO allows carbon dioxide to enter the Calvin-Benson cycle, and to perform the metabolic activity as described in paragraph §1.2 (Chi et al., 2011). Anyway, during this process the pH of the cytosol increases towards alkaline values: when the bicarbonate ion is converted into CO_2 , in fact, there is an excess of OH^- inside the microalgae cells. Internal pH needs to be buffered to

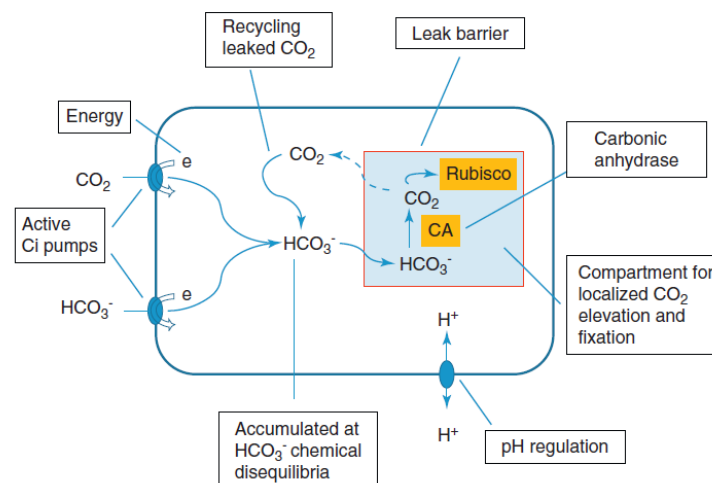


Figure 1.9: Schematic representation of the inorganic carbon uptake process and the pH regulation (Chi et al., 2011).

neutral (about 7) values to allow metabolic pathways to undergo efficiently. So, H^+ is up taken inside the cells, while OH^- ions are released. This process, finally, leads to an increase of the pH in the extracellular environment (Chi et al., 2011). A schematic representation of the metabolism is reported in *Figure 1.9*.

1.6.3.1 *Arthrospira* spp. relevance in microalgae market

There are lot of species able to survive at alkaline pH and to exploit bicarbonate ions for metabolic purposes. Among the others, *Spirulina* is one of the most common microorganisms exploited for different industrial purposes around the world. Actually, “*Spirulina*” is the commercial name of a specific genus of cyanobacteria: *Arthrospira* spp., with *Arthrospira maxima* and *Arthrospira platensis* being the most industrially relevant species (Lafarga et al., 2020; Vazquez & Sanchez, 2022).

Because of the wide range of applications, *Arthrospira* spp. is one of the most cultivated microalgae genera at industrial level and the annual production reaches 15,000 tons/year (Abreu et al., 2022), with an expected market of \$968.6 million by 2028 with a CAGR (Compound Annual Growth Rate) of 13.2% between 2021 and 2028 (R. Fernandes et al., 2023). According to the JRC (*Joint Research Centre*), in Europe, there are currently 213 companies cultivating *Spirulina* based in 15 countries, with France as the production leader (134 companies), followed by Italy (20) and Spain (18) (Vazquez & Sanchez, 2022).

The industrial importance of *Arthrospira* spp. is mainly linked to its biomass composition. In particular, it shows a high content of proteins which can reach up to 70% on a dry weight basis when it is not limited by nitrogen (Lafarga et al., 2021). From a qualitative point of view, these proteins are “complete” because all the essential amino acids are present (leucine, valine and isoleucine show the highest percentages), so no additional treatment are required to improve their content promoting the simplicity of the production system (Ragaza et al., 2020). Instead, the lipid content achieves the 6-8% of the dry weight, and the total composition is a balance between saturated and polyunsaturated fatty acids (the essential are linoleic acid and γ -linoleic acid) (Ragaza et al., 2020). Additionally, *Arthrospira* spp. shows a certain content of carbohydrates (13.6% in particular galactose and glucose), vitamins and minerals (around the 6% and examples are calcium, iron, magnesium, potassium and others) (Lafarga et al., 2020; Ragaza et al., 2020). Also, some other valuable compounds must be taken into account: apart from chlorophylls and carotenoids (such as astaxanthin, zeaxanthin and β -carotene), phycobiliproteins (PBPs) (phycocyanin, allophycocyanin and phycoerythrin) represent a valuable and requested product in the market (Costa et al., 2019; R. Fernandes et al., 2023). In particular, phycocyanin (PC), a brilliant blue water-soluble pigment protein, that can constitute up to 15-20% of the total biomass dry weight (Thevarajah et al., 2022). *Arthrospira* spp. is, nowadays, the primary source of PBPs that, according to its level of purity (25 €/mg when partially purified to 200€/mg for high purity levels), can be used for different applications in cosmetics, pharmaceuticals, textiles or food (R. Fernandes et al., 2023). To remark the economic relevance of these proteins some data can be

considered: PC market is expected to reach \$279.6 million by 2030, at a CAGR of 28.1% from 2023 to 2030, with a market volume projected towards up to 3,500 tons at a CAGR of 33.8% from 2023 to 2030 (<https://www.meticulousresearch.com/product/phycoocyanin-market-5126>).

Also, Chlorophyll, a green-coloured pigment, could be exploited as a colourant and as an ingredient with potential health benefits (Costa et al., 2019). An example of the detailed biochemical composition of *Arthrospira* spp. is reported in *Table 1.1*.

As a consequence of the abovementioned components, Spirulina biomass applications are mainly the food and feed market sector. In fact, it is also considered a “superfood” and it has been certified as Safe (GRAS) by the Food and Drug Administration (FDA); it is also commercialised without the need to comply with Regulation (EU) 2015/2283 known as novel food regulation (only microalgae known as GRAS can be sold for human consumption while the others have to be registered as novel food): consumers consider product containing Spirulina as safe, nutritious and sustainable (R. Fernandes et al., 2023; Magwell et al., 2023a).

Despite the use for human food, *Arthrospira* spp. can be involved in other different applications. For example, because of its rich nutrient profile, animal feed can be produced, with a particular attention for aquaculture products (Thevarajah et al., 2022). It can be considered for biofuels production (biodiesel and bioethanol) as well: this is mainly due to the widespread and easy cultivation of such microorganisms (Costa et al., 2019).

Other relevant applications regard the co-accumulation of bioplastics, due to the significant amount of polyhydroxyalkanoates (PHAs), which are naturally produced by prokaryotic organisms as storage material in response to stress conditions, and polyhydroxy-butyrate (PHB), which have a function in carbon energy storage as well (Costa et al., 2019; Thevarajah et al., 2022). Also, the adhibition as an organic source for biofertilizer can be considered (Thevarajah et al., 2022).

Table 1.1: Example of *Arthrospira* spp. biomass composition. Image adapted from (Ragaza et al., 2020).

Components	Contents (mg per 100 g)	Components	Contents (mg per 100 g)	Amino acids	Contents	
					(mg per 100 g dry matter)*	(g per 100 g of protein)**
Vitamins				Essential amino acids		
Vitamin B1 (Thiamine)	0.5–5.8	Minerals		Isoleucine	3500	5.71–6.70
Vitamin B2 (Riboflavin)	4.5–4.65	Calcium (Ca)	468–922.28	Leucine	5380–5400	9.26–10.17
Vitamin B3 (Niacin)	14.9–15.35	Potassium (K)	1660–2085.28	Lysine	2900–2960	4.42–4.99
Vitamin B6 (Pyridoxine)	0.94–0.96	Magnesium (Mg)	119.02–319	Methionine	1170–1400	2.05–2.50
Vitamin B12 (Analogue)	0.16–0.175	Sodium (Na)	1540.46	Phenylalanine	2750–2800	4.42–5.30
Folic acid	9.92	Phosphorous (P)	961–2191.71	Threonine	2860–3200	4.65–6.20
Inositol	60.45	Copper (Cu)	0.47–1.215	Tryptophan	900–1090	0.08–1.93
Vitamin E	9.86	Iron (Fe)	87.4–273.2	Valine	3940–4000	6.08–7.10
Vitamin K	1.09–1.096	Iron (Fe)	87.4–273.2	Non-essential amino acids		
Pantothenate	0.108	Manganese (Mn)	5.66	Alanine	470–4590	8.51–9.50
Biotin	0.008	Zinc (Zn)	1.45–3.62	Arginine	430–4310	7.09–8.0
		Chromium (Cr)	0.325	Aspartic acid	610–5990	9.86–11.80
		Selenium (Se)	0.04–25.5	Cystine	60–590	0.57–1.11
		Boron (B)	2.88	Glutamic acid	910–9130	9.47–13.69
		Molybdenum (Mo)	0.372	Glycine	320–3130	1.10–5.70
				Histidine	100–1000	2.20–10.41
Fatty acids				Proline	270–2380	3.33–4.35
		Nomenclature	Contents (%)	Serine	320–2760	4.56–5.10
Lauric acid		C 12:0	0.84–3.10	Tyrosine	300–2500	3.61–5.69
Myristic acid		C 14:0	0.2–3.60			
Palmitic acid		C 16:0	25.0–43.65			
Palmitoleic acid ($\omega - 6$)		C 16:1	0.52–3.8			
Stearic acid		C 18:0	0.95–8.82			
Oleic acid ($\omega - 6$)		C 18:1	0.33–16.6			
Linoleic acid ($\omega - 6$)		C 18:2	9.43–17.19			
Gamma linolenic acid ($\omega - 6$)		C 18:3	3.64–40.1			
Behenic acid		C 22:0	Trace – 20.01			

1.7 Purpose of the thesis

One of the major limits for high-scale cultivation of microalgae is represented by the high production costs, that result from many concomitant causes. Hence, to address or mitigate this issue it is necessary to optimize cultivation conditions, aiming to production costs decrease. The substitution of expensive substrates such as CO₂ can be a further improvement toward a sustainable cultivation in an economic perspective. The exploitation of alternative inorganic forms of carbon (BICCAPS) and alkaliphilic microalgae species could make this strategy feasible, without any productivity loss.

In this work the commercially relevant cyanobacterium *Arthrospira maxima* (SAG 49.88) is cultivated in LED photobioreactors at 400 $\mu\text{mol m}^{-2}\text{s}^{-1}$ worked in continuous. The aim is both to experimentally evaluate the pH influence on bicarbonate uptake and microalgae growth and to perform a numerical model to describe the phenomenon. This two-stage work leads to a comprehensive description of *A. maxima* growth in function of bicarbonate as a substrate in continuous PBRs, that represents to date the first attempt. Moreover, the optimization of bicarbonate concentration and air sparging in Zarrouk medium has been addressed. First, the possibility to control on-demand culture pH by mean of hydrochloric acid is evaluated. Then, different concentrations (6, 15, 30 and 45 g L⁻¹) of sodium bicarbonate were supplied in order to evaluate biomass productivity and carbonaceous species consumption. The best condition is then tested for different bubbling composition (Air, Air+CO₂ and No Bubbling) inside the PBR. Finally,

experimental results are validated through a mathematical description of bicarbonate uptake, starting from the references available and using MATLAB® software to implement the material balances equations. By mean of a fitting procedure the kinetic parameters, half-saturation constant related to the limiting substrate (HCO_3^-) and the biomass maximum specific growth rate, are determined.

Chapter 2

Materials and methods

In the following chapter, materials and methods applied to perform the experimental section are described. The experiments were carried out in LED photobioreactors working in continuous, with *Arthrospira maxima* SAG 49.88 (SAG Goettingen) as model species. The aim of the experimental part was either to test the effect of different sodium bicarbonate (NaHCO_3) concentrations in the medium and the effect of different gas composition supplied on the growth performances of *A. maxima*. Moreover, the possibility to use an on-demand pH controller (by mean of hydrochloric acid) to keep constant this variable during cultivation has been investigated.

2.1 *Arthrospira maxima* cultivation conditions

The filamentous cyanobacteria *Arthrospira maxima* SAG 49.88 (SAG Goettingen) (Figure 2.1) was cultivated at different sodium bicarbonate concentrations and at different CO_2 -Air composition, in order to find the optimal condition in terms of biomass productivity. All the experiments were performed in a thermostatic incubator set at 30 ± 1.0 °C, according to the optimal temperature growth range for this species (29-35 °C) (Soni et al., 2017). Artificial light was provided by a LED which emits white light in the PAR range. The incident light intensity, I_0 , was set equal to $400 \mu\text{mol m}^{-2} \text{s}^{-1}$, that is the



Figure 2.1: Image of *Arthrospira maxima* view at optical microscope.

value demonstrated to be able to guarantee the best results in terms of productivity (Borella, Ortolan, et al., 2021) and was daily measured with a photo radiometer Delta OHM (HD 2102.01). pH was also recorded daily using a pH meter (Hanna - HI 9124). A modified Zarrouk medium was used throughout the experimental assessment, by doubling all micro- and macro-nutrients concentrations (2X), in order to avoid nutrient starvation and by varying NaHCO_3 concentration (Zarrouk, 1966). Medium was autoclaved at 121°C for 20 minutes prior to its utilization. The detailed medium composition is reported in *Table 2.1*.

Table 2.1: Zarrouk medium composition (2X).

Component	Concentration (2X) [mg L⁻¹]
$\text{Na}_2\text{Mg EDTA}$	2.00
Ferric Ammonium Citrate	12.00
Citric Acid · 1H ₂ O	12.00
$\text{CaCl}_2 \cdot 2\text{H}_2\text{O}$	72.00
$\text{MgSO}_4 \cdot 7\text{H}_2\text{O}$	150.00
K_2HPO_4	61.00
H_3BO_4	5.72
$\text{MnCl}_2 \cdot 4\text{H}_2\text{O}$	3.60
$\text{ZnSO}_4 \cdot 7\text{H}_2\text{O}$	0.444
$\text{CuSO}_4 \cdot 5\text{H}_2\text{O}$	0.158
$\text{CoCl}_2 \cdot 6\text{H}_2\text{O}$	0.10
$\text{Na}_2\text{MoO}_4 \cdot 2\text{H}_2\text{O}$	0.782
$\text{FeSO}_4 \cdot 7\text{H}_2\text{O}$	20.00
NaNO_3	$3.00 \cdot 10^3$
NaCl	$10.00 \cdot 10^3$
NaHCO_3	$30.00 \cdot 10^3$

2.1.1 Laboratory-scale photobioreactors

All the experiments were carried out in continuous photobioreactors, whose features are reported in *Figure 2.2*.

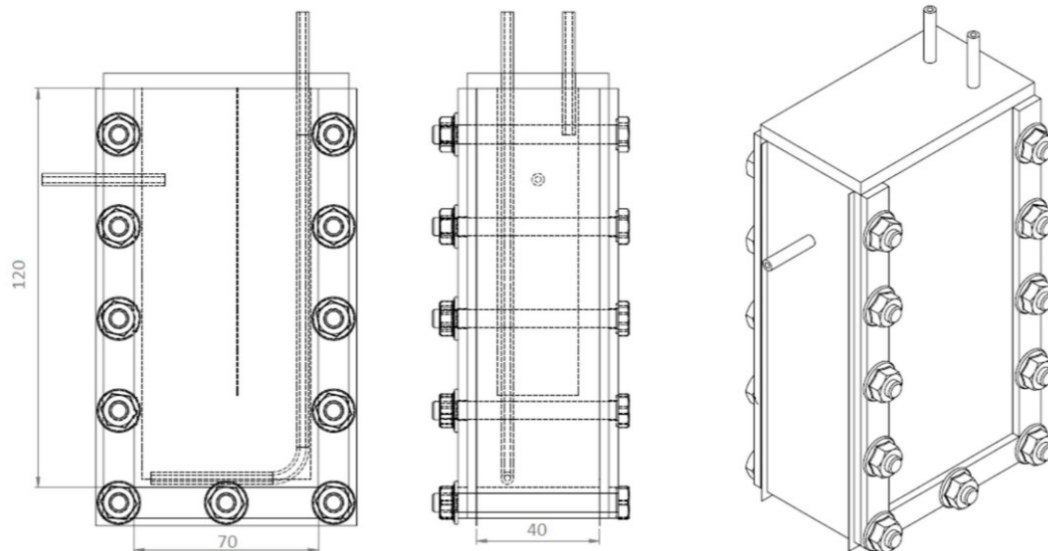


Figure 2.2: Schematic representation of laboratory-scale PBR used to perform the experimental assessment (Barbera et al., 2019).

PBRs employed simulate a flat panel PBR configuration, with a working volume of 0.350 L and 4.1 cm, 7 cm and 12 of depth, width and height, respectively. Mixing was ensured thanks to a magnetic stirring bar and an air stream bubbling, in order to simulate a continuous stirred tank reactor (CSTR). To ensure a continuous inlet stream of fresh medium a peristaltic pump (Watson-Marlow 205s) was used with Marprene® tubes with known diameter. The inlet stream was collocated on the opposite direction respect to the outlet one and no direct contact with the culture medium has to be ensured to avoid obstructions due to the biomass growth. The culture volume was kept constant thanks to an overflow tube which cause the culture discharge when it exceeds the maximum PBR's working volume. The residence time (τ), defined as the ratio between the PBR volume (V [ml]) and the volumetric flowrate (\dot{V} [ml day⁻¹]) (Eq. 2.1), was fixed at 1.2 days, previously demonstrated to be the optimal value for biomass productivity in *A. maxima* (Colta & al., 2023):

$$\tau = \frac{V}{\dot{V}} \quad (2.1)$$

Moreover, the following figure represents a scheme of the experimental arrangement involved:

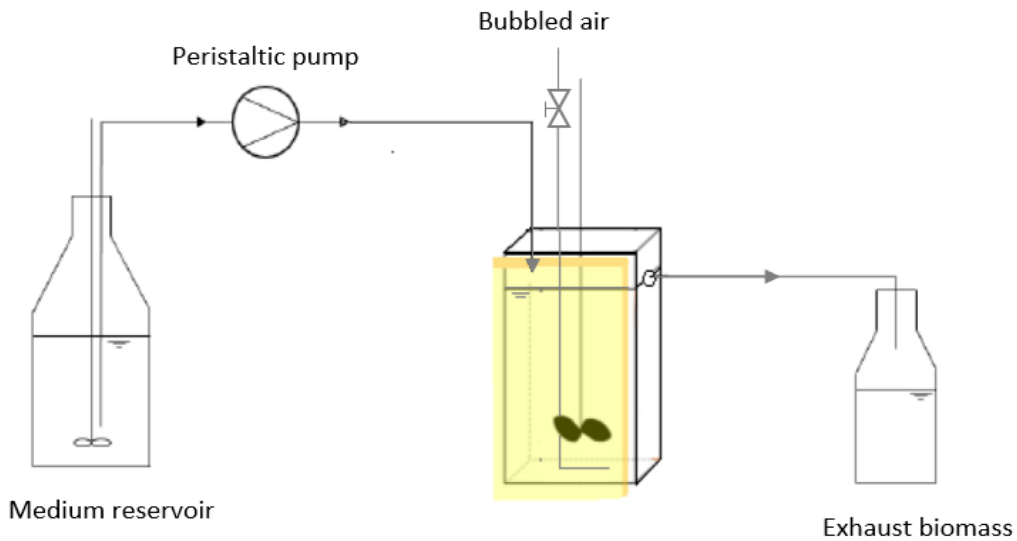


Figure 2.3: Experimental arrangement for the continuous cultivation mode experiments. Image adapted from (Colta et al., 2023).

2.1.2 Experimental conditions

Experiments were carried out first by gradually increasing NaHCO_3 concentration in the medium (6 g L^{-1} , 15 g L^{-1} , 30 g L^{-1} , 45 g L^{-1}) (R1). Once bicarbonate influence on productivity was addressed, the most productive culture was subsequently tested for air composition by insufflating atmospheric air, air+ CO_2 (5% v/v) and without any air stream (R2). Tested experimental conditions are summarized in *Table 2.2*.

Experiments using pH controller to investigate the effect of such variable on NaHCO_3 uptake were also addressed (*Table 2.3*). pH was buffered to 8.5 and 9.5 by the mean of a pH controller probe inside the PBR connected to a HCl (1M) reservoir through a peristaltic pump. HCl was injected on-demand inside the PBR whenever pH shifted from the imposed setpoint. To avoid acidification, only atmospheric air was insufflated as gaseous stream. A schematic representation of the set-up is reported in *Figure 2.4*.

Table 2.2: Summary of the different experimental conditions for R1 (bicarbonate concentration) and R2 (air stream composition) variables investigated.

	R1	R2
I₀ [$\mu\text{mol m}^{-2} \text{s}^{-1}$]	400	400
T [$^{\circ}\text{C}$]	30	30
τ [days]	1.2	1.2
Medium	Zarrouk (2X) with 30 g L ⁻¹ NaHCO ₃	Zarrouk (2X): <ul style="list-style-type: none"> • 6 g L⁻¹ NaHCO₃ • 15 g L⁻¹ NaHCO₃ • 30 g L⁻¹ NaHCO₃ • 45 g L⁻¹ NaHCO₃
Air	<ul style="list-style-type: none"> • Air + 5% v/v CO₂ • Compressed air • Without any air stream 	Air + 5% v/v CO ₂

Table 2.3: Experimental conditions for the reactor working with the pH-controller.

pH_{setpoint}	<ul style="list-style-type: none"> • 8.5 • 9.5
I₀ [$\mu\text{mol m}^{-2} \text{s}^{-1}$]	400
T [$^{\circ}\text{C}$]	30
τ [days]	1.2
Medium	Zarrouk (2X) with 30 g L ⁻¹ NaHCO ₃
Air	Compressed air

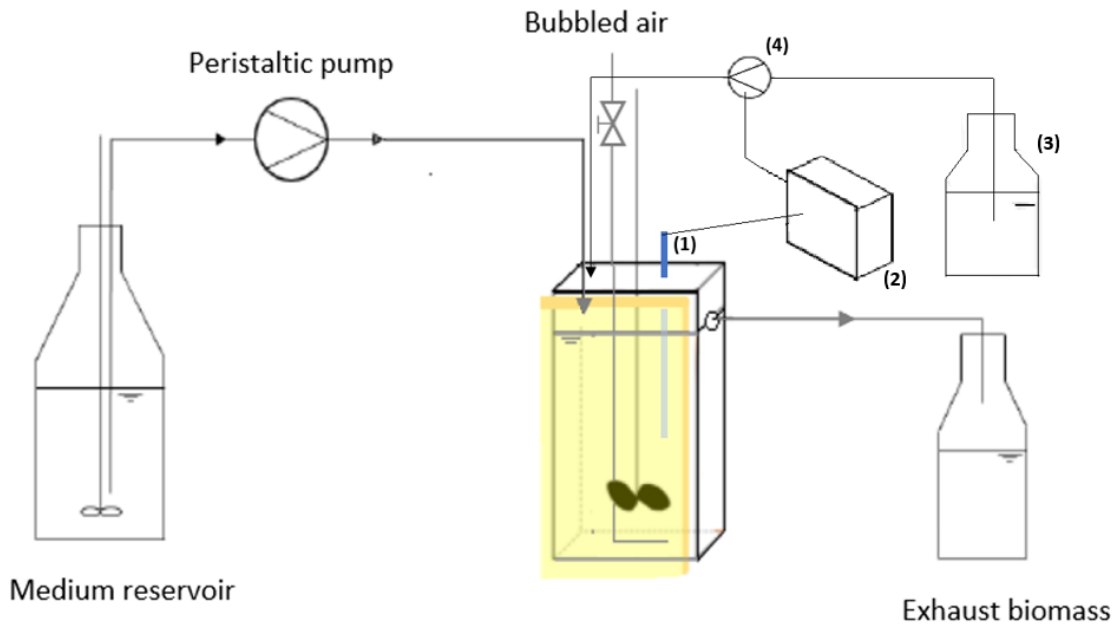


Figure 2.4: Schematic representation of the experimental set-up for the experiments performed with the pH-controller system, which main components are: (1) pH sensor; (2) the transmitter; (3) HCl 1.0 M reservoir and (4) a peristaltic pump. Image adapted from (Colta et al., 2023).

2.2 Analytic measurements

In the following paragraphs, analytical measurements used throughout the experimental campaign are described in detail. For each condition tested, once the steady-state was reached, a sample was collected every day from the PBRs for at least four days and the following analysis have been performed.

2.2.1 Optical density

Optical density (OD) measurements were performed using a double beam spectrophotometer (Shimadzu – UV 1900) and plastic cuvettes with 1 cm light path (l). The instrument was set at 750 nm to avoid interference by pigment's absorption. Absorbance was measured daily by using 2 mL of microalgae sample and loading the blank reference that consisted of Zarrouk medium (Table 2.1). Biomass concentration was then calculated according to the Lambert-Beer Law:

$$A = \varepsilon C l \quad (2.2)$$

where A is the absorbance measured, l [cm] is the optical path length, C [g L⁻¹] is the biomass concentration and ε [mol⁻¹ L cm⁻¹] is the molar absorption coefficient, (constant

for a specific substance once it has been determined and it is valid for the range of absorbance in the range between 0.1-1).

2.2.2 Dry cell weight

Biomass concentration was evaluated also by mean of dry weight (DW) measurements. First, a nitrocellulose filter (from Whatman®) with pores diameter of 0.45 µm was heated in an oven at 110°C for at least 10 min, to remove the humidity, and then weighted with a precision balance (Atilon Acculab Sartorius Group®). A know volume of sample was filtered under vacuum with a steel funnel connected with a vacuum flask and washed two times with deionized water to remove residual salts onto the filter. The filter was heated again at 110°C for at least two hours. After this time, the filter was weighted and the dry biomass concentration was calculated using the following equation:

$$C_X = \frac{m_{tot} - m_{filter}}{V_{sample}} \quad (2.2)$$

where C_X is the dried biomass concentration [g L^{-1}], m_{tot} is the gross weight of the dried filter [g], m_{filter} is the mass of the filter (after been heated the first time) [g] and V_{sample} is the volume of the sample considered [L].

2.2.3 Analytical measurements

Analytical measurements are performed to evaluate the consumption of bicarbonate during the cultivation together with the characterization of biomass for pigments phycobiliproteins and external polysaccharides (EPS).

2.2.3.1 Titration

Titration was performed in order to determine the concentration of carbonate (CO_3^{2-}) and bicarbonate (HCO_3^-) ions in both culture inside the PBR and medium. Acid-base titration consists of a reaction between an acid and a base where the equivalence point is described by a chromatic pH indicator. In this case indicators are represented by phenolphthalein (IUPAC: 3,3-Bis(4-hydroxyphenyl)-2-benzofuran-1(3H)-one) and bromocresol green (IUPAC:3,3-Bis(3,5-dibromo-4-hydroxy-2-methylphenyl)-2,1λ6-benzoxathiole-1,1(3H)-dione). The first is transparent in an acid mixture and purple in the case of a basic one; instead, the second is blue in a basic solution and yellow in an acid one. Both were prepared in 0.1% methanol solution.

For carbonaceous species inside the reactor a known volume of sample was filtered as described in 2.2.2 and the filtrate was collected. For medium titration a known volume of sample was collected from fresh autoclaved medium. Filtered solutions to be titrated were then collected into a beaker and constantly stirred to ensure homogeneous mixing. Firstly, three drops of phenolphthalein were added and the colour becomes purple, then HCl (0.5 M) is added drop by drop (20 μL) until the sample becomes colourless: this is the equivalence point where the number of moles of acid are equal to the number of moles of the carbonate ion. At this point three drops of bromocresol green are added, in this case the initial colour is blue, then hydrochloric acid is added (with the same procedure described before) until the mixture becomes yellow. At the equivalence point the number of moles of HCl are equal to the sum of bicarbonate and carbonate ions' number of moles. In the following figure an example of the sample colour changes during the measurement is reported:

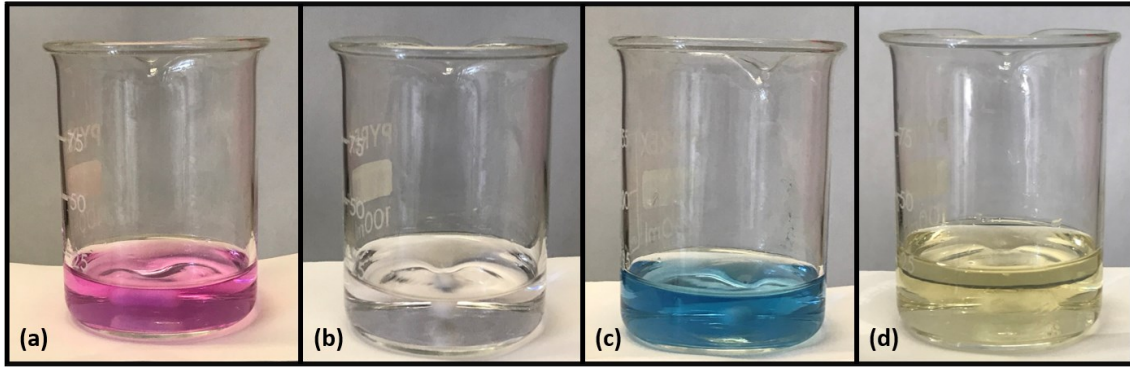


Figure 2.5: Example of the sample colour changes when titration procedure is applied: (a) represents the sample after that three drops of phenolphthalein are added and (b) represents the corresponding equivalent point after that HCl (0.5M) is added; (c) represents the colour assumed by the sample after the addition of three drops of bromocresol green and (d) is the corresponding colour at the equivalence point.

The calculations are based on molarity definition and can be described as follow:

$$n_i = n_{\text{HCl}} = \frac{M_{\text{HCl}}}{V_{\text{HCl}}} \quad (2.3)$$

where n_i is the number of moles with $i = (\text{HCO}_3^-, \text{CO}_3^{2-})$, M_{HCl} is the HCl molarity [mol L^{-1}] and V_{HCl} is the volume of acid required to achieve the equivalence point [L]. Knowing the number of moles of the carbonaceous species and the volume of the sample, it is possible to determine its concentration in terms of carbon quantity:

$$C_i = M_i \times MW_C = \frac{n_i}{V_{\text{sample}}} \times MW_C \quad (2.4)$$

with C_i the concentration of the carbonaceous species [g L^{-1}], M_i is the molar concentration of i [mol L^{-1}] and MW_C is carbon molecular weight [g mol^{-1}].

Notice that the number of moles of bicarbonate are determined as difference between the number of moles of the total carbonaceous species and the ones of carbonate.

2.2.3.2 Chlorophyll *a* and carotenoids extraction and quantification

Chlorophyll *a* and carotenoids extraction was performed according to Moran & Porath, (1980). This protocol relies on *N-N dimethylformamide* (DMF), a non-polar solvent that causes cell wall and membrane disruption as well as the solubilization and stabilization of chlorophylls and carotenoids. 1 mL of culture sample is centrifuged for 10 minutes at 13,500 rpm. Then the supernatant was discarded and cell's pellet was resuspended in DMF (1 mL) and then stored in the dark at -18°C for at least 24 hours. Samples were centrifuged as described above prior to analysis, to avoid absorption interference by cell debris. The supernatant was then collected and absorption spectra in the range 350 – 750 nm were acquired using DMF as blank. Quantification of pigments was performed by means of the following equations according to Wellburn (1994):

$$Chl_a = (Abs_{664} - Abs_{750}) \times D \times \xi_{Chl_a} \times \frac{V_{DMF}}{V_s} \quad (2.5)$$

$$Car = [(Abs_{461} - Abs_{750}) - (Abs_{664} - Abs_{750}) \times 0.04] \times D \times \xi_{car} \times \frac{V_{DMF}}{V_s} \quad (2.6)$$

where Chl_a and Car represent the amount of chlorophyll *a* and carotenoids, respectively [$\mu\text{g mL}^{-1}$], Abs_{664} , Abs_{750} and Abs_{461} are the absorbance at the wavelength of 664 nm, 750 nm and 461 nm respectively, D is the dilution coefficient, ξ_{Chl_a} and ξ_{car} are the absorption coefficients of chlorophylls *a* (11.92) and carotenoids (4), respectively, V_{DMF} and V_s are the volume [mL] of DMF and of the sample respectively and referred to the initial acquisition. All the calculations are normalized to 750 nm (Abs_{750}) to avoid possible interferences caused by debris and residuals absorption.

2.2.3.3 Phycobiliproteins extraction and quantification

Phycobiliproteins extraction was performed with a freeze and thaw cycles protocol, generally used for filamentous cyanobacteria according to Kannaujiya et al. (2017). In particular, cells are subjected to a fast thermic shock that causes cell disruption and PBPs releasing in the buffer. A sample of 5 mL was collected and centrifuged at 7500 rpm for 8 minutes. The supernatant was discarded and 1mL of CaCl_2 buffer (10 g L^{-1}) was used to resuspend biomass. Samples were freezed in the dark at -18°C and after at least 24 hours were defrost at +4°C and this freeze-thaw cycle was repeated three times. Once the cycles were completed, the samples were centrifuged at 6000 rpm for 5 minutes. In

Figure 2.6 is reported an example of the characteristic blue colour assumed by the sample, after that phycobiliproteins have been extracted.

Quantification of the different PBPs was firstly performed through the acquisition of absorption spectra in the range 350-750 nm and by determining concentration using the following equations (Bennett & Bogorad, 1973):

$$C_{PC} = \frac{(Abs_{615} - Abs_{750}) - 0.474 \cdot (Abs_{652} - Abs_{750})}{5.34} \quad (2.7)$$

$$C_{APC} = \frac{(Abs_{652} - Abs_{750}) - 0.208 \cdot (Abs_{652} - Abs_{750})}{5.09} \quad (2.8)$$

$$C_{PE} = \frac{(Abs_{652} - Abs_{750}) - \xi_{PC} \cdot C_{PC} - \xi_{APC} \cdot C_{APC}}{\xi_{PE}} \quad (2.9)$$

where C_i is the PBP concentration [$\mu\text{g mL}^{-1}$] and ξ_i is the molar absorption coefficient [$\text{mL mg}^{-1} \text{cm}^{-1}$] at the wavelength of 562nm with $i=(\text{PC}, \text{APC}, \text{PE})$, Abs_j is the absorbance at different wavelengths $j = (615 \text{ nm}; 652 \text{ nm}; 750 \text{ nm})$. The following values are assumed $\xi_{PC} = 2.41$, $\xi_{APC} = 0.849$ and $\xi_{PE} = 9.62$.

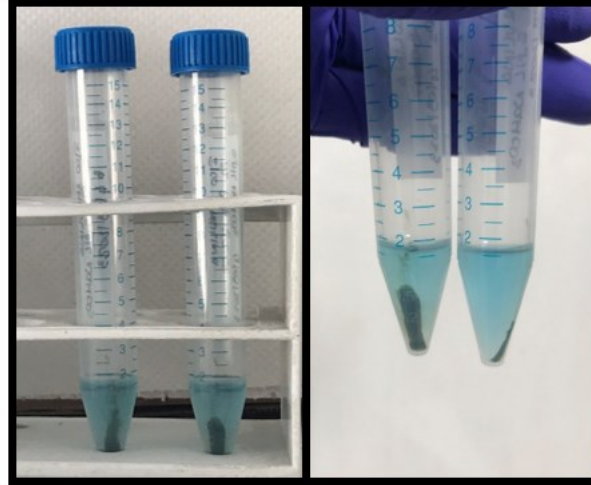


Figure 2.6: Example of the colour assumed by the sample after the extraction of phycobiliproteins.

2.2.3.4 Exopolysaccharides quantification

The exopolysaccharides are quantified following the procedure described by (Dubois et al., 1951), for which two reactants are required: sulfuric acid (H_2SO_4) (95-98%) and phenol (5% v/v). H_2SO_4 is able to hydrolyse polysaccharides to monosaccharides when used at high temperatures. Then, monosaccharides are dehydrogenated generating 5-hydroxymethylfurfural. This last component reacts with phenol to produce a component

that absorbs at a wavelength of 488 nm. To perform the analysis, 2 ml of sample were collected and centrifuged for 25min at 1,800 rpm. Then 200 μ L of the supernatant were added to the reactant (200 μ L of phenol and 1 mL of sulfuric acid). The sample was incubated at room temperature for at least 10 minutes and then incubated at 30 °C for 15 minutes. The resulting solution was analysed at the spectrophotometer using a wavelength equal to 488 nm. The reference sample to measure the absorbance is given by 200 μ L of deionized water to which the reactant is added. To calculate the EPS concentration was used a calibration curve (Fig. 2.7 and Eq. 2.10):

$$C_{C_6H_{12}O_6} = 125.87 \cdot abs + 9.9662 \quad (2.10)$$

with $C_{C_6H_{12}O_6}$ being the concentration of galactose [μ g mL⁻¹] and *abs* the recorded absorbance. If the absorbance measured exceeded the maximum value reported in the calibration curve, a dilution of the sample with deionized water.

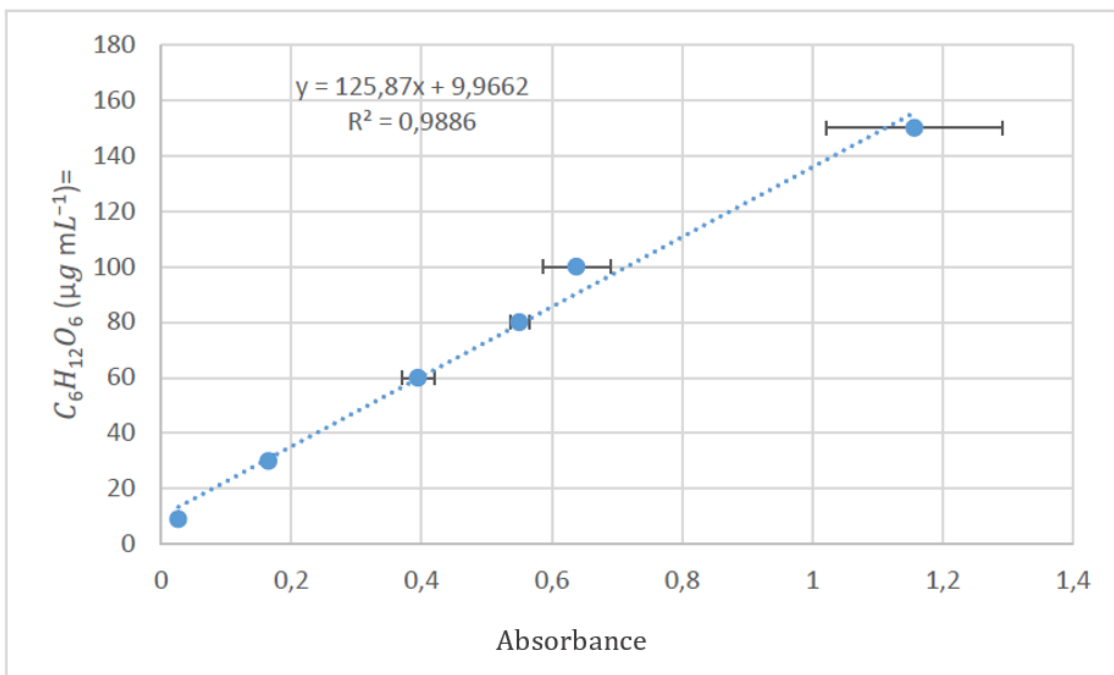


Figure 2.7: Calibration curve for the EPS quantification.

2.3 Statistical analysis

Statistical analysis has been required to check if there are statistically significant differences between the mean values of the experimental data collected.

It has been assumed that the variances among test conditions are equal: this is the basic assumption to ensure the applicability of ANOVA and Tukey's tests. The reference p.value has been fixed at 0.05 for both tests. The statistical analysis has been performed with MINITAB® Statistical Software. Regarding the results presentation and discussion, when data present the same letter it means they are not statistically different.

Chapter 3

Kinetic model description

The importance to present a suitable model able to describe the growth of *Arthrospira maxima*, when it is cultivated in continuous mode, is mainly due to a lack of information available in literature. Specifically, in this chapter, the equations considered for the numerical description of the biomass bicarbonate uptake are presented.

Equations are based on material balances written according to the most important chemical species involved in the process. Each equation contains specific terms necessary to consider the kinetic and equilibrium phenomena involved, through the corresponding constants. The most important issue regards the consideration of a proper kinetic term which accounts for the substrate consumption (bicarbonate ion in this case) and on the determination of suitable values for its parameters. The model, together with the experimental data collected, has been implemented in MATLAB[®], with the final aim to determine, through a fitting procedure, two important kinetic parameters: the half-saturation constant (K_{HCO_3}), which is referred to bicarbonate ion, and the biomass maximum specific growth rate (μ_{max}), according to a kinetic of biomass growth based on Monod model. It is important to underline that, the mathematical equations proposed in this work are different from other equations available in literature which are able to describe the effect of pH on bicarbonate concentration but they are unable to represent the experimental data in a suitable way, specifically when the correlation between carbon dioxide and bicarbonate is considered.

3.1 The importance of a mathematical model

The development of suitable mathematical models is crucial to support the research efforts for the interpretation and description of many experimental campaigns. They represent a link between the laboratory-scale observations, on which the large-scale is based, and the industrial scale itself, assuming an important role also for the scale-up of the process. In particular, a rigorous mathematical description allows us to better understand the influence of a specific process variable and to determine key production parameters (Barbera et al., 2019). According to this, particular attention is given to continuous cultivation systems because of the many advantages they show, as reported in

paragraph §1.5. Specifically, once the model has been established, it might be useful to describe the effect of a change of a process variable also without the necessity to perform experimental campaigns. However, at the initial phase of the development many important issues have to be faced, among the others, the complexity of the model itself which need to account for different phenomena that affect the cultivation system and that in most cases are strictly interconnected (Darvehei et al., 2018).

Regarding photosynthetic microorganisms, this represents a considerable challenge as a consequence of the higher complexity of their cell cycle and metabolism as well as the wide range of mechanisms that they can trigger to respond to environmental factors (Barbera et al., 2019). Additionally, among the others, it is important to focus on the kinetic growth modelling, since it is crucial both for the estimation and the optimisation of production parameters and for process variables control (Darvehei et al., 2018). In this work the kinetic of the biomass growth has been considered, since it represents a pivotal point for the description of *A. maxima* cultivation as a function of bicarbonate uptake. In this case, the phenomenon is described by one of the simplest and the most common used model which has been proposed by Monod, which considers the effect of the specific substrate without accounting for the inhibition caused by the substrate itself (Darvehei et al., 2018). The general equation of such kinetic is the following:

$$\mu = \mu_{max} \frac{C_s}{K_s + C_s} \quad (3.1)$$

where μ and μ_{max} are the specific and the maximum biomass specific growth rate respectively, C_s is the concentration of a specific substrate and K_s is the half-saturation constant, numerically equal to the concentration of the substrate when $\mu = \mu_{max}/2$.

According to *Figure 3.1*, in the region between A and B the concentration of the substrate is in excess and the growth velocity is equal to the maximum value; instead from A to C, when its concentration starts to decrease, the same happens for the growth rate, since limiting nutrient conditions start to arise. It is important to underline that the value assumed by K_s gives an estimation of the affinity that exists between the microorganism considered and the specific substrate. Low K_s values are representative of high affinity, i.e., the effect of substrate is not relevant on biomass growth until it reaches very low concentrations; on the contrary high K_s values demonstrate low affinity so that the growth rate can be drastically affected even at high concentration of substrate (Stanbury et al., 2017). Moreover, the kinetic parameters change according to different microalgae species (Darvehei et al., 2018)

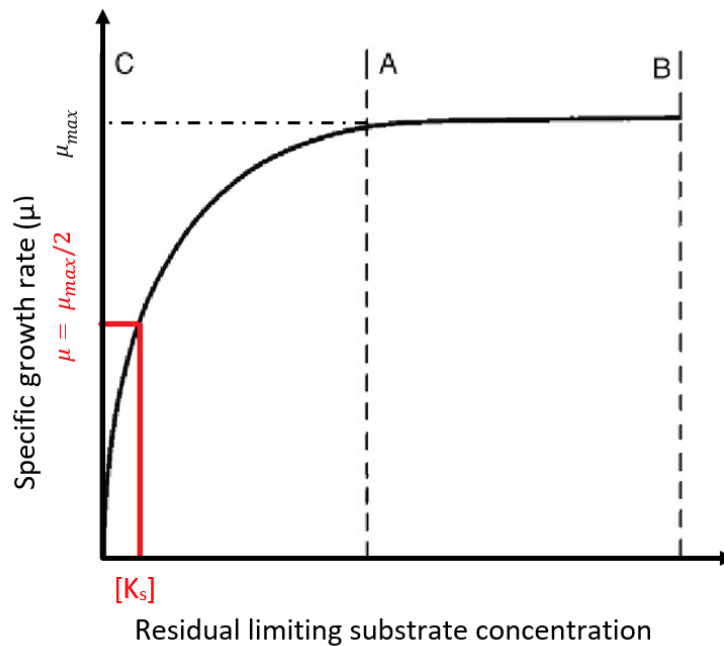


Figure 3.3: Graphical representation of the specific growth rate according to substrate concentration. Image adapted from (Stanbury et al., 2017).

3.2 Material balances

The first aim of this part of the work is to write a mathematical model able to describe the biomass growth as a function of the most important process variables. A continuous cultivation mode is adopted, according to the experimental set-up described in paragraph §2.1. It is important to remember, as anticipated in paragraph §1.3, that the selection of variables proper values could be quite complex, because of the strong interdependence that exists among them, and because they are strictly correlated with the microalgae or cyanobacteria specie considered. However, the aim of this thesis project is to investigate and to describe the effect of different sodium bicarbonate concentrations and of different insufflated air composition for *Arthrospira maxima* cultivation. To isolate the contribution of the medium or of air composition on biomass growth, the other parameters, mainly the incident light at the laboratory-scale PBR wall, the temperature and the residence time are kept constant and at fixed values which represents the optimum ones in terms of productivity. Additionally, it is fundamental to consider the chemical equilibrium correlations in which the carbonaceous species are involved and which have been described in *Equation 1.7* in subparagraph §1.6.3.2.

The model is based on material balances equations written according to a CSTR (*Continuous Stirred Tank Reactor*), whose terms mainly refer to the work of Solimeno et al., 2015 and of Pastore et al., 2022. They have been written both for the biomass and for

the most important carbonaceous species involved in the process that are strictly related to the use of sodium bicarbonate and of air (CO_2 , HCO_3^- and CO_3^{2-}). The pH of the culture has been also considered (through a material balance of H^+ and OH^-): pH description is fundamental since a buffer system is created when NaHCO_3 is added at high concentration and CO_2 is sparged inside the working volume.

The general equation that describes the material balance of a CSTR reactor, referring to concentration terms, is the following:

$$\frac{dC_i V}{dt} = C_i^{IN} \dot{q}_i^{IN} - C_i^{OUT} \dot{q}_i^{OUT} + r_i V \quad (3.2)$$

where $\frac{dC_i V}{dt}$ accounts for the mass retained inside the reactor, C_i [g m^{-3}] is the concentration of the specie i , \dot{q} [$\text{m}^3 \text{s}^{-1}$] is the volumetric flowrate, r_i is the rate of production or consumption of the specific specie i (indicated with “+” or “-” sign respectively) and V [m^3] is the reactor volume. The apex “IN” or “OUT” refers to inlet and outlet streams respectively. Since the steady-state condition is established and the reactor working volume is kept constant (so $\dot{q}_i^{IN} = \dot{q}_i^{OUT} = \dot{q}$) the previous equation can be simplified as:

$$0 = C_i^{IN} - C_i^{OUT} + r_i \tau \quad (3.3)$$

where τ [s^{-1}] is the residence time defined as $\tau = V / \dot{q}$. Additionally, since the CSTR reactor ensure a perfect mixing, process variables do not change with space so their value inside the reactor is equal to the one in the outlet stream.

The material balance equation has to be adapted to the specific specie that is considered and according to the specific phenomenon in which this is involved.

3.2.1 Biomass material balance

The biomass material balance equation results from the general equation of a CSTR according to:

$$0 = \frac{-C_X^{OUT}}{\tau} + r_X \quad (3.4)$$

Since the steady-state condition is considered, the inlet biomass term is negligible. C_X [g m^{-3}] is the biomass concentration, τ is the residence time [day^{-1}] and r_X [$\text{g m}^{-3} \text{day}^{-1}$] is the overall biomass growth rate. The latter one, in turn, accounts for a series of different contributions. Specifically:

$$r_X = R_X - R_e \quad (3.5)$$

where R_e accounts for cell maintenance and respiration. It is a function of light intensity, as maintenance requirements increases at high light intensities, as more energy is dissipated. This velocity is described by a Monod-like function (Pastore et al., 2022):

$$R_e(I) = \mu_{e,max} \frac{I_0}{I_0 + K_{I,m}} C_X^{OUT} \quad (3.6)$$

where $\mu_{e,max}$ [day^{-1}] is the maximum specific growth rate, I_0 [$\mu\text{mol photons m}^{-2} \text{s}^{-1}$] is the incident light intensity at the PBR's wall and $K_{I,m}$ [$\mu\text{mol m}^{-2} \text{s}^{-1}$] is the half-saturation constant.

Instead R_X accounts for the biomass production rate and it is a function of temperature $f(T)$, light, $f(I)$ and nutrients, mainly carbon, $f(C)$ (Borella, Ortolan, et al., 2021). So, it can be expressed as:

$$R_X = \mu_{max} \cdot f(T) \cdot f(I) \cdot f(C) \cdot C_X^{OUT} \quad (3.7)$$

where μ_{max} [day^{-1}] is the maximum specific growth rate. It is possible to better explain and report the equation of each function:

$$f(T) = \frac{(T - T_{max})(T - T_{min})^2}{T_{opt} - T_{min}[(T_{opt} - T_{min})(T - T_{opt}) - (T_{opt} - T_{max})(T_{opt} + T_{min} - 2T)]} \quad (3.8)$$

where the three parameters refer to the minimum temperature (T_{min} [$^{\circ}\text{C}$]) and the maximum temperature (T_{max} [$^{\circ}\text{C}$]), below and above which there is no growth nor respiration; instead T_{opt} [$^{\circ}\text{C}$] and T [$^{\circ}\text{C}$] represents the temperature at which the growth rate achieves its maximum value and the working temperature, respectively (Barbera et al., 2019).

The function of light accounts for its decreasing intensity according to the reactor depth (z [m]): it is described by a modified Haldane function and modelling the light extinction according to the Lambert-Beer law, which allows to consider the light absorption by microalgae and self-shading effect. It results in the following equation:

$$f(I) = \frac{1}{L} \int_0^L \frac{I(z)}{I(z) + K_I \left(\frac{I(z)}{I_{opt} - 1} \right)^2} dz \quad (3.9)$$

where L [m] is the reactor depth $K_{I,W}$ [$\mu\text{mol photons m}^{-2} \text{s}^{-1}$] and $I_{opt,W}$ [$\mu\text{mol photons m}^{-2} \text{s}^{-1}$] are two kinetic parameters (in this case, specific for white light) and a specific expression has been found for $I(z)$:

$$I(z) = I_0 \exp(-\bar{k}_a C_X^{OUT} z) \quad (3.10)$$

where \bar{k}_a [$\text{m}^2 \text{g}^{-1}$] is the average biomass absorption coefficient in the PAR range and which depends on the light source used (Borella, Ortolan, et al., 2021; Pastore et al., 2022).

Regarding the effect of the nutrients, it has been accounted with a Monod function considering HCO_3^- as the limiting substrate, according to paragraph §1.6.4 and also the Equation 3.1:

$$f(C) = \mu_{max} \frac{C_{\text{HCO}_3}}{K_{\text{HCO}_3} + C_{\text{HCO}_3}} \quad (3.11)$$

μ_{max} is the specific growth rate [day^{-1}], K_s is the half-saturation constant and C_{HCO_3} [gC m^{-3}] is the concentration of bicarbonate ion. In this model only bicarbonate is considered as limiting substrate, despite by the common model proposed in literature in which both carbon dioxide and bicarbonate are considered.

In the following table, the value of kinetic parameters already determined and used in the model have been summarized:

Table 3.1: Value of known kinetic parameters involved in the biomass material balance equation (Pastore et al., 2022).

Parameter	Value
$\mu_{e,max}$ [day^{-1}]	10.51
$K_{I,m}$ [$\mu\text{mol photons m}^{-2} \text{s}^{-1}$]	1224.0
$K_{I,w}$ [$\mu\text{mol photons m}^{-2} \text{s}^{-1}$]	207.1
$I_{opt,w}$ [$\mu\text{mol photons m}^{-2} \text{s}^{-1}$]	458.9
\bar{k}_a [$\text{m}^2 \text{g}^{-1}$]	0.0362
T_{\min} [$^{\circ}\text{C}$]	6.57
T_{\max} [$^{\circ}\text{C}$]	47.21
T_{opt} [$^{\circ}\text{C}$]	28.98

3.2.2 Carbonaceous species material balance

Besides the biomass material balance, other ones have to be written for the main carbonaceous species involved in the process. In particular, it has been considered the carbonate and bicarbonate ions which are a consequence of the use of the Zarrouk medium, for which different NaHCO_3 concentrations have been tested, and CO_2 which enters the reactor through a bubbled air stream. The general structure of the material balance can be the following one:

$$\frac{dC_i}{dt} = \frac{C_i^{IN} - C_i^{OUT}}{\tau} + r_i \quad (3.12)$$

where C_i [g m^{-3}] is the concentration and r_i is the reaction rate for each chemical species involved in the process ($i = \text{CO}_2, \text{HCO}_3, \text{CO}_3^{2-}$). What is important to notice is that, referring to the work of Solimeno et al., (2015) it is possible to introduce a specific term which accounts for both the kinetic and the equilibrium process. Three main chemical equilibrium processes (j) can be considered (according with the discussion presented in subparagraph §1.6.3.2):



according to which it is possible to define the chemical equilibrium reactions as:

$$\rho_j = k_{eq,j} (C_i - C_{i,eq}) \quad (3.16)$$

where ρ_i [$\text{g m}^{-3} \text{ day}^{-1}$] is the rate of the chemical reactions, $k_{eq,i}$ [day^{-1}] is the dissociation constant of the reaction and C_i [g m^{-3}] and $C_{i,eq}$ [g m^{-3}] are the concentration and the concentration at equilibrium of the component i , respectively. Specifically, $C_{i,eq}$ is written through the definition of chemical equilibrium constant, which is a function of temperature. As a consequence of all these considerations, it results that:

$$r_i = \sum_j \nu_{j,i} \cdot \rho_j \quad (3.17)$$

in which $\nu_{j,i}$ are specific stoichiometric coefficients with index $j=1,2,3$ (it refers to the process).

3.2.2.1 Additional terms

In case of carbon dioxide material balance, an additional term has to be considered. In fact, the transfer of gases to the atmosphere must be considered as follows:

$$\rho_{CO_2,atm} = k_{L,CO_2} (C_{CO_2}^* - C_{CO_2}) \quad (3.18)$$

where K_{L,CO_2} [day⁻¹] is the CO₂ mass transfer coefficient according to the correlation and $C_{CO_2}^*$ [gC m⁻³] and C_{CO_2} [gC m⁻³] are the concentration at equilibrium and inside the reactor respectively. In particular, the equilibrium concentration is calculated through the Henry's Law (Ji et al., 2017a):

$$C_{CO_2}^* = \frac{P_{CO_2} \rho_{H_2O}}{H_{CO_2} M_{H_2O}} \quad (3.19)$$

with H_{CO_2} [Pa] Henry's constant, P_{CO_2} [Pa] is the partial pressure of CO₂, ρ_{H_2O} [g L⁻¹] is the water density and M_{H_2O} [g mol⁻¹] is the water molecular weight. According to the unit of measure involved in the equations, it is necessary to correct Equation 3.18 introducing a product for the CO₂ molecular weight.

For the bicarbonate ion an additional term must be also considered in the corresponding material balance: it accounts for its consumption due to biomass uptake. It is given by the product of the biomass rate (r_X) and the yield (Y [gC gbiomass⁻¹]) of biomass respect to bicarbonate ion concentration considered in terms of carbon:

$$r_{cons} = - \left(\mu_{max} \cdot f(T) \cdot f(I) \cdot f(C) - \mu_{e,max} \frac{I_0}{I_0 + K_{I,m}} \right) \cdot C_X^{OUT} \cdot Y = - r_X \cdot Y \quad (3.20)$$

3.2.3 Hydrogen species material balance

The last material balances are written for the hydrogen ion and hydroxide ions, since they are also involved in the equilibrium process described in *Equation 3.12-3.14*. Moreover, they are strictly correlated with culture pH that has already been underlined as an important process variable for the considered system. The overall equation is the one reported in *Equation 3.3*. Specifically, the concentration of hydroxide ions has been calculated according to the definition of pH (Wolf-Gladrow et al., 2007):

$$C_H = 10^{-pH_{med}} \quad (3.21)$$

where C_H [gH m⁻³] is the concentration of H⁺ ions and pH_{med} is the medium pH experimentally measured. Instead, the hydroxide ions concentration C_{OH} [gH m⁻³] is

calculated from the one of hydroxide ions with the following equation (Wolf-Gladrow et al., 2007):

$$C_{OH} = \frac{10^{-14}}{C_H} \quad (3.22).$$

Regarding the rate of the process, the references are *Equations 3.15-3.16*, considering, in this case, $i = H^+, OH^-$.

The stoichiometric coefficient values involved in *Equation 3.17* are reported in Table 3.3 as well as additional parameters involved Table 3.4. Table 3.5 contains a summary of all the material balances equations.

Table 3.2: Equations for the chemical equilibrium reactions (Solimeno et al., 2015).

Process	Equation
$j=1: \rho_1$ [gC m ⁻³ day ⁻¹]	$\rho_1 = k_{eq,1} \left(C_{CO_2} - \frac{C_H \cdot C_{HCO_3}}{K_{EQ,1}} \right)$
$j=2: \rho_2$ [gC m ⁻³ day ⁻¹]	$\rho_2 = k_{eq,2} \left(C_{HCO_3} - \frac{C_H \cdot C_{CO_3}}{K_{EQ,2}} \right)$
$j=3: \rho_3$ [gH m ⁻³ day ⁻¹]	$\rho_3 = k_{eq,3} \left(1 - \frac{C_H \cdot C_{OH}}{K_{EQ,w}} \right)$

Table 3.3: Stoichiometric coefficient used to describe the different process in which each chemical specie is involved (Solimeno et al., 2015).

Component → Process ↓	$i = CO_3$	$i = HCO_3$	$i = CO_2$	$i = H$	$i = OH$
$j=1$	/	$\nu_{1,HCO_3} = 1$	$\nu_{1,CO_2} = -1$	$\nu_{1,H} = 1/12$	/
$j=2$	$\nu_{2,CO_3} = 1$	$\nu_{2,HCO_3} = -1$	/	$\nu_{2,H} = 1/12$	/
$j=3$	/	/	/	$\nu_{3,H} = 1$	$\nu_{1,OH} = 1$

Additional data, such as the residence time, the incident light intensity and the working temperature, are fixed according to experimental set-up described in Chapter 2. Moreover, the inlet concentration of the different carbonaceous ions (HCO_3^- and CO_3^{2-}) are evaluated thanks to titration performed on the medium according to the procedure

described in subparagraph 2.2.3.1. H^+ concentration have been, instead, evaluated through pH measurements, according to Equations 3.20-3.21 to account for the inlet CO_2 concentration has been approximated to the equilibrium one.

Table 3.4: Values and correlations of additional parameters involved in the material balances equations (Ji et al., 2017b; Ranganathan et al., 2017; Solimeno et al., 2015).

Chemical equilibrium constant $K_{EQ,j}$ (for process $j=1,2,3$ according to Eq. 3.12-3.14)	
$K_{EQ,1}$ [gH m ⁻³]	$10^{17.843 - \frac{3404.71}{273.15+T} - 0.032786(273.15+T)}$
$K_{EQ,2}$ [gH m ⁻³]	$10^{9.494 - \frac{2902.39}{273.15+T} - 0.02379(273.15+T)}$
$K_{EQ,3}$ [gH ² m ⁻⁶]	$10^{-\frac{4470.99}{273.15+T} + 12.0875 - 0.01706(273.15+T)}$
Dissociation constant $k_{eq,j}$ (for process $j=1,2,3$ according to Eq. 3.12-3.14)	
$k_{eq,1}$ [day ⁻¹]	10000
$k_{eq,2}$ [day ⁻¹]	1000
$k_{eq,3}$ [g m ⁻¹ day ⁻¹]	1000
Henry's Law	
H_{CO_2} [Pa]	$1.66 \cdot 10^8$
ρ_{H_2O} [g L ⁻¹]	1000
M_{H_2O} [g mol ⁻¹]	18
Mass transfer coefficient CO_2	
K_{L,CO_2} [day ⁻¹]	22.5

balances equations.

Material balances	
Biomass (X)	$0 = \frac{-C_X^{OUT}}{\tau} + r_X \cdot C_X^{OUT}$
Carbonate ion (CO₃)	$0 = \frac{(C_{CO_3}^{IN} - C_{CO_3}^{OUT})}{\tau} + k_{eq,2} * \left(C_{HCO_3} - \frac{C_H \cdot C_{CO_3}}{K_{Eq,2}} \right)$
Bicarbonate ion (HCO₃)	$0 = \frac{(C_{HCO_3}^{IN} - C_{HCO_3}^{OUT})}{\tau} - r_X \cdot Y_{HCO_3/X} + k_{eq,1} \cdot \left(C_{CO_2} - \frac{C_H \cdot C_{HCO_3}}{K_{Eq,1}} \right) - k_{eq,2} \cdot \left(C_{HCO_3} - \frac{C_H \cdot C_{CO_3}}{K_{Eq,2}} \right)$
Carbon dioxide (CO₂)	$0 = \frac{(C_{CO_2}^{IN} - C_{CO_2}^{OUT})}{\tau} + k_{L,CO_2} (C_{CO_2}^* - C_{CO_2}) - k_{eq,1} \cdot \left(C_{CO_2} - \frac{C_H \cdot C_{HCO_3}}{K_{Eq,1}} \right)$
Hydrogen ion (H)	$0 = \frac{(C_H^{IN} - C_H^{OUT})}{\tau} + \frac{1}{12} \cdot k_{eq,1} \left(C_{CO_2} - \frac{C_H \cdot C_{HCO_3}}{K_{Eq,1}} \right) + \frac{1}{12} \cdot k_{eq,2} \cdot \left(C_{HCO_3} - \frac{C_H \cdot C_{CO_3}}{K_{Eq,2}} \right) + k_{eq,w} \left(1 - \frac{C_H \cdot C_{OH}}{K_{Eq,w}} \right)$
Hydroxide ion (OH)	$0 = \frac{(C_{OH}^{IN} - C_{OH}^{OUT})}{\tau} + k_{eq,w} * \left(1 - \frac{C_H \cdot C_{OH}}{K_{Eq,w}} \right)$

3.3 Kinetic parameters determination

Once the material balances equations have been established, it is possible to proceed with the fitting procedure implementation. In particular, it is possible to notice that, if all parameters are set, the number of equations is equal to the one of unknown variables ensuring an exact numerical solution when the system of equations is solved. As previously anticipated, the final aim of the work is to verify if the Monod model could be suitable for the description of the biomass kinetic when such a culture is considered, also determining the most suitable values for the unknown parameters linked with the biomass growth:

- half-saturation constant of bicarbonate (K_{HCO_3} [gC m⁻³])
- maximum biomass specific growth rate (μ_{max} [day⁻¹]).

To achieve this result, the use of the software MATLAB® has been applied. In particular, starting from the solution of a system of differential equations (which represent the material balances equations and which have been solved at transient state in order to ensure the solver convergence) and the use of the experimental data, a fitting procedure has been implemented.

The basic idea relies on the ability of the solver to adjust the results of the equations according to the experimental data. The main output of this process is parameters estimation towards those values that are the most proper to ensure a good approximation between numerical and experimental data, since it minimizes the difference among them. Specifically, the use of an optimization routine is involved to minimize the value of the objective function, defined as the summation of the square relative errors. Relative errors have been required in this case because of the significative difference in terms of order of magnitude among the different variables involved in the equations. The objective function (OF) equation is reported:

$$OF = \sum_{i=1}^n (err_{rel,i})^2 = \sum_{i=1}^n \left(\frac{y_i - f(x_i, \mathbf{p})}{f(x_i, \mathbf{p})} \right)^2 \quad (3.23)$$

with y_i which refers to experimental data, x_i represents the calculated variables and \mathbf{p} is a vector which contains all the fitted parameters values.

Additionally, for each independent variable the determination coefficient R^2 has been considered. It is important to check if this value assumes values between 0 and 1: the more R^2 is close to 1, the more suitable are the parameters values fitted. The following equations describe the calculation of the abovementioned coefficient:

$$R^2 = 1 - \frac{SS_{res}}{SS_{tot}} \quad (3.24)$$

with:

$$SS_{res} = \sum_{i=1}^n (err_{abs,i})^2 = \sum_{i=1}^n (y_i - f(x_i, \mathbf{p}))^2 \quad (3.25)$$

that represents the sum of all the absolute errors (calculated between the experimental and the calculated values);

$$SS_{tot} = \sum_{i=1}^n (y_i - \tilde{y})^2 \quad (3.26)$$

which represents the total sum of squares, so the sum of the squared difference between the experimental data and the corresponding mean value (\tilde{y}), where

$$\tilde{y} = \frac{1}{n} \sum_{i=1}^n y_i \quad (3.27)$$

Chapter 4

Results and Discussion

4.1 Experimental results

Experimental campaign has been performed according with the discussion presented in Chapter 1, in which the importance of supporting the development of alternative microalgae cultivation systems has been underlined, focusing on BICCAPS strategy as a suitable and economic solution for those species that are alkaliphilic and able to exploit bicarbonate ion. Specifically, as anticipated in Chapter 2, the final aim of the experimental campaign is to investigate the effect of different specific process variables (namely the different insufflated air stream composition, the different concentration of sodium bicarbonate in the medium supplied and the culture pH) on *Arthrospira maxima* when a continuous cultivation mode is adopted. The importance to focus on such a cultivation mode is mainly due to a lack of information available in literature concerning this aspect. As explained in sub-subparagraph 1.6.4.1 the economic importance of *A. maxima*. Is also related to pigments production. Particular attention has been reserved to the quantification of PBPs, especially phycocyanin, that represents one of the most valuable bioactive compounds extracted from this species. However, also the chlorophyll *a* and carotenoids cell content has been reported in order to observe if a specific stress condition might be raised due to the cultivation conditions.

4.1.1 Effect of different sodium bicarbonate concentrations

For the first experimental campaign which aims at investigating the effect of different sodium bicarbonate concentrations, the bubbled air supplied to the PBR culture medium contains an additional 5% v/v of CO₂ in order to control the pH possibly separating the combined effect of this variable, strictly related to carbonate equilibrium, to the growth. In fact, CO₂ injection is specifically useful to shift the equilibrium among the different carbonaceous specie, in particular, in favour of HCO₃⁻ which is the carbonaceous specie mainly exploited by *A. maxima* (Lafarga et al., 2021; Pastore et al., 2022).

4.1.1.1 Effect of NaHCO₃ on biomass concentration on biomass and on carbonaceous species concentration

In *Figure 4.1*, the results obtained for the dried biomass weighted with the corresponding pH values at different concentrations of NaHCO₃ have been reported. It is possible to notice an interesting trend: biomass concentration increases as NaHCO₃ concentration increases, with a maximum registered at 30 g L⁻¹ (0.95 ± 0.046 [g L⁻¹]). The same trend was reported also by Colta et al., (2023) when *A. maxima* was cultivated in continuous LED photobioreactors at lower PFDs (100 μmol m⁻²s⁻¹): maximum biomass concentration (~0,6 g L⁻¹) was recorded at 30 g L⁻¹ of NaHCO₃ and a similar plateau-trend at higher bicarbonate concentration was observed. However, growth performance in function of NaHCO₃ supply seems to be dependent on species cultivated as well as cultivation mode. For example, Kim et al., (2017) studied the effect of different sodium bicarbonate concentrations on *Dunaliella salina* batch cultivation, observing that in the range between 0-30 g L⁻¹ NaHCO₃ the higher specific growth rate has been achieved at lower values (5 g L⁻¹) than those reported for continuous systems. A similar observation was made by Kim et al., (2019) on different several microalgae species. Also, pH increases as salts concentration does and this can be mostly caused by a stronger buffer capability of NaHCO₃ with respect to the carbon dioxide insufflated, besides the most significative microorganism growth. However, the difference is not so marked as in the case of biomass, ranging from 8.78 ± 0.214 to 9.06 ± 0.159 . An important observation regards the fact that with high bicarbonate concentrations in the inlet stream and working in continuous mode, referring to steady-state condition, the buffer capability of sodium bicarbonate increases avoiding that pH arises too much. Anyway, when NaHCO₃ concentration reaches higher concentrations (45 g L⁻¹), a corresponding decrease in biomass concentration (0.53 ± 0.265 [g L⁻¹]) has been observed. This significant result might be caused by the intervention of a possible inhibition effect, that is not necessarily due to the excess of bicarbonate, as demonstrated experimentally by the bicarbonate species measurement. It is reasonable, instead that the inhibition is related to the increased salinity. For example, an interesting investigation regard the deleterious effect produced by high amount of Na⁺ accumulation within the culture medium. In fact, as demonstrated by Ravelonandro et al., (2011), who worked in batch system, testing different NaCl concentrations (13,20,25,30,35 g L⁻¹), *Arthrospira* spp. shows a significative decrease of 50% for the productivity and 44% for the dried weight when salinity increases from the minimum to the maximum value tested. Therefore, a further specific investigation is needed to clarify this point.

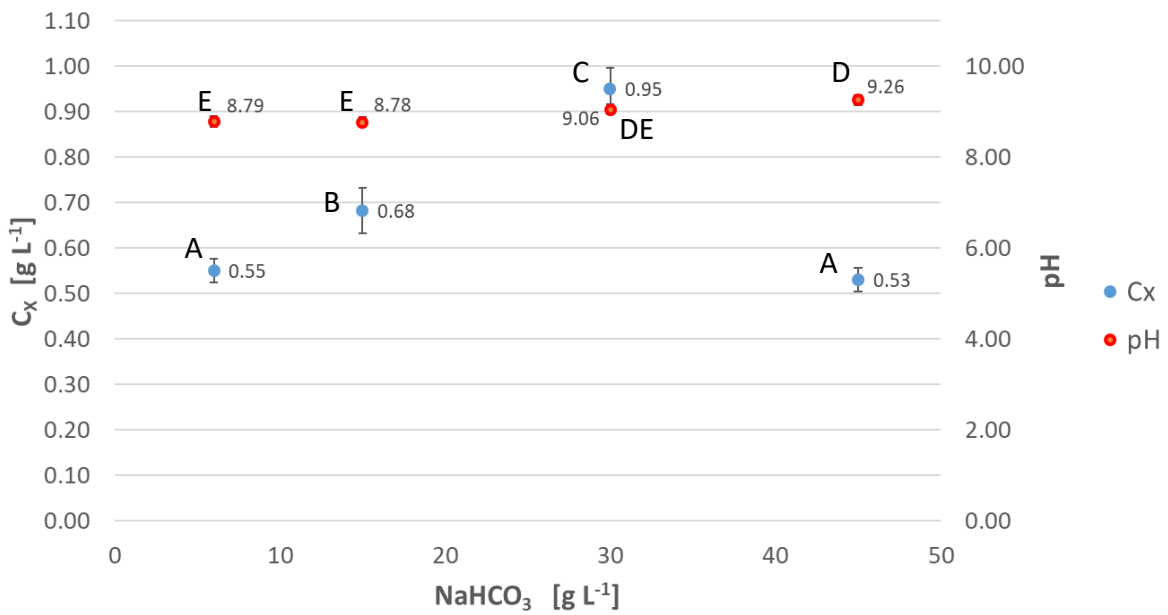


Figure 4.1: Mean biomass concentration and pH measured at steady state according to different concentration of sodium bicarbonate and air + 5% CO₂ v/v insufflation.

In Figure 4.2 and Figure 4.3 are represented the results for the titration performed on the medium fed and in the reactor respectively.

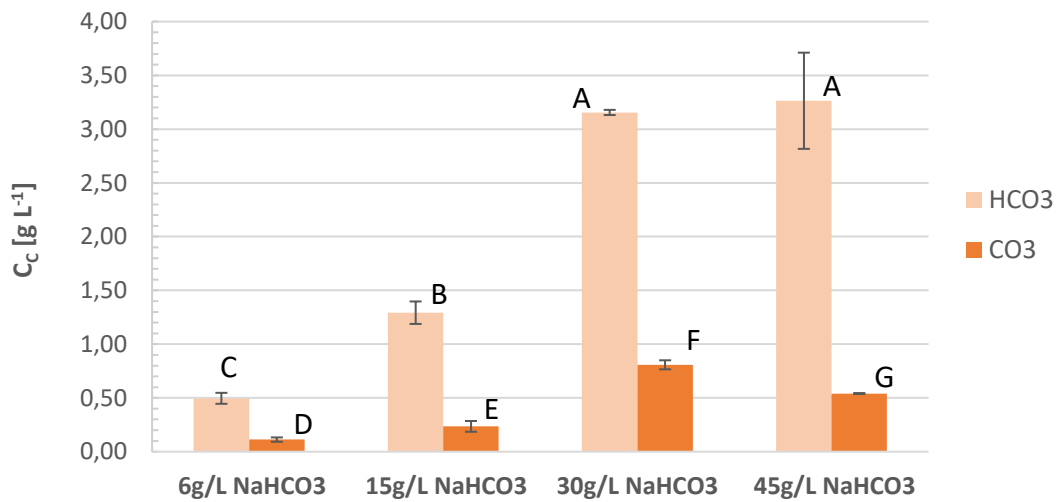


Figure 4.2: Mean carbonate and bicarbonate concentrations measured at steady state according to different concentration of sodium bicarbonate in the medium fed.

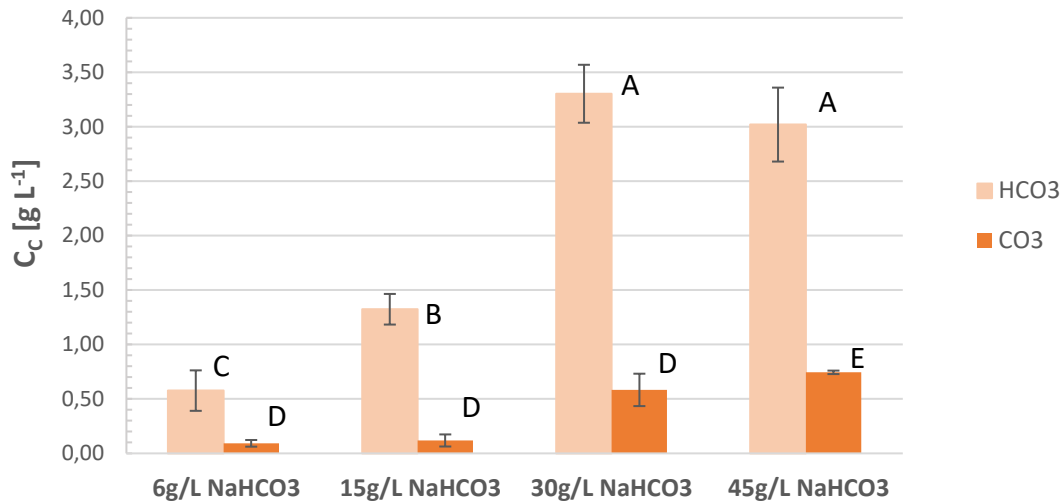


Figure 4.3: Mean carbonate and bicarbonate concentrations measured at steady state according to different concentration of sodium bicarbonate and air + 5% CO₂ v/v insufflation.

According to *Figure 4.3* it is possible to see that the bicarbonate concentration increases according to the NaHCO₃ increment in the medium fed. The same trend is observed for the carbonate ion concentration, in fact as described in *Figure 1.8* (Chapter 1) it increases with higher alkalinity conditions.

4.1.1.2 Effect of NaHCO₃ on pigments production

Additional investigation has been referred to the pigments content, in order to check if sodium bicarbonate could affect their synthesis.

In *Figure 4.4* the amount (mg g⁻¹) of the chlorophyll *a* and carotenoids with respect to biomass concentration as well as the respective ratio (Car/Chl-*a*) have been reported. The possibility of an induced stress condition mainly caused by light intensity supply can be excluded since the ratio between carotenoids and chlorophyll *a* is always quite low. This is important according to the fact that carotenoids start to increase in quantity especially when it is necessary to protect the photosynthetic apparatus as anticipated (according to Pagels et al., 2020) in paragraph 1.2.1. Nevertheless, the condition which ensures the higher chlorophyll *a* content is 30 g L⁻¹ of NaHCO₃ according to the results reported for the dried biomass concentration (Fig. 4.1). Referring to the work of Markou et al., 2023, who tested the effect of different NaCl concentrations on *Spirulina* cultivation, it is possible to demonstrate that the pigments content can be proportional to the biomass concentration, since the chlorophyll *a* amount per cell is quite constant. The same corresponding trend between the two analytical measures has been observed also in the experimental assessment performed in this thesis, observing that at the higher biomass concentration the amount of chlorophyll *a* recorded increase as well. However, this trend

is disregarded at 45 g L⁻¹, where chlorophyll accumulation is impaired with respect to the other conditions, while carotenoids quantity is comparable to the other ones. This result strongly supports the idea that a stressful condition is imposed on *A. maxima* when NaHCO₃ concentration exceeds a certain threshold value.

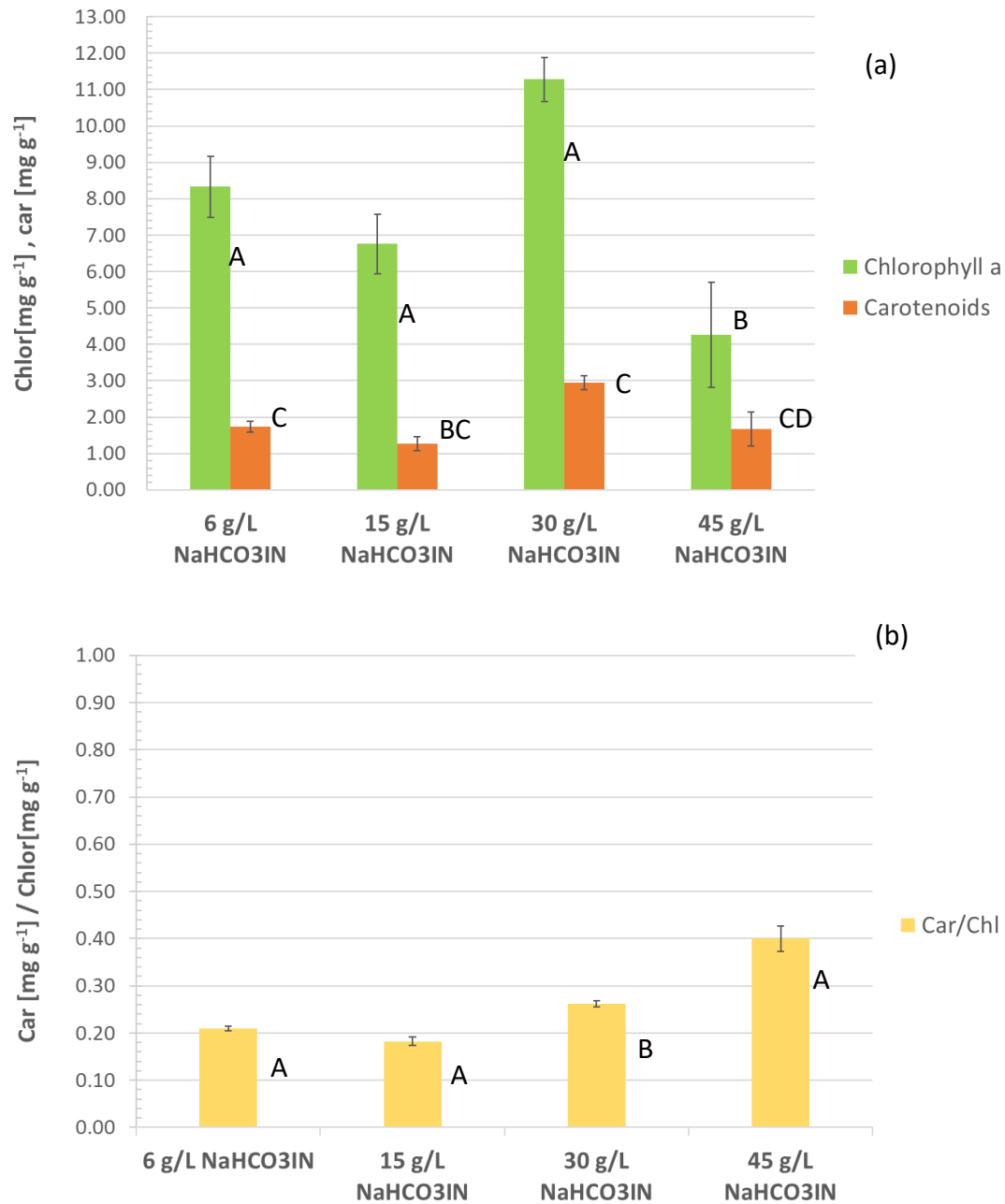


Figure 4.4: a) Mean Chlorophyll a and Carotenoids (normalised respect to the corresponding dried biomass) and b) Ratio Carotenoids/Chlorophyll a, measured at steady-state according to different concentration of sodium bicarbonate and air + 5% CO₂ v/v insufflation

Additionally, in *Figure 4.5* the results in terms of PBPs production have been reported. It is interesting to observe that, regarding the sole PC proteins, results obtained are almost the same except for the 45 g L⁻¹ NaHCO₃ condition, which reflect the results obtained for the dried biomass and pigments already discussed, confirming the hypothesis that an excess of sodium bicarbonate could cause a negative influence on biomass growth as well as pigments accumulation. It has been possible to demonstrate that the use of high concentration of NaHCO₃ doesn't affect the phycobiliproteins synthesis except for very high concentration.

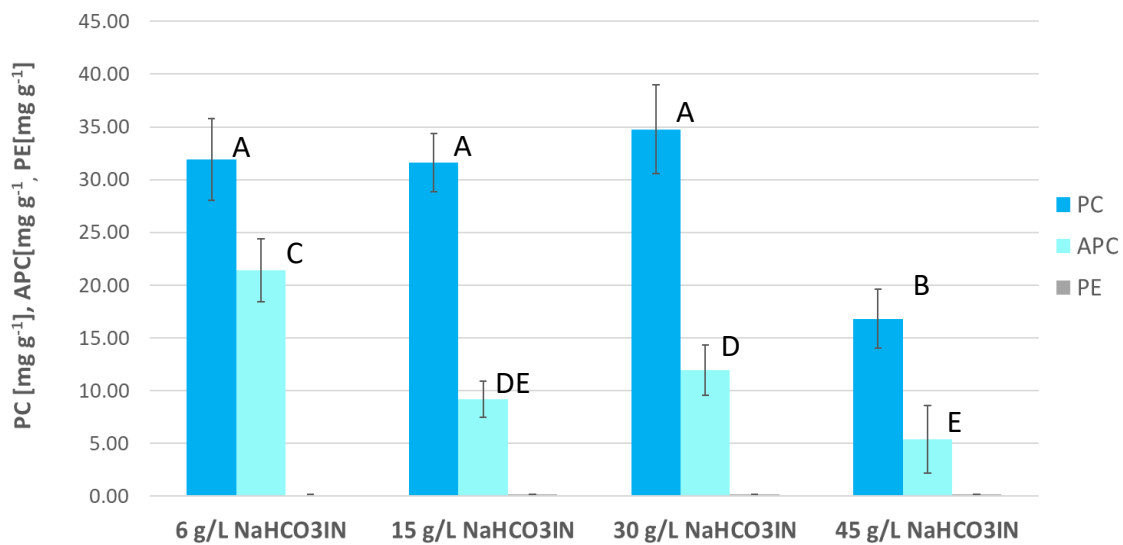


Figure 4.5: Phycobiliproteins content normalised respect to the corresponding dried biomass according to different concentration of sodium bicarbonate in the medium fed. Data refer to a continuous mode cultivation when steady-state is achieved.

4.1.2 Effect of different air composition

According to the discussion presented in Chapter 1, microalgae and cyanobacteria are usually cultivated with an insufflated air stream enriched with CO₂, whose quantity required varies among the different species. For *Arthrospira maxima* the CO₂ supplied is mostly involved for the pH control of the culture medium. Because of the necessity to reduce as much as possible the carbon dioxide amount supplied to the culture different bubbled air composition have been considered: (1) air enriched with a 5% v/v CO₂, (2) atmospheric air and (3) without any inlet stream. The final aim is to investigate what might be the effect of different carbon dioxide concentrations when a continuous cultivation is adopted. Regarding the sodium bicarbonate concentration, the value

considered is the one which ensures the highest biomass productivity according to the previous results reported. In this case, it is important to consider not only the effect of air on *Arthrospira maxima* growth but also referring to the different carbonaceous species concentration. In fact, CO₂ is involved in the equilibrium reactions and so it might be useful to understand which could be the effect on different carbon-based component.

4.1.2.1 Effect of different air composition on biomass growth.

In *Figure 4.6*, the results reported refer to the biomass concentration measured varying inlet air composition. According to this, there are no significant difference in biomass production whether the CO₂ is supplied or not in the air inlet stream. The values reported are 0.95 ± 0.046 [g L⁻¹] and 0.94 ± 0.114 [g L⁻¹] for air enriched with CO₂ and atmospheric air respectively. These results are in contrast with the ones reported by Ravelonandro et al., 2011, who tested the effect of different percentage of carbon dioxide when *A. platensis* is cultivated in a bubbled column and in batch condition. In this case, the higher biomass concentration is obtained for an addition of 1% of CO₂ to the air insufflated and also the chlorophyll *a* content increases. Otherwise, the cultivation without any inlet air stream seems to lead to a decrease of the biomass value (0.41 ± 0.030 [g L⁻¹]) maybe caused by an inhibition effect which can be caused by different aspects: first of all, the operation of the system was a batch, causing an accumulation of carbonate, an increase of pH which cannot be compensated by the CO₂ absorbed by the atmosphere (as the *k_{la}* is possibly very low in flasks). Another reasonable aspect to be considered is the possible accumulation of oxygen due to the absence of a stripping effect improved by the bubbled air, as known an excessive quantity of this chemical specie causes disruptive effects on microalgae growth (Zhou et al., 2017).

Concerning the pH, it is possible to observe that in the case of a cultivation where any additional percentage of carbon dioxide is involved, the alkalinity of the culture tends to arise since the buffer capability of CO₂ is lost. In fact, it has been found that, referring to mean values, pH is equal to $9,06 \pm 0.159$ with carbon dioxide addition instead of $9,59 \pm 0.0104$ for atmospheric air. However, *Arthrospira maxima* is an alkaliphilic specie, so the increment of this process variable does not strongly affect its growth capability, as it is in our results.

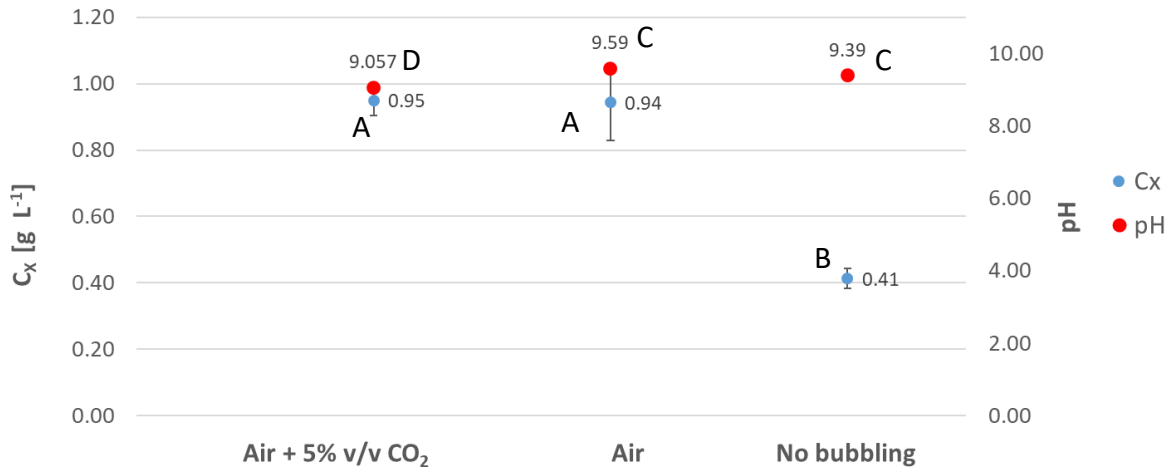


Figure 4.6: Mean values and standard deviation of dried biomass with three different insuflated air composition: a) air + 5% v/v CO₂; b) atmospheric air and c) without any air stream. Additionally, also the pH of the culture is reported in the corresponding three different cases.

4.1.2.2 Carbonaceous species distribution

According to the discussion presented above, it is interesting to investigate the effect of different composition of air supplied also referring to the nutrient exploitation.

The mean values and the corresponding standard deviation, both for the reactor cultivation and for the medium fed, have been summarize in *Figure 4.7*.

To better explain the results, it is important to consider a comparison between the residual carbonaceous species in the reactor and the medium fed to the culture system. The

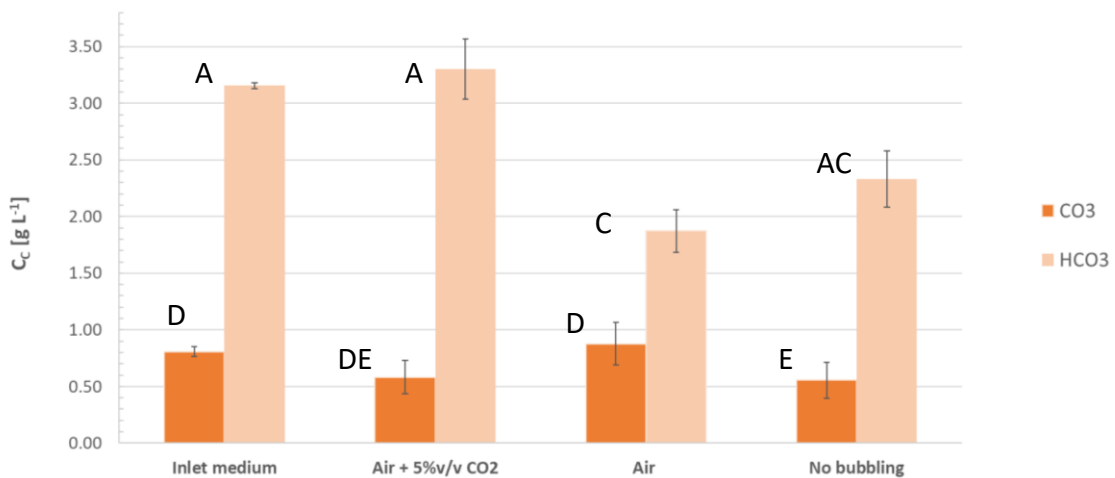


Figure 4.7: Mean values and standard deviation of carbonaceous species with three different insuflated air composition: a) air + 5% v/v CO₂; b) atmospheric air and c) without any air stream. Evaluated considering a continuous cultivation mode when steady-state is achieved.

carbonate ion concentration is quite similar among the different cases investigated and this is due to the fact that it is not exploited by *A. maxima*. An important observation regards the comparison between the bicarbonate concentration of the culture and the fresh medium fed. Specifically, when air is supplied with a 5% enrichment of CO₂ the bicarbonate available is almost constant despite the cyanobacterium exploitation (3.30 ± 0.227 [g L⁻¹] for the culture and 3.15 ± 0.024 [g L⁻¹] for fresh medium) This suggest that CO₂ might work as a HCO₃⁻ reservoir being involved in the equilibrium reactions explained in sub-subparagraph 1.6.3.1. The lower result in terms of concentration have been seen for the only air supplement which maybe causes a stripping effect of this component.

4.1.2.3 Pigments and PBPs production

In the following figures it is possible to observe the different results obtained in terms of chlorophyll *a* and carotenoids amount (mg g⁻¹) for the three different conditions of supplied air. According to data reported in *Figure 4.8*, the main observation regards that in all cases the Chlorophyll *a* amount exceeds the carotenoids one, even if the best condition seems to be the one in which CO₂ enriched air stream is involved. However, when the atmospheric air is supplied, almost acceptable mean value has been found and the absence of air stream causes a decrease of pigments quantity. Also, in this case it is possible to observe that the pigments content is representative of the biomass concentration, since also for this experimental campaign when a stress condition arises also the chlorophyll content decreases. It is possible to recognise that pigments are mainly affected by light intensity, since their biological role is to capture and supply light as energy source to perform the metabolic activities. Since during this experimental campaign different light supply has not been considered and the value is the one which ensures the highest productivity, it is possible to confirm that change of air supply didn't affect the pigments amount. However, further investigations are required to evaluate a possible inhibitory effect due to Reactive Oxygen Species (ROS) which could be accumulate when cultures without the bubbled air (which improves the stripping effect of O₂) are considered. In fact, they could deleteriously affect the photosynthetic efficiency of the microorganisms, as suggested by the significative decrease in Chlorophyll *a* content when any air bubbling stream is considered (De Farias Silva et al., 2017).

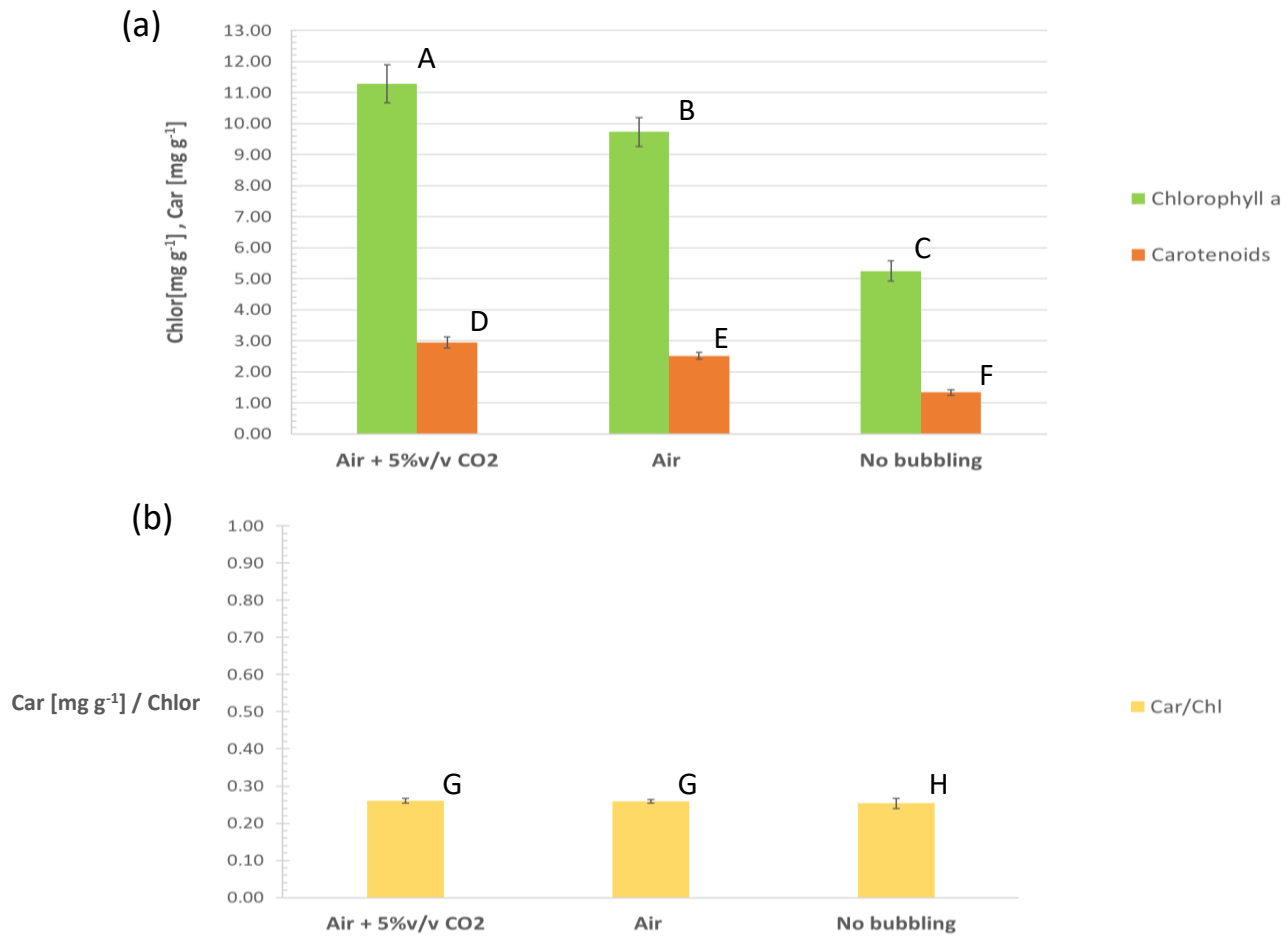


Figure 4.8: Mean values and standard deviation for Chlorophyll a and carotenoids normalised to the dried biomass [mg g⁻¹] has been reported. All data refer to three different bubbled air composition: a) air + 5% v/v CO₂; b) atmospheric air and c) without any air stream.

Regarding phycobiliproteins, as it is expected, the phycoerythrin content is quite low and almost negligible. In fact, *A. maxima* is a cyanobacterium with phycocyanin (PC) as main characteristic phycobiliprotein. According to *Figure 4.9*, it is possible to establish that the air composition didn't affect the content of this pigments. This is a very important result, if compared with the observations reported by Mehar et al., 2019. In that case, the CO₂ supply is required in order to ensure an automatization pH control for the culture when *Arthrospira* sp. is grown in an open raceway pond. To ensure the highest phycocyanin content (14%), the pH had to be fixed in a range between 8.5 -9.5. However, according to the results above reported it is possible to demonstrate that in a continuous cultivation mode the pH set to a specific value that is almost constant when the steady-state condition is established and the value is one of the most suitable to guarantee a considerable content of PC (27.96 ± 3.91 [mg g⁻¹ biomass]) without the use of carbon dioxide supply.

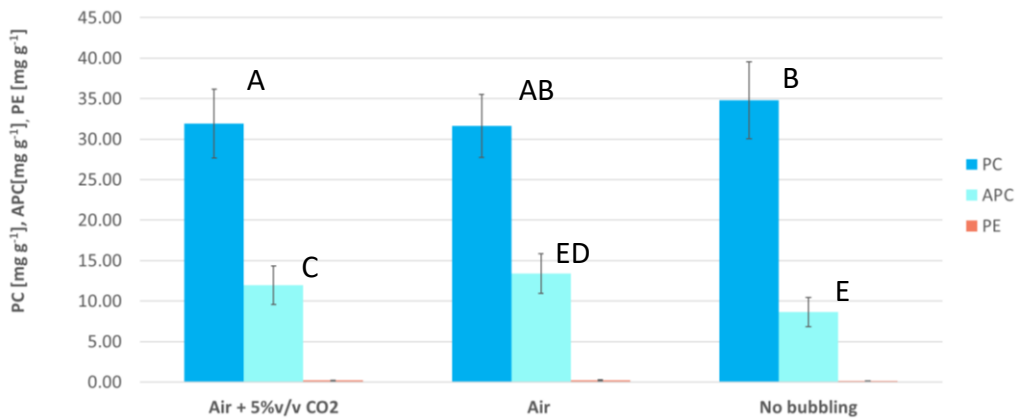


Figure 4.9: Mean values and standard deviation for phycobiliproteins normalised to the dried biomass [mg g⁻¹] has been reported. All data refer to three different bubbled air composition: a) air + 5% v/v CO₂; b) atmospheric air and c) without any air stream.

4.1.3 The effect of pH

Another important aspect to be considered is to investigate the effect produced by the pH control of the culture. In fact, also this process variable could be used to enhance the synthesis of specific bioactive compounds (Meher et al., 2019). Additionally, since the carbonaceous species concentration is strictly related to the pH (according to *Figure 1.8* in Chapter 1) it could be useful to find the optimal pH value in order to ensure the maximum bicarbonate ion concentration. As a consequence, this might result in higher biomass concentration, following the example reported by Gris et al., 2014. in which *Chlorella protothecoides* results in more suitable biomass concentration in continuous mode cultivation when the culture pH is set to the one which ensures a higher carbon dioxide concentration. In *Figure 4.10* the results obtained for the dried biomass concentration have been reported according with the different pH set point tested and also with a comparison with the case in which the pH controller is not exploited. What is important to observe is that, in case of a continuous cultivation the best results in terms of dried biomass concentration have been obtained when no pH-controller is involved in the process and pH, once the steady-state condition is established, naturally set to 9.6 which is almost the optimal value indicated for the cultivation of *Arthrospira maxima* (Pastore et al., 2022). However, the use of a pH controller drastically changes biomass concentration when comparing to the non-controlled culture: 0.68 ± 0.0153 [g L⁻¹] and 0.69 ± 0.0702 [g L⁻¹] for a pH set-point of 9.5 and 8.5 respectively, instead without pH controller the dry weight is equal to 0.94 ± 0.1137 [g L⁻¹]. This could be a result of an important aspect to be considered, namely a suitable compromise between the HCl molarity and its inlet flowrate. In fact, the acid concentration has to be suitable enough to guarantee the survival capability of the microorganism but at the same time it has not to

affect the reactor working volume that must be kept to a constant value. In fact, if the acid concentration is too low it means that it might not be able to compensate the pH increment with a reasonable flowrate, but it is continuously required by the control system leading to a wash-out condition. For this reason, a suitable alternative to control the pH of the culture could be represented by the use of carbon dioxide which supply is controlled by an automatic system. Some examples of such application are reported in literature, such as the work of Chen et al., 2016 or of Mehar et al., 2019 even if they refer to a different system (e.g. open raceway pond). However, in the second case, they considered that *Arthrospira* spp. has been mostly cultivated with CO₂ as carbon inorganic source finding that the biomass productivity is comparable with the standard Zarrouk medium if pH is set to 8.572 ± 2.88 [mg L⁻¹ day⁻¹]. So, a deeper investigation is required in order to find suitable pH controller strategies but minimizing as much as possible the use of carbon dioxide.

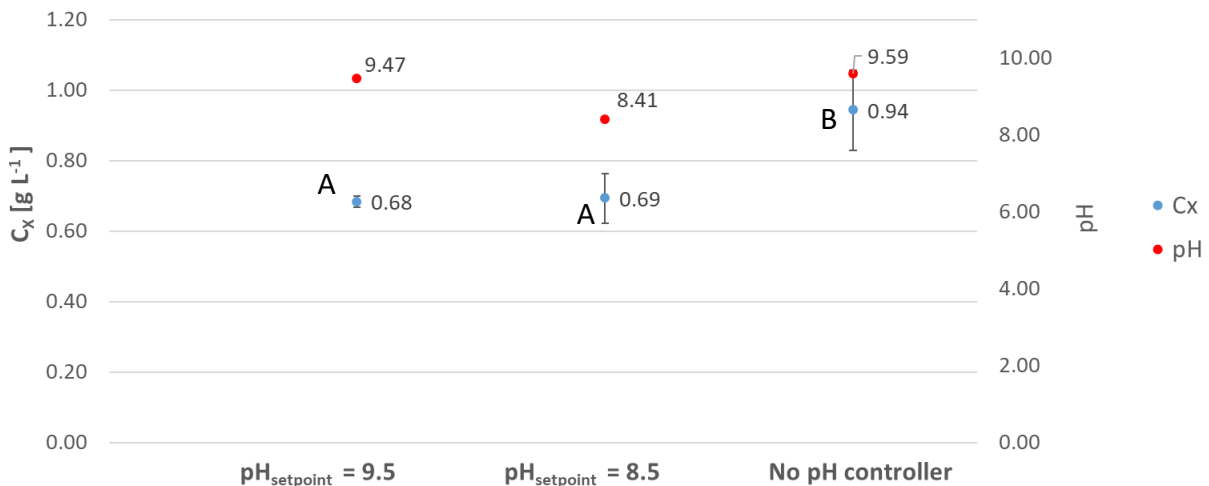


Figure 4.10: Mean dried biomass concentration for a continuous cultivation of *Arthrospira maxima*, when the steady-state condition has been established and with a pH controller. The different cases investigated are: a) pH-setpoint =9.5; b) pH-setpoint =8.5 and c) without any pH controller.

4.2 Kinetic parameters

According to the discussion presented in the previous chapters, one of the important purposes of this thesis project is to determine the most suitable values of two kinetic parameters present in the model, namely, the bicarbonate half-saturation constant (K_{HCO_3}) and the maximum biomass specific growth rate (μ_{max}). According to the method described in Chapter 3, this is possible through a fitting procedure implemented in MATLAB®, which requires both experimental data and a numerical model.

4.5.1 Input data

If from one side the numerical model has been deeply described in Chapter 3, the additional data required need to be briefly described and summarized. In particular, they refer to results obtained from the experimental campaigns, to the composition of the inlet medium and to suitable starting values for the kinetic parameters.

Firstly, concerning the data obtained from the experiments, they refer to results presented in paragraph §4.1, which describe the effect produced by different sodium bicarbonate inlet concentrations on biomass growth, besides the bicarbonate ion concentration and pH, measured in the cultivation culture. These results are also calculated numerically solving the material balances equations presented in *Table 3.4*. Both are strongly necessary to ensure the solver capability to construct and to minimize the object function based on relative errors (see paragraph §3.3).

Table 4.1: Data obtained for dried biomass and bicarbonate concentrations and pH inside the reactor and considering three different concentrations of sodium bicarbonate in the medium fed. The reactor worked with a continuous cultivation mode and data refer to steady-state condition.

	6 [g L ⁻¹] NaHCO ₃ ^{IN}		15 [g L ⁻¹] NaHCO ₃ ^{IN}		30 [g L ⁻¹] NaHCO ₃ ^{IN}		45 [g L ⁻¹] NaHCO ₃ ^{IN}	
	Mean	Stand. dev.	Mean	Stand. dev.	Mean	Stand. dev.	Mean	Stand. dev.
Biomass [g L⁻¹]	0.550	0.026	0.683	0.054	0.950	0.046	0.530	0.027
HCO₃ [gC L⁻¹]	0.577	0.186	1.324	0.141	3.302	0.266	3.020	0.340
pH	8.787	0.214	8.770	0.152	9.057	0.159	9.260	0.040

In addition to the values of the parameters involved in the model, more data have been required as input information in order to guarantee the univocal determination of the

unknown variables (so to ensure that the number of equations is equal to the number of variables to be determined). According to the material balances equations and also to the fact that for each experimental campaign the inlet medium composition doesn't change, it has been possible to assume the corresponding term as constant. The inlet concentration of bicarbonate and carbonate ions are calculated through the titration procedure described in paragraph § 2.2.3.1, the inlet concentration of hydrogen and hydroxide ions have been calculated from the pH experimental value thanks to *Equation 3.21-3.22*, instead the inlet concentration of carbon dioxide has been approximated to equilibrium concentration with *Equation 3.19*. Both for the pH and for carbon dioxide equations, they have been directly involved in the MATLAB® script.

Table 4.2: pH, carbonate and bicarbonate concentrations in the medium involved to perform the experimental assessment of different sodium bicarbonate concentration in the medium fed when a continuous cultivation mode is adopted.

	6 [g L ⁻¹] NaHCO ₃ ^{IN}		15 [g L ⁻¹] NaHCO ₃ ^{IN}		30 [g L ⁻¹] NaHCO ₃ ^{IN}		45 [g L ⁻¹] NaHCO ₃ ^{IN}	
	Mean	Stand. dev.	Mean	Stand. dev.	Mean	Stand. dev.	Mean	Stand. dev.
CO ₃ [gC L ⁻¹]	0.112	0.020	0.235	0.050	0.808	0.042	0.541	0.005
HCO ₃ [gC L ⁻¹]	0.496	0.051	1.292	0.104	3.155	0.024	3.266	0.447
pH	9.12	0.020	9.12	0.020	9.31	0.010	8.39	0.015

Finally, also a starting value for the parameters to be fitted is required and it has to be the most reasonable as possible, so the corresponding values reported from Pastore et al., 2022 and Colta, 2023 are considered, as reported in the following table.

Table 4.3: Tentative value for unknown kinetic parameters.

Kinetic parameter	Tentative value
K_{HCO_3} [gC m ⁻³]	140
μ_{max} [day ⁻¹]	8.66

In order to be able to obtain suitable fitted values specific boundaries values have been set: the lower limit is zero, since negative values has no physical meaning, instead the upper limits have been fixed at 400 and 15 for the half saturation constant and for the maximum specific growth rate respectively.

4.5.1 Fitting results

Once all data required have been collected, it has been possible to proceed with the fitting procedure. The results obtained are discussed considering the most important variables of the process considered: the biomass concentration, the bicarbonate ion concentration that represent the main inorganic carbon source and the pH which is an important process variable because it strongly influences the equilibrium among the different carbonaceous species.

Table 4.4: Fitted values for the unknown kinetic parameters.

Kinetic parameter	Fitted value
K_{HCO_3} [gC m ⁻³]	108.85
μ_{max} [day ⁻¹]	4.76

Regarding the maximum biomass specific growth rate, we can suppose that the value obtained is acceptable. As expected, it is lower than the one reported in the reference work where the growth biomass rate equation reported by Pastore et al. (2022) does not contain a specific term which could account for the nutrient consumption, but there is a coherence between the order of measure. Instead regarding the half-saturation constant, it is acceptable being a lower value which ensures the higher affinity between *Arthrospira maxima* and the bicarbonate ion which represent the preferred inorganic carbon source when is available. In the following figures (Fig 4.8, 4.9 and 4.10) the results obtained from the fitting procedure are presented. Specifically, they refer to the biomass concentration (C_x), to the bicarbonate concentration (C_{HCO_3}) and to the pH.

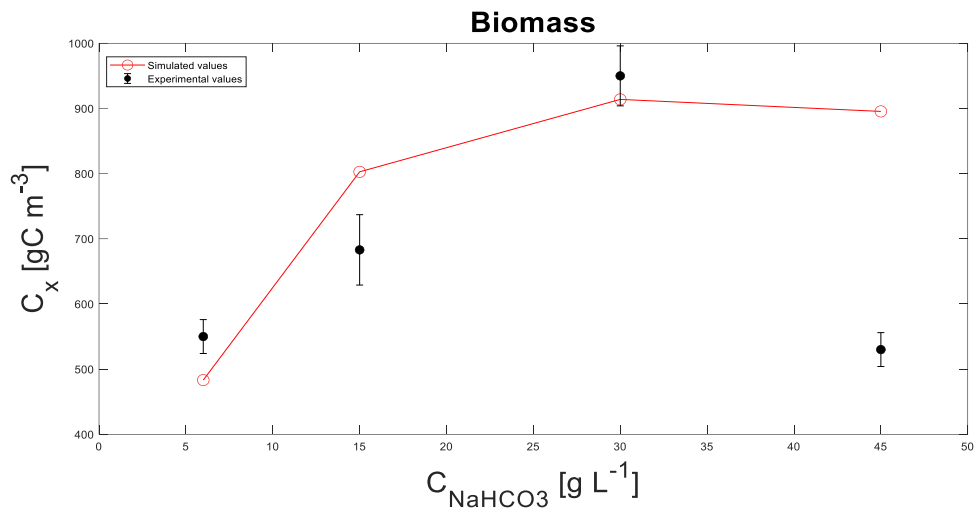


Figure 4.10: Results of the fitting procedure for the biomass data.

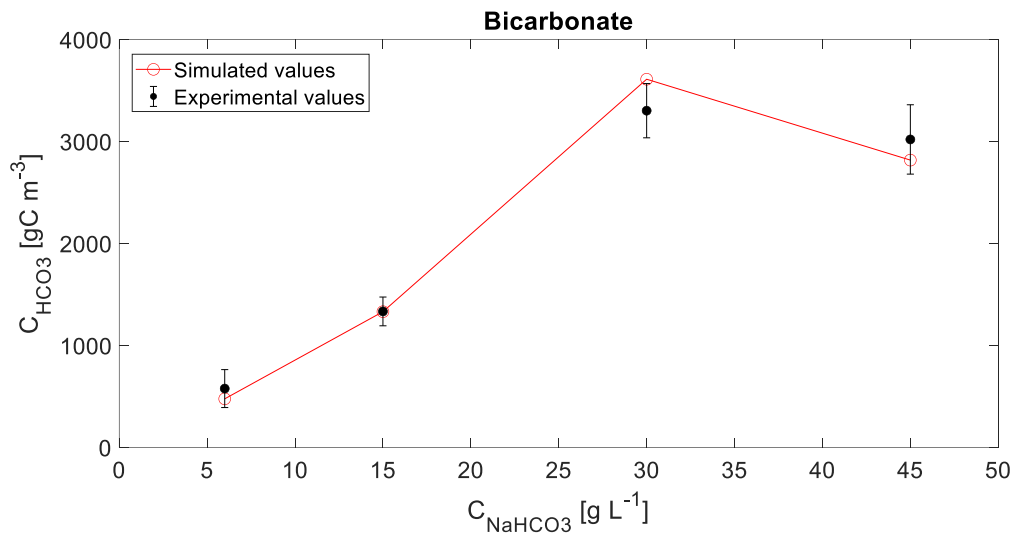


Figure 4.11: Results of the fitting procedure for the bicarbonate data.

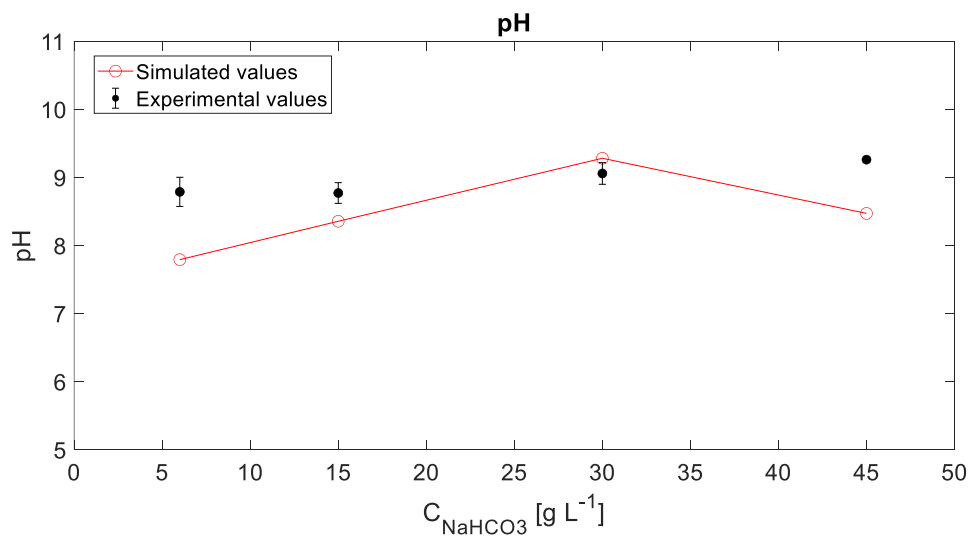


Figure 4.12: Results of the fitting procedure for the pH data.

It is possible to conclude that the model proposed by Solimeno et al. (2015) allows to consider both the variation of pH and of bicarbonate ion in a continuous microalgae culture. The importance to consider a model that is able to well approximated the behaviour of this process variables is mainly due to their importance, since bicarbonate represents the limiting substrate (namely, the fundamental inorganic carbon source) and pH drives the equilibrium among the different species. Additionally, also the choice of the Monod kinetic to describe the bicarbonate exploitation by the cyanobacterium is reasonable, in fact the biomass data are well fitted until an inlet sodium bicarbonate concentration equal to 30 [g L⁻¹]. It is also important to underline that, even if for the limiting substrate only bicarbonate ion has been considered (differently from Solimeno et al. (2015) who considered also carbon dioxide), this choice doesn't impact on the predictive capability of the model. In fact, as it has been demonstrated in paragraph 4.1 *Arthrospira maxima* preferentially exploits the bicarbonate ion. Despite this, further improvements are required in order to better consider the possible inhibiting effects, that have causes different from the accumulation of substrate as deeply described in previous paragraphs and that at the moment have not been considered in the mathematical equations. So, since the inhibition effect can be caused mainly by the high salinity content, in particular by the high content of sodium additional experiments have to be performed in order to verify this hypothesis and to add the most suitable term which allows to consider this effect in the predictive model. However, also the increase of carbonate ion concentration required to be considered and the trend has to be better studied with more experiments.

Conclusions

The aim of this thesis is to present a suitable mathematical model able to describe the bicarbonate uptake of the commercially relevant alkaliphilic cyanobacteria *Arthrospira maxima* when cultivated in continuous mode and with high concentration of sodium bicarbonate as inorganic carbon source. Due to the ability of this species to grow even at alkaline pH, BICCAPS (Bicarbonate Inorganic Carbon Capture and Algae Production System) can be used as a strategic tool to overcome most of the energetic and economic barriers of the traditional cultivation process. Specifically, the use of alternative inorganic carbon source is suitable to minimize as much as possible the use of carbon dioxide towards a cheaper production system. In order to emphasize the suitability of such an approach, this work uses an experimental assessment to improve and simplify the mathematical description of *A. maxima* growth in function of sodium bicarbonate as major nutrient. It has been possible to demonstrate that the highest biomass concentration can be achieved with a concentration of sodium bicarbonate equal to 30 g L^{-1} , even though at higher salts concentrations an inhibitory effect was observed whether on cellular growth as well as pigments accumulation. Moreover, it might be reasonable to work with the insufflation of air which does not contain CO_2 enrichment. This is possible because *Arthrospira* spp., in general, preferentially exploit bicarbonate ion for carbon fixation and, according to the data obtained from the experimental campaign, carbon dioxide works as a reservoir for the bicarbonate itself. Additionally, it has been demonstrated that the culture pH never exceeds $\text{pH}=10$, so the carbon dioxide supply is not required to control the pH of the culture if the conditions set in this thesis are ensured. Concerning the mathematical model, it has been demonstrated that the solution proposed is suitable to describe, in first approximation, trend of the biomass and bicarbonate ion concentrations, besides the pH one, when a cultivation in continuous mode is considered. This is an important starting point according to a lack of information available for such cultivations. The main advantage of the equations proposed is that they allow to consider the chemical equilibrium phenomena in which the main chemical species and the pH are involved in a quite simple way. Additionally, it has been demonstrated that the idea to describe the limiting substrate consumption only by considering the bicarbonate ion is reasonable, according to *Arthrospira* spp. capability to mainly exploit this compound despite CO_2 . The Monod kinetic model is suitable for such purpose, as demonstrated by fitting procedure applied. In fact, thanks to the use of the software MATLAB®, the fitting procedure, based on the experimental data collected testing different sodium bicarbonate ion concentrations and the material balances equations proposed, has been applied. In this way it has been possible to determine the values of two unknown kinetic parameters the

bicarbonate half-saturation constant ($K_{HCO_3} = 108.85 \text{ [gC m}^{-3}\text{]}$) and the maximum biomass specific growth rate ($\mu_{\max} = 4.76 \text{ [day}^{-1}\text{]}$). All these results are strongly significant to support the idea that it could be reasonable to improve researches activity as well as industrial cultivation towards the continuous mode operation exploiting alternative carbon feedings for microalgae cultivation. However, further improvements and studies are required to extend this approach to other significant microalgae species and make the model able to account for the inhibition effects which could arise (as explained before) and that are not accounted for up to this moment. At the end it also important to consider the possibility to recycle the culture medium, since high quantities of sodium bicarbonate are fed and the recycle could be suitable to enhance the cheapness of the cultivation system.

References

- Abreu, A. P., Morais, R. C., Teixeira, J. A., & Nunes, J. (2022). A comparison between microalgal autotrophic growth and metabolite accumulation with heterotrophic, mixotrophic and photoheterotrophic cultivation modes. In *Renewable and Sustainable Energy Reviews* (Vol. 159). Elsevier Ltd. <https://doi.org/10.1016/j.rser.2022.112247>
- Ahmad, I., Abdullah, N., Koji, I., Yuzir, A., & Eva Muhammad, S. (2021). Evolution of Photobioreactors: A Review based on Microalgal Perspective. *IOP Conference Series: Materials Science and Engineering*, 1142(1), 012004. <https://doi.org/10.1088/1757-899x/1142/1/012004>
- Barbera, E., Grandi, A., Borella, L., Bertuccio, A., & Sforza, E. (2019). Continuous cultivation as a method to assess the maximum specific growth rate of photosynthetic organisms. *Frontiers in Bioengineering and Biotechnology*, 7(OCT). <https://doi.org/10.3389/fbioe.2019.00274>
- Bennett, A., & Bogorad, L. (n.d.). *COMPLEMENTARY CHROMATIC ADAPTATION IN A FILAMENTOUS BLUE-GREEN ALGA*.
- Blanken, W., Cuaresma, M., Wijffels, R. H., & Janssen, M. (2013). Cultivation of microalgae on artificial light comes at a cost. In *Algal Research* (Vol. 2, Issue 4, pp. 333–340). <https://doi.org/10.1016/j.algal.2013.09.004>
- Borella, L., Ortolan, D., Barbera, E., Trivellin, N., & Sforza, E. (2021). A multiwavelength model to improve microalgal productivity and energetic conversion in a red-blue light emitting diodes (LEDs) continuous photobioreactor. *Energy Conversion and Management*, 243. <https://doi.org/10.1016/j.enconman.2021.114330>
- Borella, L., Sforza, E., & Bertuccio, A. (2021). Effect of residence time in continuous photobioreactor on mass and energy balance of microalgal protein production. *New Biotechnology*, 64, 46–53. <https://doi.org/10.1016/j.nbt.2021.05.006>
- Carvalho, A. P., Silva, S. O., Baptista, J. M., & Malcata, F. X. (2011). Light requirements in microalgal photobioreactors: An overview of biophotonic aspects. In *Applied Microbiology and Biotechnology* (Vol. 89, Issue 5, pp. 1275–1288). <https://doi.org/10.1007/s00253-010-3047-8>
- Chai, W. S., Tan, W. G., Halimatul Munawaroh, H. S., Gupta, V. K., Ho, S. H., & Show, P. L. (2021). Multifaceted roles of microalgae in the application of wastewater biotreatment: A review. *Environmental Pollution*, 269. <https://doi.org/10.1016/j.envpol.2020.116236>

- Chen, C. Y., Kao, P. C., Tan, C. H., Show, P. L., Cheah, W. Y., Lee, W. L., Ling, T. C., & Chang, J. S. (2016). Using an innovative pH-stat CO₂ feeding strategy to enhance cell growth and C-phycocyanin production from *Spirulina platensis*. *Biochemical Engineering Journal*, *112*, 78–85. <https://doi.org/10.1016/j.bej.2016.04.009>
- Chen, C. Y., Yeh, K. L., Aisyah, R., Lee, D. J., & Chang, J. S. (2011). Cultivation, photobioreactor design and harvesting of microalgae for biodiesel production: A critical review. *Bioresource Technology*, *102*(1), 71–81. <https://doi.org/10.1016/j.biortech.2010.06.159>
- Chi, Z., O'Fallon, J. V., & Chen, S. (2011). Bicarbonate produced from carbon capture for algae culture. In *Trends in Biotechnology* (Vol. 29, Issue 11, pp. 537–541). <https://doi.org/10.1016/j.tibtech.2011.06.006>
- Clippinger, J., & Davis, R. (2019). *Techno-Economic Analysis for the Production of Algal Biomass via Closed Photobioreactors: Future Cost Potential Evaluated Across a Range of Cultivation System Designs*. www.nrel.gov/publications.
- Colta, et al. (2023). *EFFETTO DEL RAPPORTO DI RICICLO IN FOTOBIOREATTORI IN CONTINUO PER LA COLTIVAZIONE DI ARTHROSPIRA MAXIMA: COMPOSIZIONE DELLA BIOMASSA E OTTIMIZZAZIONE DEL CONSUMO DI ACQUA E NUTRIENTI*. Unversità degli Studi di Padova.
- Costa, J. A. V., Freitas, B. C. B., Rosa, G. M., Moraes, L., Morais, M. G., & Mitchell, B. G. (2019). Operational and economic aspects of *Spirulina*-based biorefinery. In *Bioresource Technology* (Vol. 292). Elsevier Ltd. <https://doi.org/10.1016/j.biortech.2019.121946>
- Daneshvar, E., Wicker, R. J., Show, P. L., & Bhatnagar, A. (2022). Biologically-mediated carbon capture and utilization by microalgae towards sustainable CO₂ biofixation and biomass valorization – A review. *Chemical Engineering Journal*, *427*. <https://doi.org/10.1016/j.cej.2021.130884>
- Darvehei, P., Bahri, P. A., & Moheimani, N. R. (2018). Model development for the growth of microalgae: A review. In *Renewable and Sustainable Energy Reviews* (Vol. 97, pp. 233–258). Elsevier Ltd. <https://doi.org/10.1016/j.rser.2018.08.027>
- De Farias Silva, C. E., Sforza, E., & Bertucco, A. (2017). Effects of pH and Carbon Source on *Synechococcus* PCC 7002 Cultivation: Biomass and Carbohydrate Production with Different Strategies for pH Control. *Applied Biochemistry and Biotechnology*, *181*(2), 682–698. <https://doi.org/10.1007/s12010-016-2241-2>
- Devadas, V. V., Khoo, K. S., Chia, W. Y., Chew, K. W., Munawaroh, H. S. H., Lam, M. K., Lim, J. W., Ho, Y. C., Lee, K. T., & Show, P. L. (2021). Algae biopolymer towards sustainable

- circular economy. In *Bioresource Technology* (Vol. 325). Elsevier Ltd.
<https://doi.org/10.1016/j.biortech.2021.124702>
- Di Caprio, F., Altimari, P., & Pagnanelli, F. (2019). New strategies enhancing feasibility of microalgal cultivations. In *Studies in Surface Science and Catalysis* (Vol. 179, pp. 287–316). Elsevier Inc. <https://doi.org/10.1016/B978-0-444-64337-7.00016-1>
- Dubois, M., Gilles, K., Hamilton, J. K., Rebers, P. A., & Smith, F. (1951). A colorimetric method for the determination of sugars. *Nature*.
- Fernandes, B. D., Mota, A., Teixeira, J. A., & Vicente, A. A. (2015). Continuous cultivation of photosynthetic microorganisms: Approaches, applications and future trends. In *Biotechnology Advances* (Vol. 33, Issue 6, pp. 1228–1245). Elsevier Inc.
<https://doi.org/10.1016/j.biotechadv.2015.03.004>
- Fernandes, R., Campos, J., Serra, M., Fidalgo, J., Almeida, H., Casas, A., Toubarro, D., & Barros, A. I. R. N. A. (2023). Exploring the Benefits of Phycocyanin: From Spirulina Cultivation to Its Widespread Applications. In *Pharmaceuticals* (Vol. 16, Issue 4). MDPI.
<https://doi.org/10.3390/ph16040592>
- Fernández, F. G. A., Reis, A., Wijffels, R. H., Barbosa, M., Verdelho, V., & Llamas, B. (2021). The role of microalgae in the bioeconomy. *New Biotechnology*, *61*, 99–107.
<https://doi.org/10.1016/j.nbt.2020.11.011>
- Gris, B., Sforza, E., Vecchiato, L., & Bertucco, A. (2014). Development of a process for an efficient exploitation of CO₂ captured from flue gases as liquid carbonates for chlorella protothecoides cultivation. *Industrial and Engineering Chemistry Research*, *53*(43), 16678–16688. <https://doi.org/10.1021/ie502336d>
- Huang, Q., Jiang, F., Wang, L., & Yang, C. (2017). Design of Photobioreactors for Mass Cultivation of Photosynthetic Organisms. *Engineering*, *3*(3), 318–329.
<https://doi.org/10.1016/J.ENG.2017.03.020>
- Ighalo, J. O., Dulta, K., Kurniawan, S. B., Omoarukhe, F. O., Ewuzie, U., Eshiemogie, S. O., Ojo, A. U., & Abdullah, S. R. S. (2022). Progress in Microalgae Application for CO₂ Sequestration. *Cleaner Chemical Engineering*, *3*, 100044. <https://doi.org/10.1016/j.clce.2022.100044>
- Ji, C., Wang, J., Li, R., & Liu, T. (2017a). Modeling of carbon dioxide mass transfer behavior in attached cultivation photobioreactor using the analysis of the pH profiles. *Bioprocess and Biosystems Engineering*, *40*(7), 1079–1090. <https://doi.org/10.1007/s00449-017-1770-6>

- Ji, C., Wang, J., Li, R., & Liu, T. (2017b). Modeling of carbon dioxide mass transfer behavior in attached cultivation photobioreactor using the analysis of the pH profiles. *Bioprocess and Biosystems Engineering*, *40*(7), 1079–1090. <https://doi.org/10.1007/s00449-017-1770-6>
- Kannaujiya, V. K. S. R. P., Sundaram, S., & Sinha, R. P. (2017). Advances and Strategies of Purification Technology. In *Phycobiliproteins: Recent Developments and Future Applications*. Singapore: Springer Singapore., 99–120.
- Khan, M. I., Shin, J. H., & Kim, J. D. (2018). The promising future of microalgae: Current status, challenges, and optimization of a sustainable and renewable industry for biofuels, feed, and other products. In *Microbial Cell Factories* (Vol. 17, Issue 1). BioMed Central Ltd. <https://doi.org/10.1186/s12934-018-0879-x>
- Kim, G. Y., Heo, J., Kim, H. S., & Han, J. I. (2017). Bicarbonate-based cultivation of *Dunaliella salina* for enhancing carbon utilization efficiency. *Bioresource Technology*, *237*, 72–77. <https://doi.org/10.1016/j.biortech.2017.04.009>
- Kim, G. Y., Roh, K., & Han, J. I. (2019). The use of bicarbonate for microalgae cultivation and its carbon footprint analysis. *Green Chemistry*, *21*(18), 5053–5062. <https://doi.org/10.1039/c9gc01107b>
- Lafarga, T., Fernández-Sevilla, J. M., González-López, C., & Acién-Fernández, F. G. (2020). Spirulina for the food and functional food industries. In *Food Research International* (Vol. 137). Elsevier Ltd. <https://doi.org/10.1016/j.foodres.2020.109356>
- Lafarga, T., Sánchez-Zurano, A., Villaró, S., Morillas-España, A., & Acién, G. (2021). Industrial production of spirulina as a protein source for bioactive peptide generation. In *Trends in Food Science and Technology* (Vol. 116, pp. 176–185). Elsevier Ltd. <https://doi.org/10.1016/j.tifs.2021.07.018>
- Lau, N. S., Matsui, M., & Abdullah, A. A. A. (2015). Cyanobacteria: Photoautotrophic Microbial Factories for the Sustainable Synthesis of Industrial Products. In *BioMed Research International* (Vol. 2015). Hindawi Publishing Corporation. <https://doi.org/10.1155/2015/754934>
- Lee, Y. K., Chen, W., Shen, H., Han, D., Li, Y., Jones, H. D. T., Timlin, J. A., & Hu, Q. (2013). Basic Culturing and Analytical Measurement Techniques. In *Handbook of Microalgal Culture: Applied Phycology and Biotechnology: Second Edition* (pp. 37–68). Wiley. <https://doi.org/10.1002/9781118567166.ch3>
- Magwell, P. F. R., Djoudjeu, K. T., Minyaka, E., Tavea, M. F., Fotsop, O. W., Tagnikeu, R. F., Fofou, A. M., Darelle, C. K. V., Dzoyem, C. U. D., & Lehman, L. G. (2023a). Sodium Bicarbonate (NaHCO₃) Increases Growth, Protein and Photosynthetic Pigments

- Production and Alters Carbohydrate Production of *Spirulina platensis*. *Current Microbiology*, 80(2). <https://doi.org/10.1007/s00284-022-03165-0>
- Magwell, P. F. R., Djoudjeu, K. T., Minyaka, E., Tavea, M. F., Fotsop, O. W., Tagnikeu, R. F., Fofou, A. M., Darelle, C. K. V., Dzoyem, C. U. D., & Lehman, L. G. (2023b). Sodium Bicarbonate (NaHCO₃) Increases Growth, Protein and Photosynthetic Pigments Production and Alters Carbohydrate Production of *Spirulina platensis*. *Current Microbiology*, 80(2). <https://doi.org/10.1007/s00284-022-03165-0>
- Markou, G., Kougia, E., Arapoglou, D., Chentir, I., Andreou, V., & Tzovenis, I. (2023). Production of *Arthrospira platensis*: Effects on Growth and Biochemical Composition of Long-Term Acclimatization at Different Salinities. *Bioengineering*, 10(2). <https://doi.org/10.3390/bioengineering10020233>
- Markou, G., Vandamme, D., & Muylaert, K. (2014). Microalgal and cyanobacterial cultivation: The supply of nutrients. In *Water Research* (Vol. 65, pp. 186–202). Elsevier Ltd. <https://doi.org/10.1016/j.watres.2014.07.025>
- Mehar, J., Shekh, A., Nethravathy, M. U., Sarada, R., Chauhan, V. S., & Mudliar, S. (2019). Automation of pilot-scale open raceway pond: A case study of CO₂-fed pH control on *Spirulina* biomass, protein and phycocyanin production. *Journal of CO₂ Utilization*, 33, 384–393. <https://doi.org/10.1016/j.jcou.2019.07.006>
- Mitra, R., Das Gupta, A., Kumar, R. R., & Sen, R. (2023). A cleaner and smarter way to achieve high microalgal biomass density coupled with facilitated self-flocculation by utilizing bicarbonate as a source of dissolved carbon dioxide. *Journal of Cleaner Production*, 391. <https://doi.org/10.1016/j.jclepro.2023.136217>
- Moran, R., & Porath, D. (1980). Chlorophyll Determination in Intact Tissues Using N,N-Dimethylformamide. In *Plant Physiol* (Vol. 65). <https://academic.oup.com/plphys/article/65/3/478/6076103>
- Pagels, F., Salvaterra, D., Amaro, H. M., & Guedes, A. C. (2020). Pigments from microalgae. In *Handbook of Microalgae-Based Processes and Products: Fundamentals and Advances in Energy, Food, Feed, Fertilizer, and Bioactive Compounds* (pp. 465–492). Elsevier. <https://doi.org/10.1016/B978-0-12-818536-0.00018-X>
- Pastore, M., Primavera, A., Milocco, A., Barbera, E., & Sforza, E. (2022). Tuning the Solid Retention Time to Boost Microalgal Productivity and Carbon Exploitation in an Industrial Pilot-Scale LED Photobioreactor. *Industrial and Engineering Chemistry Research*, 61(23), 7739–7747. <https://doi.org/10.1021/acs.iecr.2c01031>

- Ragaza, J. A., Hossain, M. S., Meiler, K. A., Velasquez, S. F., & Kumar, V. (2020). A review on Spirulina: alternative media for cultivation and nutritive value as an aquafeed. In *Reviews in Aquaculture* (Vol. 12, Issue 4, pp. 2371–2395). Wiley-Blackwell.
<https://doi.org/10.1111/raq.12439>
- Ranganathan, P., Amal, J. C., Savithri, S., & Haridas, A. (2017). Experimental and modelling of Arthrospira platensis cultivation in open raceway ponds. *Bioresource Technology*, 242, 197–205. <https://doi.org/10.1016/j.biortech.2017.03.150>
- Ravelonandro, P. H., Ratianarivo, D. H., Joannis-Cassan, C., Isambert, A., & Raherimandimby, M. (2011). Improvement of the growth of Arthrospira (Spirulina) platensis from Toliara (Madagascar): Effect of agitation, salinity and CO₂ addition. *Food and Bioprocess Technology*, 89(3), 209–216. <https://doi.org/10.1016/j.fbp.2010.04.009>
- Reichert, C. C., Reinehr, C. O., & Costa, J. A. V. (n.d.). SEMICONTINUOUS CULTIVATION OF THE CYANOBACTERIUM *Spirulina platensis* IN A CLOSED PHOTOBIOREACTOR. 23(01), 23–28. www.abeq.org.br/bjche
- Schulze, P. S. C., Barreira, L. A., Pereira, H. G. C., Perales, J. A., & Varela, J. C. S. (2014). Light emitting diodes (LEDs) applied to microalgal production. In *Trends in Biotechnology* (Vol. 32, Issue 8, pp. 422–430). Elsevier Ltd. <https://doi.org/10.1016/j.tibtech.2014.06.001>
- Shankar, S., Singh, J., Chakravarty, N., Mathur, A., & Singh, R. P. (2022). Algal biorefinery: Challenges and opportunities. In *Production of Top 12 Biochemicals Selected by USDOE from Renewable Resources: Status and Innovation* (pp. 41–79). Elsevier.
<https://doi.org/10.1016/B978-0-12-823531-7.00001-9>
- Sirohi, R., Kumar Pandey, A., Ranganathan, P., Singh, S., Udayan, A., Kumar Awasthi, M., Hoang, A. T., Chilakamarry, C. R., Kim, S. H., & Sim, S. J. (2022). Design and applications of photobioreactors- a review. In *Bioresource Technology* (Vol. 349). Elsevier Ltd.
<https://doi.org/10.1016/j.biortech.2022.126858>
- Solimeno, A., Samsó, R., Uggetti, E., Sialve, B., Steyer, J. P., Gabarró, A., & García, J. (2015). New mechanistic model to simulate microalgae growth. In *Algal Research* (Vol. 12, pp. 350–358). Elsevier. <https://doi.org/10.1016/j.algal.2015.09.008>
- Soni, R. A., Sudhakar, K., & Rana, R. S. (2017). Spirulina – From growth to nutritional product: A review. In *Trends in Food Science and Technology* (Vol. 69, pp. 157–171). Elsevier Ltd.
<https://doi.org/10.1016/j.tifs.2017.09.010>
- Stanbury, F. P., Whitaker, A., & Hall, S. J. (2017). *Principles of Fermentation Technology - Chapter 2 - Microbial growth kinetics* (Third Edition).
<https://doi.org/https://doi.org/10.1016/B978-0-08-099953-1.00002-8>

- Thevarajah, B., Nishshanka, G. K. S. H., Premaratne, M., Nimarshana, P. H. V., Nagarajan, D., Chang, J. S., & Ariyadasa, T. U. (2022). Large-scale production of Spirulina-based proteins and c-phycoerythrin: A biorefinery approach. *Biochemical Engineering Journal*, 185. <https://doi.org/10.1016/j.bej.2022.108541>
- Vale, M. A., Ferreira, A., Pires, J. C. M., & Gonçalves, G. A. L. (2020). CO₂ capture using microalgae. In *Advances in Carbon Capture: Methods, Technologies and Applications* (pp. 381–405). Elsevier. <https://doi.org/10.1016/B978-0-12-819657-1.00017-7>
- Van Den Hende, S., Vervaeren, H., & Boon, N. (2012). Flue gas compounds and microalgae: (Bio-)chemical interactions leading to biotechnological opportunities. In *Biotechnology Advances* (Vol. 30, Issue 6, pp. 1405–1424). <https://doi.org/10.1016/j.biotechadv.2012.02.015>
- Vazquez, C. F., & Sanchez, L. J. (2022). An overview of the algae industry in Europe. In *Joint Research Centre (JRC) to the European Commission's Knowledge Centre for Bioeconomy*. <https://doi.org/10.2760/813113>
- Wang, B., Lan, C. Q., & Horsman, M. (2012). Closed photobioreactors for production of microalgal biomasses. In *Biotechnology Advances* (Vol. 30, Issue 4, pp. 904–912). <https://doi.org/10.1016/j.biotechadv.2012.01.019>
- Wellburn, A. R. (1994). The Spectral Determination of Chlorophylls a and b, as well as Total Carotenoids, Using Various Solvents with Spectrophotometers of Different Resolution. *Journal of Plant Physiology*, 144(3), 307–313.
- Wolf-Gladrow, D. A., Zeebe, R. E., Klaas, C., Körtzinger, A., & Dickson, A. G. (2007). Total alkalinity: The explicit conservative expression and its application to biogeochemical processes. *Marine Chemistry*, 106(1-2 SPEC. ISS.), 287–300. <https://doi.org/10.1016/j.marchem.2007.01.006>
- Yarish, C., & Kim, J. K. (2012). *Gracilaria Culture Handbook for New England*. <https://www.researchgate.net/publication/311561454>
- Zarrouk, C. (1966). *Contribution a l'étude d'une Cyanophyce. Influence de Divers Facteurs Physiques et Chimiques Sur La Croissance et La Photosynthese de Spirulina Mixima*. Ph.D. Thesis [Ph.D. Thesis]. University of Paris.
- Zhou, W., Wang, J., Chen, P., Ji, C., Kang, Q., Lu, B., Li, K., Liu, J., & Ruan, R. (2017). Bio-mitigation of carbon dioxide using microalgal systems: Advances and perspectives. In *Renewable and Sustainable Energy Reviews* (Vol. 76, pp. 1163–1175). Elsevier Ltd. <https://doi.org/10.1016/j.rser.2017.03.065>

Zhu, C., Chen, S., Ji, Y., Schwaneberg, U., & Chi, Z. (2022). Progress toward a bicarbonate-based microalgae production system. In *Trends in Biotechnology* (Vol. 40, Issue 2, pp. 180–193). Elsevier Ltd. <https://doi.org/10.1016/j.tibtech.2021.06.005>

Zhu, C., Xi, Y., Zhai, X., Wang, J., Kong, F., & Chi, Z. (2021). Pilot outdoor cultivation of an extreme alkalihalophilic Trebouxiophyte in a floating photobioreactor using bicarbonate as carbon source. *Journal of Cleaner Production*, 283. <https://doi.org/10.1016/j.jclepro.2020.124648>

Website:

<https://www.meticulousresearch.com/product/phycoocyanin-market-5126>

Ringraziamenti

Ringrazio la Prof.ssa Eleonora Sforza per avermi concesso la possibilità di svolgere l'attività di tesi presso il laboratorio di Microalghe.

Un ringraziamento sincero a Danilo, per essere stato un punto di riferimento e un sostegno morale fondamentale durante questi mesi di lavoro.

Ringrazio i miei compagni di laboratorio, non solo per aver condiviso con me questo percorso, ma anche per l'amicizia sincera.

Infine, un ringraziamento doveroso ai miei genitori per essermi sempre stati accanto e per avermi sempre sostenuta durante tutto il percorso di studi.